Whole-embryo culture of mouse embryos to study vascular development

Inaugural-Dissertation

zur Erlangung des Doktorgrades
der Mathematisch-Naturwissenschaftlichen Fakultät
der Heinrich-Heine-Universität Düsseldorf

vorgelegt von

Martin Zeeb
aus Hechingen

Düsseldorf, November 2012

aus dem Institut für Stoffwechselphysiologie
der Heinrich-Heine Universität Düsseldorf

Gedruckt mit der Genehmigung der
Mathematisch-Naturwissenschaftlichen Fakultät der
Heinrich-Heine-Universität Düsseldorf

Referent: Prof. Dr. Eckhard Lammert
Korreferent: Prof. Dr. Christopher Bridges

Tag der mündlichen Prüfung:

Contents

Abstract

Formation of functional blood vessels is a prerequisite for all higher organisms, as blood circulation is required for the delivery of nutrients, oxygen and metabolic signals to tissues, as well as the removal of waste products and carbon dioxide. Blood vessels are also implicated in many diseases such as cancer, stroke or diabetic retinopathy. It is therefore of vital importance to understand and potentially manipulate blood vessel development in mammalian systems in order to find suitable targets for therapeutic treatments.

Both major modes of blood vessel formation, vasculogenesis and angiogenesis, require polarization of endothelial cells prior to lumenization. Up until recently, intracellular vacuole coalescence was thought to be the most important mechanism of lumen formation, whereas now, the focus has shifted towards extracellular lumen formation. Remodeling of vascular junctions, emergence of an apical membrane, and separation of apposing endothelial cell membranes are critical steps during this process. As the functional mechanisms and molecules underlying these processes become unraveled, an accurate and high-quality technique of manipulation and imaging is required to advance our knowledge.

Previous vessel formation studies have mostly been conducted in zebrafish (*Danio rerio*) embryos, as they are cheap, easy to handle and to manipulate, and transparent during development. However, zebrafish embryos show striking differences to mammals such as mouse or humans concerning heart morphogenesis, intersomitic vessel sprouting, dorsal aorta formation, and the site of hematopoiesis. Therefore, molecular investigations of mouse embryonic vessel development are necessary and nicely complement zebrafish studies.

In order to meet the requirements of blood vessel development studies in the mouse, I have refined and improved the method for whole-embryo *ex vivo* culture of mouse embryos. Now, mouse embryos can be isolated from the maternal uterus, vessel formation can be manipulated, and embryos can subsequently be cultured for up to 24 hours. After culture, mouse embryos can be subjected to whole-embryo staining, immuno-histochemistry, *in situ* hybridization or cell sorting.

Manipulation of mouse embryos can be achieved by local injection of pharmacological compounds or antibodies to block or activate specific signaling pathways. This treatment requires minimal amounts of substance, locally restricts its effects, and allows using internal controls.

The new culture media are free of serum or only contain calf serum, thus reducing the price of culture by up to 90 % and allowing the use of primary antibodies from all common species.

Following this technique, vasculogenesis and angiogenesis can be analyzed in a complete mouse embryo with simple confocal microscopy. Additionally, other developmental processes can be analyzed as required by the researcher.

We have used this technique to investigate the influence of negatively charged sialomucins, namely Podocalyxin (PODXL), on the process of lumen formation. We could show that sialic acids and, more specifically, their negative charges are necessary for slit formation between apposing endothelial cells during aortic lumen formation. Removal or masking of negative charges suppressed lumen formation, an effect that could be rescued by addition of artificial negative charges. Slit-formation, driven by negative charges on sialomucins was thereby identified as the initial step of vascular lumen formation in the mouse dorsal aorta following its polarization.

Zusammenfassung

Entstehung funktioneller Blutgefäße ist eine Grundvoraussetzung für das Überleben aller höherer Organismen, da Blutzirkulation für den Transport von Nährstoffen, Atemgasen und Stoffwechselsignalen zu den Geweben, so wie für den Abtransport von Abfallstoffen und Kohlendioxid unentbehrlich ist. Blutgefäße sind außerdem in die Entstehung von Krankheiten wie Krebs und Schlaganfall verwickelt. Deshalb ist es von essentieller Bedeutung, die Entstehung der Blutgefäße zu verstehen und zu manipulieren, um neue Ziele für therapeutische Maßnahmen zu finden.

Die zwei wichtigsten Formen der Gefäßentstehung, Vasculogenese und Angiogenese, beinhalten beide die Polarisierung von Endothelzellen, vor der eigentlichen Lumenbildung. Bis vor kurzem dachte man, dass die Verschmelzung intrazellulärer Vakuolen der wichtigste Mechanismus der Lumenbildung sei. Nun jedoch, richtet sich die Aufmerksamkeit mehr auf die extrazelluläre Lumenbildung. Der Umbau vaskulärer Verknüpfungspunkte, das Entstehen einer apikalen Membran, so wie die Trennung gegenüberliegender Endothelzellmembranen sind entscheidende Schritte dieses Prozesses.

Die Aufklärung der zu Grunde liegenden Mechanismen und Moleküle erfordert eine präzise und reproduzierbare Technik zur Manipulation und Darstellung. Bisherige Studien wurden zumeist in Embryonen der Fischgattung *Danio rerio* durchgeführt, da diese billig, leicht zu handhaben und zu manipulieren sind, da sie in der Embryonalentwicklung transparent sind. Zebrabärblinge (*Danio rerio*) zeigen jedoch auffällige Unterschiede zu Mäusen und Menschen bei der Herzentstehung, der Sprossung der intersomitischen Gefäße, der Bildung der Aorta, sowie dem Ort der Blutbildung. Deshalb sind Studien der embryonalen Mausentwicklung auf molekularer Ebene dringend notwendig und hervorragend geeignet um Studien am Zebrabärbling zu ergänzen.

Um die Anforderungen zu erfüllen, die an diese neuen Studien der Blutgefäßentwicklung in der Maus gestellt werden, habe ich die Methode der *ex vivo*-Kultivierung ganzer Mausembryonen verbessert. Mausembryonen können jetzt nach Manipulation der Gefäßentwicklung für bis zu 24 Stunden weiter kultiviert werden. Nach der Kultur können sie im Ganzen oder in Schnitten gefärbt oder mit anderen Methoden untersucht werden.
Die Manipulation erreicht man durch die Injektion pharmakologischer Substanzen oder Antikörper, die spezifisch Signalwege blockieren oder aktivieren. Diese Behandlung erfordert nur kleinste Mengen an Substanz und grenzt die Effekte lokal, auf die Injektionsregion, ein, wodurch interne Kontrollen verwendet werden können.
Die neu entwickelten Medien zur Kultur kommen gänzlich ohne oder nur mit Kälberserum aus, so dass der Preis der Kultur um bis zu 90 % sinkt und primäre Antikörper jeder verbreiteten Spezies verwendet werden können. Unter Anwendung dieser Technik können Vasculogenese und Angiogenese jetzt im vollständigen Mausembryo mittels Konfokalmikroskopie untersucht werden. Zusätzlich zur Gefäßentwicklung können beliebige weitere Entwicklungsprozesse, die im selben Zeitrahmen ablaufen, untersucht werden.

Wir haben frühe Versionen dieser Technik dazu verwendet, um den Einfluss der negativ geladenen Sialomucine, insbesondere von Podocalyxin, auf die Lumenbildung zu untersuchen. Wir konnten zeigen, dass die Sialinsäurereste, bzw. ihre negativen Ladungen notwendig und entscheidend für die Bildung des ersten Spalts zwischen zwei aneinander liegenden Endothelzellen sind. Das Entfernen oder Verdecken der negative Ladungen hatte einen Rückgang der Lumenbildung zur Folge, ein Effekt der durch die künstliche Zugabe von negativen Ladungen verhindert werden konnte. Die Bildung eines Spalts zwischen Endothelzellen, die durch negative Ladungen hervorgerufen wird, wurde dabei nach der Polarisierung als initialer Schritt in der Lumenbildung der Aorta identifiziert.

1 Introduction

1.1 Introduction to the topic

1.1.1 Reading and using this thesis

This thesis consists of three independent publications that were produced and published between 2009 and 2012:

- Zeeb, M.; Strilić, B.; Lammert, E. - Resolving cell-cell junctions: Lumen formation in blood vessels – Current Opinion in Cell Biology - 2010
  A review article describing the molecular events during vascular lumen formation with special emphasis on endothelial cell junctions (Zeeb et al., 2010).
- Strilić, B.; Eglinger, J.; Krieg, M.; Zeeb, M.; Axnick, J.; Babál, P.; Müller, D. and Lammert, E. - Electrostatic cell surface repulsion initiates lumen formation in developing blood vessels – Current Biology – 2010
  A primary scientific article establishing negative charges on sialomucins as the initializing factor of vascular lumen formation (Strilic et al., 2010a).
- Zeeb, M.; Axnick, A.; Planas-Paz, L.; Hartmann, T.; Strilić, B. and Lammert, E. - Pharmacological manipulation of blood and lymphatic vascularization in ex vivo cultured mouse embryos – Nature Protocols – 2012
  A methodological paper describing in detail the procedure to isolate, inject, cultivate, and analyze blood and lymphatic vessel formation during mouse embryonic development (Zeeb et al., 2012).

To facilitate reading and understanding of this thesis, the publications are not presented in chronological order. Instead, the publications are presented in logical succession, starting with the review article (Zeeb et al., 2010), which gives a theoretical introduction and shows the state of the art in blood vessel formation.
Next, the protocol introduces the reader to the detailed materials and methods used to study vessel development in the mouse (Zeeb et al., 2012).
Finally, the scientific article shows results that were obtained using this technique (Strilic et al., 2010a). It should be noted, that not all changes and updates described in (Zeeb et al., 2012) were established when finishing (Strilic et al., 2010a).

As the publications offer an overview of theory and methodology in and of themselves, only a brief introduction into the development and architecture of the blood vascular system will be given in this introduction. Subsequently, all publications will be set into the scientific context of their time, to understand their relevance and significance.

1.1.2 The vascular system in vertebrates

During embryonic development of higher animals, the cardiovascular system is the first functional organ system that forms.
Whereas animals smaller than a few millimeters can rely solely on diffusion to supply all of their tissues, all larger animals require a transport and circulation system to deliver oxygen and

nutrients to the tissues and carry away carbon dioxide and metabolic products, as diffusion is no longer sufficient.

In invertebrates, this system usually consists of cardioblasts (as in arthropods (Yarnitzky and Volk, 1995)) or mesothelial cells (as in annelids (Graupera et al., 2008)) lining a central tubing with their basal cell surfaces and an extracellular matrix (ECM), that is degraded to form the vascular lumen (Kucera et al., 2009). In general, there are no endothelial cells (ECs) present in invertebrate vessels (Shigei et al., 2001). Their system can be open towards the body cavity (coelom) or closed (Strilic et al., 2010b).

In vertebrates such as zebrafish, mouse or human, however, all vessels are endothelial-lined tubes, in which the lumen is formed by apical cell surfaces.
The vascular system of vertebrates is always closed, is highly complex and organized hierarchically with vessel diameters ranging from 5 μm to over 2 cm (Eichmann et al., 2005).
Vessels carrying blood from the heart to the consumptive tissues are called arteries, the largest of which is the dorsal aorta that branches into arteries and those into arterioles. Nutrient and gas exchange occurs in the smallest vessels, the capillaries that bridge the arterial network to the venous system. Venules, draining the blood into larger veins and thus, back to the heart complete the circulatory system.
All vessels are surrounded by mural cells, subdivided into pericytes and smooth muscle cells (Gerhardt and Betsholtz, 2003; Betsholtz et al., 2005). Pericytes surround smaller capillaries.
Bigger vessels show a three-layered organization (see Fig. 1.1). The innermost layer, the *intima*, consists of the endothelial cells and their adjacent basement membrane. The *tunica media* harbors several layers of smooth muscle cells innervated by nerves and separated by layers of ECM. The biggest vessels even contain small capillaries to supply this layer of smooth muscle cells. The outermost layer is called *tunica externa*, or *adventitia*, and represents a protective coat consisting of collagen fibers and fibroblasts.
Indeed, veins are morphologically quite different from arteries. They harbor much less muscle cells and contain valves that prevent backflow of blood. These valves are made of endothelial cells supported by basement membrane.
Arteries are much thicker and more muscular, as they have to withstand higher pressure.

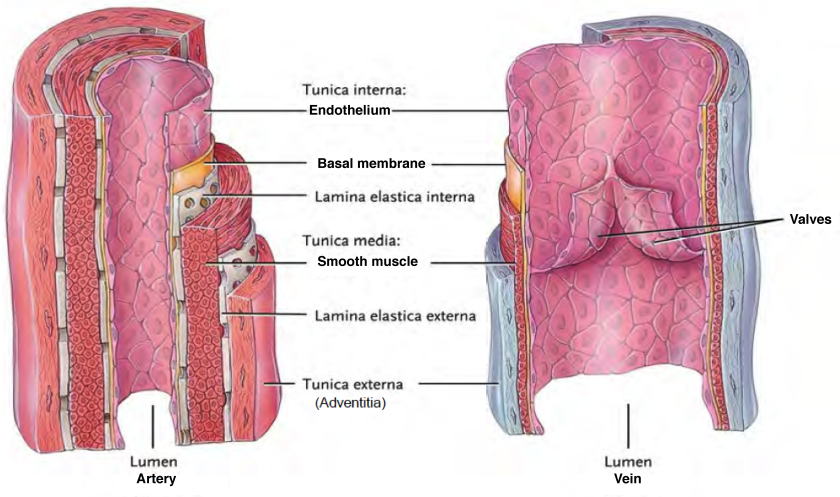

Figure 1.1: Multilayered structure of larger arteries and veins.
Adapted from (Tortora, Derrickson, 2006)

Even among the capillaries there is a high degree of variability, depending on the specific needs of the tissue or organ. Capillaries can be extremely tight, as in the brain (Lammert, 2008), preventing any leakage, or can be discontinuous and leaky as in the liver sinusoids (Buschmann, 2010).

Another kind of vessel originates from the cardinal vein after E10.5, the lymphatic system (Wigle and Oliver, 1999; Planas-Paz et al., 2012). Lymphatic vessels are also lined by endothelial cells. However, the lymphatic system is not circulatory, but blind-ended. It serves to drain fluid that escaped the blood vessels back to the circulatory system. It is also responsible for the transport of lipids and immune cells. In order to exert this function, collecting lymph vessels are leaky, contain discontinuous junctions and no basement membrane. They also contain valves to direct the flow of the lymph.

Finally, formation of vessels is not just a physiological process during development and wound healing, but also occurs in many pathological states, including cancer and diabetic retinopathy. Especially in the development of cancer, attraction or formation of blood vessels to the tumor tissue is a critical step, as without vessel supply, a tumor cannot grow beyond a certain size. Therefore, blood vessels are important drug targets in many cancer types (Chung et al., 2010). Consequently, new therapies to normalize or suppress vessel formation are in constant need, especially because some classical paradigms of vessel formation haven proven to be incorrect against the background of tumor vascularization (Miles et al., 2010).

1.1.3 The mouse as a model organism

The mouse (*mus musculus*) is commonly used as a model organism all around the globe, as it shares a close genetic relationship to humans, with a high degree of genetic homology and identity. Compared with other mammals, mice are relatively robust and easy to keep. Mouse models for many human diseases exist, offering the possibility of *in vivo* studies and initial target screening.
The mouse is a well-established model system for geneticists with a plethora of knockout strains being available, ranging from whole-body knockouts to time- and site-specific knockouts and even inducible knockout systems.

For a mammal, mice produce a lot of offspring, due to the short generation time of around 9 weeks.
The first part of this period, the embryonic development, lasts for approximately 3 weeks (usually 19-20 days), dependent on the mouse strain.
The next 3 weeks after birth, mouse pups critically depend on the mother for nourishment by lactation. They develop fur and open their eyes. The phase finishes with weaning.
The mice now feed independently and lab mice are separated from the mother and genotyped shortly thereafter. After three more weeks, at the age of 6-7 weeks, the mice become pubescent and can produce new offspring.

Mouse strains commonly used in the laboratory include C57BL/6, BALB/c, CD1, and NMRI mice.
C57BL/6, called “black 6” is the most common strain, of which lots of knockout strains exist. They usually show pronounced and distinct phenotypes. BALB/c is an albino strain that is most commonly used in cancer and immunology research. CD1 and NMRI mice are both SWISS-type albino mouse strains having larger litters and a high resistance to diseases and other stressors.
The first two mentioned strains are inbred strains, where brothers ad sisters were mated for at

least 20 generations, resulting in more pronounced effects and a homogenous genotype. The latter two strains are outbred strains, where wildtype mice a regularly crossed in, in order to retain a heterogeneous genotype commonly resulting in longer life span.

As mice are nocturnal, conception happens around midnight and is usually indicated by a vaginal plug of coagulated sperm on the next morning, termed E0.5 (embryonic day 0.5). For the next 5 days, the fertilized oocyte travels along the oviduct and passes the morula and blastula stages. At around E5.0 to E5.5, the embryos are implanted into the uterus wall. Shortly thereafter, during gastrulation, the three germ layers ectoderm, mesoderm, and endoderm are created.
After neurulation, the first somites begin to develop lateral to the neural tube from E8.0 onwards. Simultaneously, the circulatory system, initially only consisting of the heart and the two dorsal aortae as the first vessels, begins to develop. The dorsal aortae lumenize and sprout extensively to form e.g. the intersomitic vessels (ISVs). This occurs in parallel to a process called turning, in which the embryo turns its ventral body surface to the inside and the dorsal surface to the outside adopting the usual embryo-like orientation.
After E9.5, organogenesis continues, forming the inner organs such as liver or pancreas (Zaret and Grompe, 2008) or the lymphatic system (Wigle and Oliver, 1999).
The last days before birth are characterized by embryonic growth.

1.1.4 Development of the vascular system in the mouse

Blood vessels are formed by two major modes known as vasculogenesis and angiogenesis (see Fig 1.2, Risau and Flamme, 1995; Axnick and Lammert, 2012).
Vasculogenesis describes the *de novo* formation of blood vessels, which is relevant for the formation of the yolk sac vessels and the formation of the dorsal aorta, the first vessel within the embryo proper (Fong et al., 1999; Sato et al., 2008).
Further vessels are generally formed via angiogenesis, as this mode describes the formation of blood vessels from pre-existing ones (Adams and Alitalo, 2007).
Recently, a novel method of vessel formation, called selective cell sprouting, responsible for the formation of the cardinal vein in zebrafish was proposed (Herbert et al., 2009).

Vasculogenic formation of the mouse dorsal aorta starts at E7.5, with the differentiation of angioblast into endothelial cells on both sides of the neuroepithelium. Consequently, the dorsal aorta initially forms as two dorsal aortae, that fuse later in development (Drake and Fleming, 2000). Angioblasts are of mesodermal origin and start to express endothelial-specific markers such as PECAM-1 (CD31), or VEGFR-2 (Kdr, Flt-1) during their differentiation (Tzima et al., 2005; Woodfin et al., 2007). These cells then begin to migrate towards a gradient of VEGF-A and/or FGF and stop their migration upon reaching the outer cell layer, the endoderm. VEGF-A is one of the major molecular factors during vessel formation, as it is important for angioblast migration, lumen formation and initiation of angiogenesis (Olsson et al., 2006).
At their destination, the angioblasts that are now called endothelial cells (ECs) connect and form an EC cord, along the embryonic axis.
Subsequently, ECs lumenize in a complex process that is dependent on the polarization of the ECs, the emergence of a deadhesive apical cell surface between their apposing membranes and VEGF-A driven cell shape changes that open up a functional lumen. Lumenization in the mouse dorsal aorta requires at least two ECs and happens extracellularly (Strilic et al., 2009).

Angiogenesis occurs via sprouting of existing vessels or via intussusception (Baum et al., 2010; Axnick and Lammert, 2012). Sprouting angiogenesis is most commonly initiated by hypoxia, but can also be triggered by shear stress (Tzima et al., 2005; Adams and Alitalo, 2007). Hypoxia

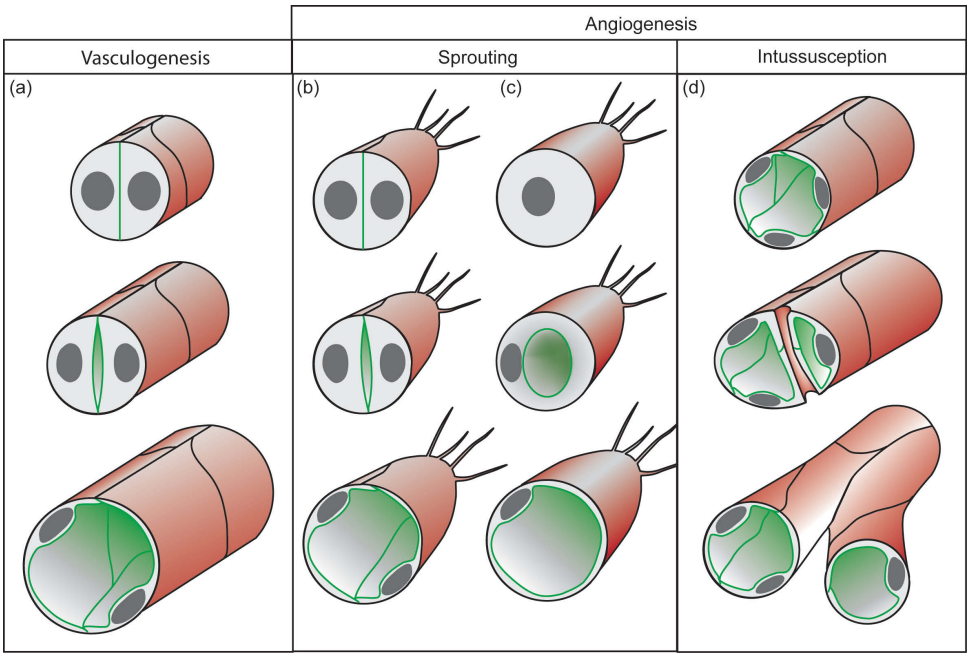

Figure 1.2: Different modes of vascular lumen formation. Taken from (Axnick and Lammert, 2012).

leads to the expression of hypoxia-inducible factors in the affected tissue, which in turn trigger the release of VEGF-A. VEGF-A is sensed by endothelial cells in a neighboring vessel and triggers the "angiogenic switch". The affected endothelial cells start to degrade the basement membrane using matrix-metalloproteinases, reverse their polarity, and begin to migrate. A single endothelial cell is selected as the tip cell of the new-forming sprout. This tip cells predominantly expresses Dll4, a transmembrane protein that acts as a ligand for the Notch receptor, which is expressed on neighboring endothelial cells, the stalk cells. Signaling downstream of Notch suppresses tip cell behavior, thus preventing the formation of additional sprouts. The sprout then connects to another vessel nearby, creating a supply route for the previously hypoxic region. The most well-understood angiogenic events to date are the formation of the intersegmental vessels (ISVs) in zebrafish, corresponding to the intersomitic vessels in the mouse. In mice, these vessels sprout from the dorsal aorta at a time when the ninth somite is formed (9 S stage), shortly after the heart starts to beat (at 6-7 S).

The vessels initially formed by vasculogenesis and angiogenesis later increase in size, a process that is critically dependent on the proliferation and migration of endothelial cells (Graupera et al., 2008). Additionally, the newly formed vessels secrete a basement membrane that attracts mural cells, such as pericytes that help to stabilize the vessel (Stratman et al., 2010). These processes are called vessel remodeling and occur from embryonic day E9.5 onwards in the mouse (Betsholtz et al., 2005). Vessel remodeling in the adult can be triggered by shear stress or vessel occlusion, the latter of which causes collateral vessel expansion as compensation, a process called arteriogenesis (Cai and Schaper, 2008).

The question, how vessels form and remodel on a molecular basis has been up for debate for over a century. Only recently, major advances have been made that are described in the following sections, in which the articles of this thesis are set into a larger scientific context.

1.2 Scientific context of the published articles

1.2.1 Strilic et al., Curr Biol, 2010 and Zeeb et al., Curr Opin Cell Biol, 2010

Although the morphological traits of vessel formation are well established, the exact molecular mechanisms of vasculogenesis and angiogenesis are still up for debate.
Until recently, it was not even clear whether lumen formation occurs intra- or extracellularly, a question that is almost 100 years old. Cord hollowing and cell hollowing have been proposed as mechanisms for tube formation (Billroth, 1856; Sabin, 1920; Lubarsky and Krasnow, 2003).
In cord hollowing, an agglomeration of cells forms a tube by creating and expanding an apical surface between the cells and by directed movements and rearrangements (Lubarsky and Krasnow, 2003). This process creates multicellular tubes.
In cell hollowing, cells form intracellular lumens that open up towards the outside only later, thus creating vessels, which are initially unicellular.

For many years, intracellular lumen formation was regarded as the actual mode of lumen formation. A detailed analysis of intracellular lumen formation in zebrafish ISVs was published in 2006 and cemented this opinion (Kamei et al., 2006). The theory was that intracellular lumens originate from pinocytotic vesicles that fuse intracellularly to give rise to large "vacuoles" that subsequently bridge two neighboring endothelial cells intracellularly (Davis and Camarillo, 1996; Davis et al., 2002). The lumen space was thought to be sealed off from the extracellular space (Kamei et al., 2006), so lumen enlargement would also rely on additional delivery of membrane and fluid to the lumen. The whole mechanism was labeled "vacuole coalescence".
However, many reports have challenged this view and have promoted multicellular lumen formation (Parker et al., 2004; Blum et al., 2008) and intercellular lumen formation (Strilic et al., 2009) via cord hollowing, a mechanism that is now widely accepted to be the most common mode of lumen formation.
The reports leading to this paradigm shift pose the basis for the Current Biology article and are reviewed in the Current Opinion in Cell Biology paper.

In brief, dorsal aorta formation was initially investigated in zebrafish embryos, showing that endothelial cells migrate towards the dorsal midline to form a multicellular tube (Parker et al., 2004; Jin et al., 2005). Molecular details were not resolved in these studies.
In 2009, our lab published a major article on lumen formation in the dorsal aorta of mouse embryos (Strilic et al., 2009). The study did not reveal any intracellular vacuoles, but explained the necessity of the junctional molecule VE-cadherin (Carmeliet et al., 1999) and the signaling molecule VEGF-A (Carmeliet et al., 1996; Ferrara et al., 1996). It was shown that endothelial cells first create an apical membrane between apposing endothelial cells via delivery of PODXL (gp135)-filled vesicles. Further, signaling downstream of VEGF-A and VEGFR2 via ROCK creates contractile fibers and cell shape changes that open up a functional lumen. It was also shown that the initial lumen is discontinuous, so directed delivery of fluid to the tube is not necessary.
In parallel or quick succession, other studies revealed more molecular details of lumen formation. Endothelial polarization was shown to involve the Par3 polarity complex (Lampugnani et al., 2010; Zovein et al., 2010) and utilizes Cdc42 to mark and target endothelial vesicles (Koh et al., 2008; Iruela-Arispe and Davis, 2009). The ccm proteins were shown to regulate endothelial junctions and thus polarity (Kleaveland et al., 2009; Lampugnani et al., 2010).

As more and more mechanistic details and molecular players were reported, a review was requested discussing the endothelial junctions, as these play a major role in polarization and

designation of the lumen site (Zeeb et al., 2010). Our review presented these details as an ordered framework of lumen formation and strongly promoted extracellular lumen formation as the most common way (and certainly only way in mouse and probably zebrafish dorsal aorta).

Although there has been a lot of progress concerning signaling prior to lumen formation, some questions remained on how lumen formation takes place once polarity is established. Therefore, research was conducted to elucidate the exact role of the glycoprotein PODXL during lumen formation (Strilic et al., 2009; Strilic et al., 2010).

1.2.2 Zeeb et al., Nat Protoc, 2012

Despite all the details being reported from dorsal aorta formation in both mouse and zebrafish, angiogenic formation of zebrafish intersegmental and mouse intersomitic vessels (ISVs) remained unclear.
As seamless and unicellular tubes have been reported for this type of vessel, it was debated if these originate from unicellular tube formation or multicellular tube formation followed by cellular rearrangements. Additionally, if the lumen is formed unicellularly, the mechanism could be extra- or intracellular.

As a first step in solving these question, it was shown that ISV lumen formation occurs between multiple endothelial cells (Blum et al., 2008).
However, under certain circumstances, unicellular tube formation also occurs. Unicellular lumen formation was observed in the formation of the dorso-lateral anastomotic vessel (DLAV) in parallel with multicellular mechanisms. In this system, unicellular lumen formation does not depend on the fusion of intracellular vacuoles but occurs extracellularly via membrane invaginations (Herwig et al., 2011).
It should be noted that blood "[...] flow is dispensable for cell rearrangements during DLAV formation and for EC polarization per se. It is, however, required for membrane invagination, which leads to the formation of unicellular tubes, indicating that blood pressure may be the driving force of this morphogenetic process." (Herwig et al., 2011).
In general, heartbeat is not required for intersegmental vessel formation, as the sprouting is initiated when the dorsal aorta is not yet lumenized (Ellertsdottir et al., 2010). In mice, sprouting from the dorsal aorta starts at 9S during late E8.5 (Walls et al., 2008), several hours after the heart starts beating and pumping blood through the lumenized aorta (at 6-7 S). To date, it is not known if heartbeat or blood flow is required for these sprouting events.

In total, vasculogenesis seems to rely on multicellular lumen formation exclusively, whereas angiogenic processes can utilize uni- and multicellular lumen formation, dependent on the specific environment (see Fig 1.2, p. 7, (Axnick and Lammert, 2012)).

Since 2010, further molecular details in aortic lumen formation became unraveled. The Ras interacting protein 1, Rasip1, was identified as a regulator of endothelial polarity and the Par3 complex (Xu et al., 2011).

In 2011, a major contribution to the research on lymphatic vessel formation was issued from our lab (Planas-Paz et al., 2012). In this article, mechanical strain was identified as an inducing factor of lymphatic endothelial cell (LEC) proliferation and jugular lymph sac (JLS) formation. Stretching of ECs and swelling of ECM is transduced into the cell by β1-integrin resulting in VEGFR-3 (Flt-4) phosphorylation and LEC proliferation.

In summary, many recent studies, which made major contributions to blood and lymphatic

vessel formation and sprouting, promoted the mouse as a model system of choice in vascular research.
With this progress and the need for further molecular studies, updating the technique to culture and investigate mouse embryos *ex vivo* was long overdue. The publication in Nature Protocols (Zeeb et al., 2012) summarizes our recent advancements of whole-embryo culture. The protocol that was used in (Strilic et al., 2009), (Strilic et al., 2010a), and (Planas-Paz et al., 2012) was improved on and tested in detail.

2 Publications

2.1 Resolving cell-cell junctions: lumen formation in blood vessels

2.1.1 Summary

Formation of a patent vascular lumen is essential for the transport of oxygen, nutrients and waste products to and from tissues. No matter whether the blood vessel arises from vasculogenesis or angiogenesis, endothelial cells first have to form a cord, which subsequently lumenizes, in order to generate a functional vessel. During these processes, cellular junctions rearrange between adjacent endothelial cells and are involved in endothelial cell polarization as a prerequisite for lumen formation.

In this article, we review *in vivo* studies of the last five years and integrate their findings into a comprehensive scheme of vascular lumen formation.
For the first time, we put these findings into a frame and transform conflicting results into a commonly accepted consensus model of lumen formation valid for multiple vascular beds.

We present and elucidate a special role for vascular junctions during obligatory EC polarization and subsequent lumen formation. In particular, the roles of cadherins, polarity complexes, deadhesive molecules, integrins and their connection to the actin cytoskeleton are presented and discussed and these molecules are put into a larger context.

Signaling downstream of integrins and Heg1/ccm regulates the formation and stabilization of endothelial cell-cell junctions containing VE-cadherin. VE-cadherin is critically required for vascular lumen formation and a prerequisite for endothelial cell polarization, as shown by the embryonic lethality of VE-cadherin-deficient mice.
Next, the Par3 polarity complex regulates the establishment of an apical surface. To do so, PTEN first defines the apical membrane. Then, exocytotic vesicles filled with negatively charged glycoproteins (such as PODXL) are targeted to this membrane. This process utilizes the small GTPase Cdc42.
At lateral positions, VE-cadherin is connected to the actin cytoskeleton via interaction with catenins to create stable junctions. These junctions are necessary to maintain cellular polarity. Cell shape changes during subsequent lumen formation are initiated by contractile fibers or actin remodeling. These changes depend on VEGF-A and ROCK and the anchorage of the apical membrane to the cytoskeleton via ERM proteins.

In total, this review promotes and significantly strengthens the understanding of extracellular lumen formation by providing detailed molecular mechanisms in a time-specific framework, thus providing a major contribution to the debate whether lumen formation occurs intra- or extracellularly.

2.1.2 Accepted review article

See pages 12 ff.

Resolving cell-cell junctions: Lumen formation in blood vessels

Martin Zeeb[1], Boris Strilic[1,2], Eckhard Lammert[1]

Addresses:

[1]Institute for Metabolic Physiology, Heinrich-Heine-University, Düsseldorf, Germany

[2]Department of Pharmacology, Max Planck Institute for Heart and Lung Research, W.G. Kerckhoff-Institute, Bad Nauheim, Germany

Corresponding Author: Lammert, Eckhard (Lammert@uni-duesseldorf.de)

Abstract

Formation of a patent vascular lumen is essential for the transport of oxygen, nutrients and waste products to and from tissues. No matter whether the blood vessel arises from vasculogenesis or angiogenesis, endothelial cells first have to form a cord, which subsequently lumenizes, in order to generate a functional vessel. During these processes, cellular junctions rearrange between adjacent endothelial cells and are involved in endothelial cell polarization as a prerequisite for lumen formation. Here we review the role of endothelial cell junctions in vascular lumen formation within different vascular beds.

Introduction

Virtually all vascular lumens develop from interconnected endothelial cells (ECs). Using mouse and zebrafish embryos, several publications in the last couple of years implicated junctions as important regulators of lumen formation in a variety of blood vessels (ranging from the aorta to capillaries). Junctions guide vascular lumen formation by regulating EC contact formation and cell polarization at apposing EC plasma membranes [1-3]. Here we describe the junctional molecules expressed in ECs (Fig. 1a (1)), their role in EC polarization, and how they are involved in vascular lumen formation. To this end, we focus on *in vivo* studies and only include *in vitro* studies when these have been supported *in vivo*.

Cell-cell junctions in endothelial cells

Cadherins

Vascular endothelial cadherin (VE-cadherin) is a cell adhesion molecule expressed in ECs and some tumor cells [4, 5]. It belongs to the cadherin protein family, whose member N-cadherin is also expressed in ECs [6] (Fig. 1a). VE-cadherin promotes homotypic interactions between ECs, but is not strictly required for the adhesion of ECs to one another. Instead, VE-cadherin-deficient mice retain EC-EC contacts and form EC cords [7]. However, VE-cadherin-deficient mice die during embryonic development because of impaired vascular lumen formation followed by EC apoptosis [7, 2]. In addition, it was observed that ECs require VE-cadherin to polarize [2, 3], similar to epithelial cells that require E-cadherin for polarization [8].

N-cadherin increases the amount of VE-cadherin at the endothelial cell-cell contact and also localizes to adherens junctions in human umbilical vein endothelial cells (HUVEC) [6]. Moreover, N-cadherin knockout mice die at mid-gestation and display a smaller aortic lumen and an overall developmental delay [6].

Initially during *de novo* vascular lumen formation, VE-cadherin and adherens junctions are located throughout the entire cell-cell contact area of apposing plasma membranes in EC cords (Fig. 1a). Later, VE-cadherin is found at lateral positions of neighboring ECs, flanking the apical, or luminal, plasma membranes (Fig. 1b) [2].

Other cell adhesion molecules

The platelet and endothelial cell adhesion molecule (PECAM-1, also known as CD31) is expressed on platelets, leukocytes and, more importantly, ECs (Fig. 1a) [9], where it is involved in homo- and heterophilic cell-cell contacts. CD31-deficient mice are viable and exhibit no obvious vascular developmental defects, showing that this

adhesion molecule is not strictly required for vascular lumen formation [10]. It is, however, part of a mechanosensory complex initiating endothelial cell sprouting, together with VE-cadherin and the vascular endothelial growth factor receptor 2 (VEGFR-2) [11].

The junctional adhesion molecules (JAM) A to C are also expressed in ECs and localize to junctions. It has been shown that JAM-B and -C interact with the polarity protein Par3 in HUVECs and possibly influence endothelial cell polarity [12]. However, JAM-deficient mice seem to have no vascular phenotype [13].

Vascular cell adhesion molecule-1 (VCAM-1) is expressed in ECs after chemokine stimulation and mediates adhesion of lymphocytes and macrophages to the endothelium [14]. To date, VCAM-1-deficient mice appear to have no striking vascular defects.

Establishing endothelial cell polarity

In order to form a patent vascular lumen, ECs need to establish an apical cell surface where the lumen develops. In contrast, the basal or basolateral cell surface mediates the interaction of the developing blood vessel with the surrounding extracellular matrix (ECM) and mural cells. The establishment of cell polarity involves translocation of junctions to lateral positions, delivery of de-adhesive proteins to the cell-cell contact via exocytosis, and rearrangement of the cytoskeleton [2]. In addition, polarity complexes might be involved [15] (Fig. 1 and see below).

The establishment of cell polarity precedes lumen formation in the mouse dorsal aortae [2] and is required for proper lumen formation in mouse arteries [3, 15], similar to other tubular systems outside the vasculature [16]. At least three kinds of signaling events could be involved in cell polarization: signaling via cell-cell interactions,

signaling induced by extracellular signals, and signaling induced by binding to the surrounding ECM [17]. To date, cell-cell interactions [2] and cell-ECM interactions [15] have been shown to play a role in EC polarization and subsequent vascular lumen formation.

Polarity complexes and Integrins

Polarity complexes have been investigated in epithelial tube formation (reviewed by [18]). At least one of these, the Par3 complex – consisting of Par3, Par6 and atypical protein kinase C (aPKC) in epithelial cells – seems to be present in mouse ECs [15] and HUVECs [19] (Fig. 1a, (2)).

One of the downstream effectors of the Par3 complex is PTEN (phosphatase and tensin homolog) that appears at the future apical plasma membrane and converts Phosphatidylinositol (3,4,5)-trisphosphate (PIP_3) to Phosphatidylinositol (4,5)-bisphosphate (PIP_2)[20]. The latter recruits Cdc42 to the apical cell surface in MDCK (Madin-Darby Canine Kidney) cells [21]. Moreover, Cdc42 was shown to be required for tube formation in HUVECs *in vitro* [19] and in the pancreas *in vivo* [16]. These effectors may also be relevant for *in vivo* vascular lumen formation, as pharmacologic inhibition of PTEN reduces aortic lumen formation in mice [2], and Cdc42 localizes to luminal EC surfaces in developing zebrafish intersomitic vessels (ISVs) [22]. However, no definitive evidence for their roles in vascular lumen formation has been provided, since PTEN-deficient mice appear to be able to form lumenized dorsal aortae [23], and Cdc42-deficient mice have not yet been analyzed for vascular defects.

The first evidence for a role of integrins in blood vessel lumenization *in vivo* was the demonstration that quails fail to form proper vascular tubes in the dorsal aorta when

injected with a β1-integrin-blocking antibody [24]. β1-integrin appears to be upstream of Par3 (and maybe the full complex) and appears to be required for vascular lumen formation in mouse arteries [15]. Other studies, however, do not report on vascular lumen defects in β1-integrin-deficient mice, but reveal vascular remodeling defects and hemorrhages [25-27]. In addition, the ECM protein fibronectin is not required for formation of a lumenized dorsal aorta in all mouse strains [28]. Moreover, when a subunit of most laminins, laminin-γ1 (LAMC1), is missing in embryonic stem cells (ESCs), lumenized blood vessels develop in embryoid bodies and harbor a larger lumen diameter. These data suggest that basement membrane is not strictly required for vascular lumen formation, but controls blood vessel enlargement [29].

De-adhesive molecules

At the apical cell surface of MDCK cells, PIP_2 may trigger the exocytosis of vesicles carrying de-adhesive molecules, such as podocalyxin/gp135 (PODXL), which is a member of the CD34-sialomucin family (Fig. 1a, (3)) [21, 30]. The presence of CD34-sialomucin-containing vesicles in ECs at the onset of aortic lumen formation suggests that CD34-sialomucins also accumulate at the apical EC surfaces via exocytosis. VE-cadherin is required for specifically targeting CD34-sialomucins to the EC-EC contact, as these proteins do not enrich apically in VE-cadherin-deficient mice [2].

The CD34-sialomucin family consists of CD34, PODXL and endoglycan [31]. PODXL and CD34 are localized apically in epithelial cells and mouse ECs [32, 2]. Since CD34-sialomucins are partially redundant, single knockouts of these proteins do not have severe vascular defects. Instead, a significant delay in aortic lumen formation has been observed in PODXL-deficient mice [2]. Interestingly, PODXL is required for

the formation of filtration slits between adjacent podocytes [33], and inhibits cell-cell adhesion in MDCK cells [34]. Being highly glycosylated, PODXL contributes to the apical glycocalyx, shown to form an exclusion zone around the luminal cell surface [35]. Therefore, the glycocalyx more likely contributes to lumen formation by promoting cell-cell repulsion rather than serves as a reservoir for growth factors. In contrast, the abluminal basement membrane binds and modulates growth factors due to the presence of heparan sulfate proteoglycans (HSPGs) and proteases [36], but does not initiate lumen formation.

Adherens junctions and tight junctions

While CD34-sialomucins are delivered to the cell-cell contact (Fig. 1a (3) and 1b (4)), VE-cadherins get translocated to the cell borders (Fig. 1b (5)). At least two possible mechanisms could be involved, e.g. VE-cadherin is endocytosed from the apical cell surface or it is pushed to the cell borders by CD34-sialomucins and other apical glycoproteins. At the lateral positions, VE-cadherin becomes part of junctions that have properties of adherens junctions (AJ) – as they harbor the VE-cadherin protein – and have properties of tight junctions (TJ) [37] – as they harbor the ZO-1 protein (zona occludens 1) [38, 39]. VE-cadherin binds to β-catenin and plakoglobin (or γ-catenin) via its C-terminal cytoplasmic tail. β-catenin and plakoglobin in turn bind to α-catenin, which connects VE-cadherin to F-actin. β-catenin-deficient mice die during embryonic development because of vascular defects. Early vasculogenesis and angiogenesis appear normal, but irregular and inconsistent vascular lumens develop, as do hemorrhages. This phenotype is probably due to alterations in the F-actin cytoskeleton as well as a reduced amount of α-catenin at the junctions [40]. VE-cadherin also binds to p120, which does not link to F-actin, but can modulate the F-

actin cytoskeleton via interaction with RhoA [41]. Thus, VE-cadherin anchors the cells to one another, while also connecting and influencing the contractile, cytoskeletal fibres necessary for lumen formation.

A mechanism of regulating junctions was recently identified in both, the mouse aorta and zebrafish branchial arteries [42]. The formation of functional junctions requires signaling downstream of the transmembrane protein Heg1 (heart of glass) and its intracellular adaptor molecule CCM2 (cerebral cavernous malformation), as mice deficient for both proteins die before embryonic day 10 (E10). These mice display hemorrhages and no patent lumen in the dorsal aorta and branchial arteries [42]. Thus, the formation of junctions is a critical step for EC polarization and forms the groundwork for lumen formation in developing blood vessels.

Under the cell surface

While several proteins get recruited to the junctions at lateral positions, the same holds true for the apical cell surface. More specifically, ERM (ezrin, radixin, moesin) proteins are recruited to the apical cell surface of ECs [2] (Fig. 1b (7)). Moesin is the most abundant ERM protein in ECs [31] and binds to CD34-sialomucins, directly or via adaptors. Deletion of moesin, however, is not lethal and does not cause major vascular defects [43], but causes a slight delay in aortic lumen formation, probably due to insufficient recruitment of F-actin to the apical CD34-sialomucins [2]. The mild phenotype could be due to the presence of the other ERM proteins in ECs and/or alternative mechanisms of linking the apical cell surface to the F-actin cytoskeleton [43, 2]. In contrast, model organisms that harbor only a single ERM protein (e.g. *D. melanogaster* or *C. elegans*) display more severe cell polarity and lumen formation defects upon ERM protein deletion [44, 45].

In general, ERM proteins can directly link F-actin to apical transmembrane glycoproteins in their open, phosphorylated conformation. However, in some cases adaptor molecules such as NHERF-1 or -2 (Na^+/H^+ exchanger regulatory factor) are required [46]. Various PKC isoforms have been shown to phosphorylate ERM proteins *in vitro* (Fig. 1b (6)) [47], and PKC inhibition also inhibits moesin phosphorylation in ECs *in vivo* [2]. Among the PKC isoforms expressed in the mouse aorta [2], PKC ζ [19] and θ [48] have been shown to be involved in tube formation and angiogenesis *in vitro*. Thus, a number of proteins are located to both the junctions and the apical cell surface to connect these to the F-actin cytoskeleton.

Lumen formation

Upon establishment of cell polarity and connection of cortical F-actin to the apical cell surfaces, the ECs proceed to form a lumen. Vascular lumen formation in zebrafish ISVs was suggested to occur via fusion of intracellular vesicles within single ECs [22] (Fig. 2a). Moreover, it was proposed that these vesicles arise from pinocytosis and subsequently fuse with other vesicles within the cytoplasm to form large intracellular vacuoles [22]. These exocytose towards adjacent ECs to form vessels that do not have any junction on cross-sections and are therefore called “seamless vessels”.

Recently, ISV lumen formation was reinvestigated and shown to occur extra- rather than intracellularly between several intermingled ECs [39], thus questioning the aforementioned model (Fig. 2a) [22]. In addition, the vacuole coalescence model has been contrasted by other studies investigating the zebrafish aorta, suggesting that the vascular lumen forms between adjacent EC upon junctional rearrangements [49, 50].

Recently, a first molecular mechanism for the formation of a developing blood vessel

was proposed (Fig. 1 and Fig. 2b) [2]. According to this model, vascular endothelial growth factor-A (VEGF-A) induces cell shape changes in polarized ECs to drive extracellular vascular lumen formation. VEGF-A interacts with its receptor VEGFR2 (also known as Kdr or Flk1) to activate Rho-dependent kinases (ROCK-1, ROCK-2 or both). ROCK subsequently increases the phosphorylation of the non-muscle myosin II light chain (MLC), thus driving the recruitment of nm-Myosin II to F-actin (Fig. 2b) [51, 2]. It is likely that force generated by the actomyosin complex as well as F-actin rearrangements trigger subsequent EC shape changes that open up a patent extracellular vascular lumen between the apposing ECs (Fig. 2b) [2]. However, single knockouts of ROCK1 [52] or ROCK2 [53] die during embryonic development, but without striking lumen formation defects, thus indicating functional redundancy for inducing actomyosin formation.

Another recent publication also reports on extracellular lumen formation in small and midsized mouse arteries (Fig. 2c) [15]. It was shown that signaling downstream of β1-integrin is necessary for lumen formation, as β1-integrin deficient arteries have occluded vascular lumens. β1-integrin-deficient mouse embryos showed altered localization of Par3 and VE-cadherin and decreased expression of Par3, indicating that β1-integrin influences the Par3 polarity complex in ECs (see Fig. 1a). Based on *in vitro* work on ECs, VE-cadherin may also interact with the Par3 complex [54]. Arterial ECs in β1-integrin-deficient mice have an increased Rab7 expression, a protein of late endosomes, and accumulate vesicles, thus pointing to an exocytotic defect. This defect was accounted for the missing increase in lumen diameter [15]. However, the failure of lumen formation may also be due to the lack of glycoproteins, such as PODXL, at the apical cell surface in the β1-integrin-deficient ECs.

A novel mechanism of lumen formation has recently been identified in the developing zebrafish cardinal vein (Fig. 2d) [55]. This kind of vessel formation was named „selective sprouting“, as single venous-fated cells migrate out ventrally from the dorsal aorta to surround erythrocytes. The amount of ventral EC migration is downregulated by VEGF-signaling in the arterial cells, involving VEGFR2 and Phospholipase Cγ (PLCγ). In contrast, VEGFR3 (a receptor for VEGF-C) is expressed in venous fated ECs, and increases ventral EC migration, involving the Phosphatidyl-inositole-3-kinase (PI3K) isoform p110α [55, 56]. In addition, VEGF-A might regulate ephrin-B2 to limit ventral EC migration, whereas EphB4 promotes it [55]. At first glance, this model completely deviates from what has previously been shown for blood vessel formation. However, the ECs are likely to polarize to present an apical cell surface towards the erythrocyte-filled lumen.

Thus, both common and distinct kinds of vascular lumen formation exist in different vascular beds. However, it appears as if (i) junctional rearrangements, (ii) establishment of an apicobasal cell polarity and (iii) cytoskeleton-driven cell shape changes are crucial for vascular lumen formation in most situations and cellular contexts.

Conclusions

Remodeling of junctions is a critical step during vascular lumen formation. During development from a vascular cord to a tube, junctions at the cell-cell contact first define the location of lumen formation. These junctions are involved in vesicle delivery to the endothelial cell-cell contact to establish apicobasal cell polarity. In addition, junctions connect to and regulate the F-actin cytoskeleton. Finally, understanding the molecular mechanisms of blood vessel lumenization can help to design therapies for inhibiting blood vessel lumen formation in tumors or for increasing the lumen diameter in collateral arteries during stenosis.

Acknowledgements

We'd like to thank Lara Planas-Paz and Jan Eglinger for critical reading and helpful comments on the manuscript. Our work entitled "Molecular investigation of vascular lumen formation in the developing mouse aorta" is supported by the Deutsche Forschungsgemeinschaft DFG (LA1216/4-1).

Recommended reading:

* of interest:

Tzima et al. [11],

This paper shows that the cell adhesion molecules VE-cadherin and PECAM-1 form a mechanosensory complex in ECs.

Zovein et al. [15]

This paper shows that β1-integrin is required for arterial lumen formation.

Carlson et al. [25], Lei et al. [26], Tanjore et al. [27]

These papers show that β1-integrin is required for vascular patterning.

George et al. [28], Jakobsson et al. [29]

These papers show that the ECM proteins fibronectin and laminin containing LAMC1 are not strictly required for vascular lumen formation.

** of special interest:

Carmeliet et al. [7]

This paper shows that VE-cadherin is required for blood vessel formation.

Blum et al. [39]

This paper questions vacuole coalescence in zebrafish blood vessel formation and suggests extracellular vascular lumen formation.

Parker et al. [49], Jin et al. [50]

These papers show that blood vessels in zebrafish develop via cord hollowing and cellular rearrangements.

Herbert et al. [55]

This paper describes a novel form of blood vessel formation, i.e. selective cell sprouting angiogenesis

1. Adams RH, Alitalo K: **Molecular regulation of angiogenesis and lymphangiogenesis**. *Nat Rev Mol Cell Biol* 2007, **8**:464-478.
2. Strilic B, Kucera T, Eglinger J, Hughes MR, McNagny KM, Tsukita S, Dejana E, Ferrara N, Lammert E: **The molecular basis of vascular lumen formation in the developing mouse aorta**. *Dev Cell* 2009, **17**:505-515.
3. Lampugnani MG, Orsenigo F, Rudini N, Maddaluno L, Boulday G, Chapon F, Dejana E: **CCM1 regulates vascular-lumen organization by inducing endothelial polarity**. *J Cell Sci* **123**:1073-1080.
4. Labelle M, Schnittler HJ, Aust DE, Friedrich K, Baretton G, Vestweber D, Breier G: **Vascular endothelial cadherin promotes breast cancer progression via transforming growth factor beta signaling**. *Cancer Res* 2008, **68**:1388-1397.
5. Cavallaro U, Liebner S, Dejana E: **Endothelial cadherins and tumor angiogenesis**. *Exp Cell Res* 2006, **312**:659-667.
6. Luo Y, Radice GL: **N-cadherin acts upstream of VE-cadherin in controlling vascular morphogenesis**. *J Cell Biol* 2005, **169**:29-34.
7. Carmeliet P, Lampugnani MG, Moons L, Breviario F, Compernolle V, Bono F, Balconi G, Spagnuolo R, Oosthuyse B, Dewerchin M, et al.: **Targeted deficiency or cytosolic truncation of the VE-cadherin gene in mice impairs VEGF-mediated endothelial survival and angiogenesis**. *Cell* 1999, **98**:147-157.
8. Nejsum LN, Nelson WJ: **A molecular mechanism directly linking E-cadherin adhesion to initiation of epithelial cell surface polarity**. *J Cell Biol* 2007, **178**:323-335.
9. Woodfin A, Voisin MB, Nourshargh S: **PECAM-1: a multi-functional molecule in inflammation and vascular biology**. *Arterioscler Thromb Vasc Biol* 2007, **27**:2514-2523.
10. Duncan GS, Andrew DP, Takimoto H, Kaufman SA, Yoshida H, Spellberg J, Luis de la Pompa J, Elia A, Wakeham A, Karan-Tamir B, et al.: **Genetic evidence for functional redundancy of Platelet/Endothelial cell adhesion molecule-1 (PECAM-1): CD31-deficient mice reveal PECAM-1-dependent and PECAM-1-independent functions**. *J Immunol* 1999, **162**:3022-3030.
11. Tzima E, Irani-Tehrani M, Kiosses WB, Dejana E, Schultz DA, Engelhardt B, Cao G, DeLisser H, Schwartz MA: **A mechanosensory complex that mediates the endothelial cell response to fluid shear stress**. *Nature* 2005, **437**:426-431.
12. Ebnet K, Aurrand-Lions M, Kuhn A, Kiefer F, Butz S, Zander K, Meyer zu Brickwedde MK, Suzuki A, Imhof BA, Vestweber D: **The junctional adhesion molecule (JAM) family members JAM-2 and JAM-3 associate with the cell polarity protein PAR-3: a possible role for JAMs in endothelial cell polarity**. *J Cell Sci* 2003, **116**:3879-3891.
13. Cooke VG, Naik MU, Naik UP: **Fibroblast growth factor-2 failed to induce angiogenesis in junctional adhesion molecule-A-deficient mice**. *Arterioscler Thromb Vasc Biol* 2006, **26**:2005-2011.
14. Preiss DJ, Sattar N: **Vascular cell adhesion molecule-1: a viable therapeutic target for atherosclerosis?** *Int J Clin Pract* 2007, **61**:697-701.
15. Zovein AC, Luque A, Turlo KA, Hofmann JJ, Yee KM, Becker MS, Fassler R, Mellman I, Lane TF, Iruela-Arispe ML: **Beta1 integrin establishes endothelial cell polarity and arteriolar lumen formation via a Par3-dependent mechanism**. *Dev Cell* **18**:39-51.
16. Kesavan G, Sand FW, Greiner TU, Johansson JK, Kobberup S, Wu X, Brakebusch C, Semb H: **Cdc42-mediated tubulogenesis controls cell specification**. *Cell* 2009, **139**:791-801.
17. Etienne-Manneville S: **Cdc42--the centre of polarity**. *J Cell Sci* 2004, **117**:1291-1300.
18. Bryant DM, Mostov KE: **From cells to organs: building polarized tissue**. *Nat Rev Mol Cell Biol* 2008, **9**:887-901.
19. Koh W, Mahan RD, Davis GE: **Cdc42- and Rac1-mediated endothelial lumen formation requires Pak2, Pak4 and Par3, and PKC-dependent signaling**. *J Cell Sci* 2008, **121**:989-1001.
20. Feng W, Wu H, Chan LN, Zhang M: **Par-3-mediated junctional localization of the lipid phosphatase PTEN is required for cell polarity establishment**. *J Biol Chem* 2008, **283**:23440-23449.
21. Martin-Belmonte F, Gassama A, Datta A, Yu W, Rescher U, Gerke V, Mostov K: **PTEN-mediated apical segregation of phosphoinositides controls epithelial morphogenesis through Cdc42**. *Cell* 2007, **128**:383-397.
22. Kamei M, Saunders WB, Bayless KJ, Dye L, Davis GE, Weinstein BM: **Endothelial tubes**

assemble from intracellular vacuoles in vivo. *Nature* 2006, **442**:453-456.
23. Suzuki A, Hamada K, Sasaki T, Mak TW, Nakano T: **Role of PTEN/PI3K pathway in endothelial cells**. *Biochem Soc Trans* 2007, **35**:172-176.
24. Drake CJ, Davis LA, Little CD: **Antibodies to beta 1-integrins cause alterations of aortic vasculogenesis, in vivo**. *Dev Dyn* 1992, **193**:83-91.
25. Carlson TR, Hu H, Braren R, Kim YH, Wang RA: **Cell-autonomous requirement for beta1 integrin in endothelial cell adhesion, migration and survival during angiogenesis in mice**. *Development* 2008, **135**:2193-2202.
26. Lei L, Liu D, Huang Y, Jovin I, Shai SY, Kyriakides T, Ross RS, Giordano FJ: **Endothelial expression of beta1 integrin is required for embryonic vascular patterning and postnatal vascular remodeling**. *Mol Cell Biol* 2008, **28**:794-802.
27. Tanjore H, Zeisberg EM, Gerami-Naini B, Kalluri R: **Beta1 integrin expression on endothelial cells is required for angiogenesis but not for vasculogenesis**. *Dev Dyn* 2008, **237**:75-82.
28. George EL, Baldwin HS, Hynes RO: **Fibronectins are essential for heart and blood vessel morphogenesis but are dispensable for initial specification of precursor cells**. *Blood* 1997, **90**:3073-3081.
29. Jakobsson L, Domogatskaya A, Tryggvason K, Edgar D, Claesson-Welsh L: **Laminin deposition is dispensable for vasculogenesis but regulates blood vessel diameter independent of flow**. *FASEB J* 2008, **22**:1530-1539.
30. Ferrari A, Veligodskiy A, Berge U, Lucas MS, Kroschewski R: **ROCK-mediated contractility, tight junctions and channels contribute to the conversion of a preapical patch into apical surface during isochoric lumen initiation**. *J Cell Sci* 2008, **121**:3649-3663.
31. Nielsen JS, McNagny KM: **Novel functions of the CD34 family**. *J Cell Sci* 2008, **121**:3683-3692.
32. Young PE, Baumhueter S, Lasky LA: **The sialomucin CD34 is expressed on hematopoietic cells and blood vessels during murine development**. *Blood* 1995, **85**:96-105.
33. Doyonnas R, Kershaw DB, Duhme C, Merkens H, Chelliah S, Graf T, McNagny KM: **Anuria, omphalocele, and perinatal lethality in mice lacking the CD34-related protein podocalyxin**. *J Exp Med* 2001, **194**:13-27.
34. Takeda T, Go WY, Orlando RA, Farquhar MG: **Expression of podocalyxin inhibits cell-cell adhesion and modifies junctional properties in Madin-Darby canine kidney cells**. *Mol Biol Cell* 2000, **11**:3219-3232.
35. Flessner MF: **Endothelial glycocalyx and the peritoneal barrier**. *Perit Dial Int* 2008, **28**:6-12.
36. Hallmann R, Horn N, Selg M, Wendler O, Pausch F, Sorokin LM: **Expression and function of laminins in the embryonic and mature vasculature**. *Physiol Rev* 2005, **85**:979-1000.
37. Bazzoni G, Dejana E: **Endothelial cell-to-cell junctions: molecular organization and role in vascular homeostasis**. *Physiol Rev* 2004, **84**:869-901.
38. Itoh M, Nagafuchi A, Moroi S, Tsukita S: **Involvement of ZO-1 in cadherin-based cell adhesion through its direct binding to alpha catenin and actin filaments**. *J Cell Biol* 1997, **138**:181-192.
39. Blum Y, Belting HG, Ellertsdottir E, Herwig L, Luders F, Affolter M: **Complex cell rearrangements during intersegmental vessel sprouting and vessel fusion in the zebrafish embryo**. *Dev Biol* 2008, **316**:312-322.
40. Cattelino A, Liebner S, Gallini R, Zanetti A, Balconi G, Corsi A, Bianco P, Wolburg H, Moore R, Oreda B, et al.: **The conditional inactivation of the beta-catenin gene in endothelial cells causes a defective vascular pattern and increased vascular fragility**. *J Cell Biol* 2003, **162**:1111-1122.
41. Anastasiadis PZ, Moon SY, Thoreson MA, Mariner DJ, Crawford HC, Zheng Y, Reynolds AB: **Inhibition of RhoA by p120 catenin**. *Nat Cell Biol* 2000, **2**:637-644.
42. Kleaveland B, Zheng X, Liu JJ, Blum Y, Tung JJ, Zou Z, Sweeney SM, Chen M, Guo L, Lu MM, et al.: **Regulation of cardiovascular development and integrity by the heart of glass-cerebral cavernous malformation protein pathway**. *Nat Med* 2009, **15**:169-176.
43. Doi Y, Itoh M, Yonemura S, Ishihara S, Takano H, Noda T, Tsukita S: **Normal development of mice and unimpaired cell adhesion/cell motility/actin-based cytoskeleton without compensatory up-regulation of ezrin or radixin in moesin gene knockout**. *J Biol Chem* 1999, **274**:2315-2321.
44. Gobel V, Barrett PL, Hall DH, Fleming JT: **Lumen morphogenesis in C. elegans requires the membrane-cytoskeleton linker erm-1**. *Dev Cell* 2004, **6**:865-873.
45. Van Furden D, Johnson K, Segbert C, Bossinger O: **The C. elegans ezrin-radixin-moesin**

protein ERM-1 is necessary for apical junction remodelling and tubulogenesis in the intestine. *Dev Biol* 2004, **272**:262-276.
46. Fehon RG, McClatchey AI, Bretscher A: **Organizing the cell cortex: the role of ERM proteins**. *Nat Rev Mol Cell Biol* **11**:276-287.
47. Koss M, Pfeiffer GR, 2nd, Wang Y, Thomas ST, Yerukhimovich M, Gaarde WA, Doerschuk CM, Wang Q: **Ezrin/radixin/moesin proteins are phosphorylated by TNF-alpha and modulate permeability increases in human pulmonary microvascular endothelial cells**. *J Immunol* 2006, **176**:1218-1227.
48. Tang S, Gao Y, Ware JA: **Enhancement of endothelial cell migration and in vitro tube formation by TAP20, a novel beta 5 integrin-modulating, PKC theta-dependent protein**. *J Cell Biol* 1999, **147**:1073-1084.
49. Parker LH, Schmidt M, Jin SW, Gray AM, Beis D, Pham T, Frantz G, Palmieri S, Hillan K, Stainier DY, et al.: **The endothelial-cell-derived secreted factor Egfl7 regulates vascular tube formation**. *Nature* 2004, **428**:754-758.
50. Jin SW, Beis D, Mitchell T, Chen JN, Stainier DY: **Cellular and molecular analyses of vascular tube and lumen formation in zebrafish**. *Development* 2005, **132**:5199-5209.
51. Sun H, Breslin JW, Zhu J, Yuan SY, Wu MH: **Rho and ROCK signaling in VEGF-induced microvascular endothelial hyperpermeability**. *Microcirculation* 2006, **13**:237-247.
52. Shimizu Y, Thumkeo D, Keel J, Ishizaki T, Oshima H, Oshima M, Noda Y, Matsumura F, Taketo MM, Narumiya S: **ROCK-I regulates closure of the eyelids and ventral body wall by inducing assembly of actomyosin bundles**. *J Cell Biol* 2005, **168**:941-953.
53. Thumkeo D, Keel J, Ishizaki T, Hirose M, Nonomura K, Oshima H, Oshima M, Taketo MM, Narumiya S: **Targeted disruption of the mouse rho-associated kinase 2 gene results in intrauterine growth retardation and fetal death**. *Mol Cell Biol* 2003, **23**:5043-5055.
54. Iden S, Rehder D, August B, Suzuki A, Wolburg-Buchholz K, Wolburg H, Ohno S, Behrens J, Vestweber D, Ebnet K: **A distinct PAR complex associates physically with VE-cadherin in vertebrate endothelial cells**. *EMBO Rep* 2006, **7**:1239-1246.
55. Herbert SP, Huisken J, Kim TN, Feldman ME, Houseman BT, Wang RA, Shokat KM, Stainier DY: **Arterial-venous segregation by selective cell sprouting: an alternative mode of blood vessel formation**. *Science* 2009, **326**:294-298.
56. Graupera M, Guillermet-Guibert J, Foukas LC, Phng LK, Cain RJ, Salpekar A, Pearce W, Meek S, Millan J, Cutillas PR, et al.: **Angiogenesis selectively requires the p110alpha isoform of PI3K to control endothelial cell migration**. *Nature* 2008, **453**:662-666.
57. Dawes-Hoang RE, Parmar KM, Christiansen AE, Phelps CB, Brand AH, Wieschaus EF: **folded gastrulation, cell shape change and the control of myosin localization**. *Development* 2005, **132**:4165-4178.
58. David DJ, Tishkina A, Harris TJ: **The PAR complex regulates pulsed actomyosin contractions during amnioserosa apical constriction in Drosophila**. *Development* **137**:1645-1655.
59. Sawyer JK, Harris NJ, Slep KC, Gaul U, Peifer M: **The Drosophila afadin homologue Canoe regulates linkage of the actin cytoskeleton to adherens junctions during apical constriction**. *J Cell Biol* 2009, **186**:57-73.
60. Lee JY, Harland RM: **Actomyosin contractility and microtubules drive apical constriction in Xenopus bottle cells**. *Dev Biol* 2007, **311**:40-52.
61. Beitel GJ, Krasnow MA: **Genetic control of epithelial tube size in the Drosophila tracheal system**. *Development* 2000, **127**:3271-3282.
62. Gervais L, Casanova J: **In vivo coupling of cell elongation and lumen formation in a single cell**. *Curr Biol* **20**:359-366.
63. Rasmussen JP, English K, Tenlen JR, Priess JR: **Notch signaling and morphogenesis of single-cell tubes in the C. elegans digestive tract**. *Dev Cell* 2008, **14**:559-569.

Box 1

Generic principles of lumen formation in several epithelial and endothelial tubes

- Role of cadherins in cell polarization and lumen formation: [2, 8]
- Exocytosis of CD34-sialomucins at the cell-cell contact: [30]
- Role of ERM proteins in cell polarization and lumen formation: [44, 45]
- Role of Rho kinases and the actomyosin complex in shaping the apical cell surface: [30, 57-60]
- Cdc42 is required for lumen formation: [16, 21]
- Requirement of an apical cell surface for lumen formation: [21, 2, 61]
- Evidence against vacuole coalescence as a mechanism of lumen formation in four different model organisms: [2, 62, 39, 63]

Figure legends:

Fig. 1: Establishing endothelial cell polarity

Schematic sections through an EC cord at an early **(a)** and later stage **(b)** of vascular lumen formation.

(a)(1) In the beginning of lumen formation, ECs express junctional molecules along the entire cell-cell contact. (2) Downstream of β1-integrin or VE-cadherin, PTEN transforms PIP_3 to PIP_2, likely via activation of the Par3 polarity complex and PTEN. (3) This induces the delivery of CD34-sialomucin-containing vesicles to the apical plasma membrane, probably involving Cdc42.

(b)(4) PODXL repels the apical cell surfaces and (5) VE-cadherin gets localized laterally and connects to the F-actin cytoskeleton or to p120 via catenins. (6) When ERM proteins become phosphorylated by PKC (7), these proteins connect PODXL to the F-actin, either directly or via involvement of an additional adaptor protein.

Two ECs without nuclei are depicted due to simplification, even though more ECs can be found on cross-sections through developing vessels.

Fig. 2: Different models of vascular lumen formation

(a) Lumen formation in the zebrafish ISVs was proposed to occur via intracellular fusion of vesicles within a single EC [22]. The resultant vacuoles arise by pinocytosis and colocalize with Cdc42.

(b) Lumen formation in the developing mouse aorta as described by [2]. VEGF-A binds to its receptor VEGFR2, which activates Rho-associated kinase (ROCK). ROCK is required for the phosphorylation of nm-myosin II light chain, which increases the interaction of nm-myosin II with F-actin to form contractile fibres. The actomyosin complex subsequently separates the apical cell surfaces to form an extracellular vascular lumen (*).

(c) Activation of β1-integrin is required for lumen formation in mouse arteries [15]. β1-integrin influences the distribution of VE-cadherin and the distribution and expression of Par3 as well as Rab7. Thus β1-integrin influences cell polarization, lumen formation and vesicular trafficking in arteries.

(d) Selective sprouting during the formation of the zebrafish cardinal vein, as described by [55]. Venous-fated ECs migrate ventrally out of the dorsal aorta (DA) to surround erythrocytes. This EC migration is driven by VEGF-C/VEGFR3-induced signaling via PI3K and expression of EphB4. Cells are retained in the DA by VEGF-A/VEGFR2-induced signaling via PLCγ and expression of ephrin-B2.

Due to simplification, cells are shown without nuclei, and signaling pathways are shown in only one EC.

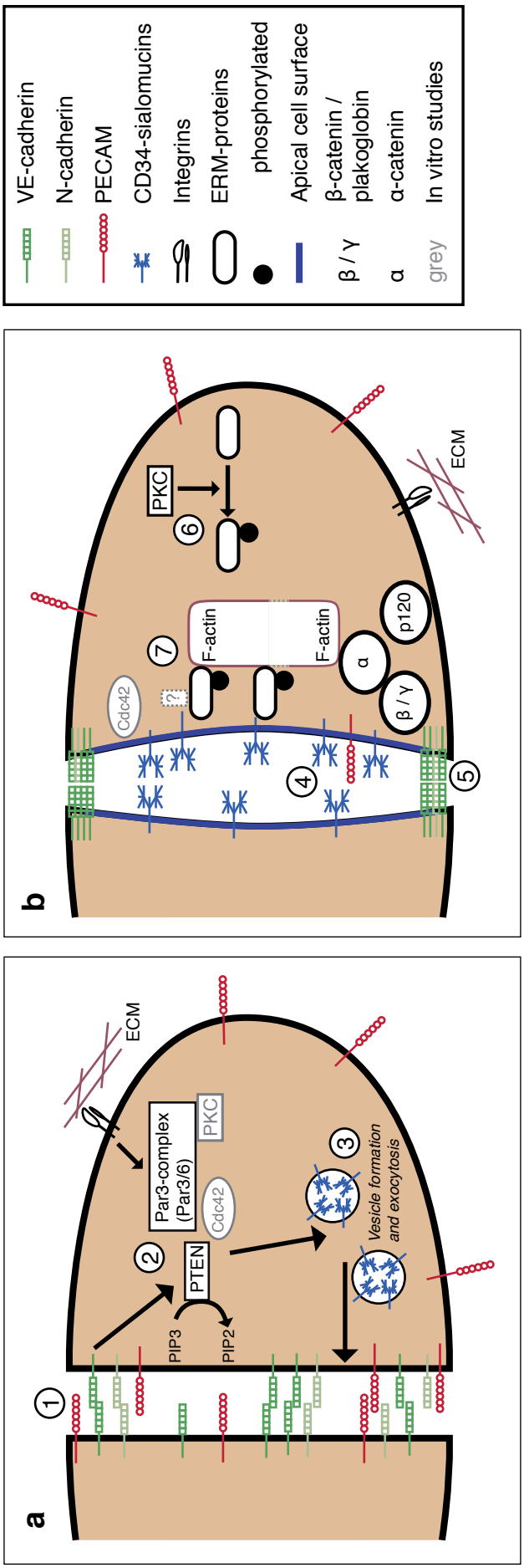

Zeeb et al., Fig. 1

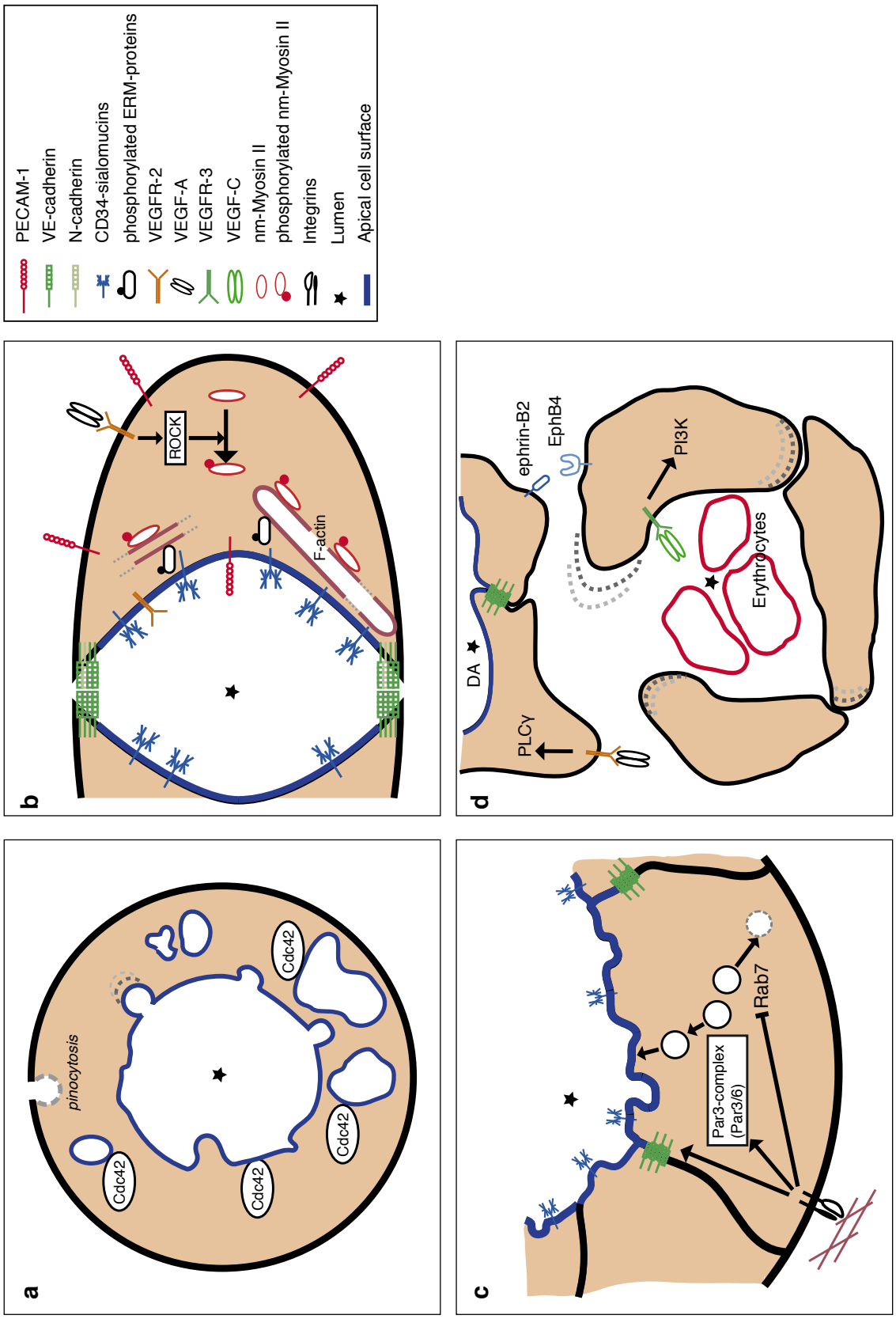

Zeeb et al., Fig. 2

2.1.3 General information and personal contribution

Name of the journal	Current Opinion in Cell Biology
Impact Factor (2011)	12.897
Personal contribution	70 %
Author position	1st author
Tasks	Literature research, manuscript writing and correction, figure preparation
Other	Protocol was commissioned by Current Opinion in Cell Biology

Contribution in detail
For this review article I chose the scope and the contents together with Prof. Eckhard Lammert. I performed the literature research constituting its contents and wrote the first draft, single-handedly. Correction and finalization was conducted in close exchange with Prof. Eckhard Lammert and Dr. Boris Strilic. The figures were prepared by myself, according to the manuscript's contents, with annotations from Prof. Eckhard Lammert.

2.2 Pharmacological manipulation of blood and lymphatic vascularization in ex vivo–cultured mouse embryos

2.2.1 Summary

Formation of new blood and lymphatic vessels is involved in many physiological and pathological processes, including organ and tumor growth, cancer cell metastasis, fluid drainage and lymphedema. Therefore, the ability to manipulate vascularization in a mammalian system is of particular interest. Here, we describe a method for pharmacological manipulation of de novo and sprouting blood and lymphatic vascular development in ex vivo cultured mouse embryos. The described protocol can also be used to evaluate the properties of pharmacological agents in growing mammalian tissues and to manipulate other developmental processes. The whole procedure, from embryo isolation to image quantification, takes 3 to 5 days, depending on the analysis and age of the embryos.

In this article, we present a detailed procedure of our *ex vivo* whole-embryo culture (WEC) of mouse embryos, based on (Strilic et al., 2009) and (Planas-Paz et al., 2011). We significantly improved the protocol to increase staining quality and to reduce running costs. We used WEC to study *de novo* and sprouting blood and lymphatic vessel development, but the protocol can be applied to all other developmental processes in the given time frame.

WEC of mouse embryos is especially well suited to study and manipulate developmental processes and to test pharmacological target substances. In general, mouse embryos are more readily accessible and cheaper than adult mice and provide simpler physiological systems to study. Pharmacological inhibition can easily be compared to or combined with a multitude of genetic approaches.
Investigation of mice is of great interest for the initial testing and development of pharmacological substances due to the close genetic relationship with humans.
In vascular biology, investigations in mice are a very good addition to zebrafish studies in light of striking differences in aorta formation, initial sprouting events, or hematopoiesis.

Our system of whole-embryo culture offers multiple advantages compared to similar or related cultivation methods.
First, targeted injection of substances results in locally restricted effects, allows the use of internal controls, and requires only minimal amounts of substance, avoiding systemic effects and high costs.
Opposite to previous conditions, our culture medium is free of rat serum and thus, rat antibodies can be used, which greatly improves staining quality. Our new cultivation media are easy to obtain and up to 90 % cheaper than commercial rat serum. Survival rates in our new media are high, even over a prolonged time, permitting longer incubation times and thus enabling the analysis of slower developmental processes. Starting with E8.0 to E9.0 embryos, culture of up to 24 hours is possible, with survival rates after 12 hours still exceeding 83 % in all conditions.

The protocol lists all required material and chemicals in detail allowing even beginners to use the method effectively. The main part of the manuscript consists of a numbered list of working steps, serving as an instruction book for the isolation, preparation, injection, and culture of mouse embryos and their subsequent analysis. Additionally, four videos showing the isolation and injection procedure are also included to visualize the most important steps, increasing understanding and usability of our protocol in the field.

We have used the method to study vessel development, to effectively inhibit *de novo* and sprouting blood and lymphatic vessel formation using a small molecule inhibitor and an inhibiting antibody, respectively.
Using our improved method, we were able to perform high-quality whole-embryo staining and imaging to visualize intersomitic vessels in the mouse using a simple confocal microscope, an approach that previously required the use of sophisticated imaging techniques.

In summary, this protocol gives a detailed description to perform *ex vivo* whole-embryo culture useful for beginners and advanced researchers alike, thus promoting, improving, and facilitating the use of mice as a model organism for the study of vascular development and beyond.

2.2.2 Accepted protocol

See pages 38 ff.

Keywords: Pharmacology; Blood vessel; Lymphatic vessel; Vasculature; Development; Whole embryo culture.

Pharmacological manipulation of blood and lymphatic vascularization in *ex vivo* cultured mouse embryos

Martin Zeeb[1,*], Jennifer Axnick[1,*], Lara Planas-Paz[1], Thorsten Hartmann[1], Boris Strilic[2], Eckhard Lammert[1,3]

Author affiliations:

1: Institute of Metabolic Physiology, Heinrich-Heine University Duesseldorf, Germany

2: Department of Pharmacology, Max Planck Institute for Heart and Lung Research, W.G. Kerckhoff-Institute, D-61231 Bad Nauheim, Germany

3: German Diabetes Center (DDZ), Paul-Langerhans-Group for Beta Cell Biology, 40225 Duesseldorf, Germany

* the authors contributed equally to this work

Corresponding author: Eckhard Lammert, lammert@hhu.de

Summary

Formation of new blood and lymphatic vessels is involved in many physiological and pathological processes, including organ and tumor growth, cancer cell metastasis, fluid drainage and lymphedema. Therefore, the ability to manipulate vascularization in a mammalian system is of particular interest. Here, we describe a method for pharmacological manipulation of *de novo* and sprouting blood and lymphatic vascular development in *ex vivo* cultured mouse embryos. The described protocol can also be used to evaluate the properties of pharmacological agents in growing mammalian tissues and to manipulate other developmental processes. The whole procedure, from embryo isolation to image quantification, takes 3 to 5 days, depending on the analysis and age of the embryos.

Introduction

Analyses of defects in gene-deficient mouse embryos have led to the discovery of novel drug targets for the treatment of human diseases in which blood and lymphatic vessels are altered, including, but not limited to, VEGF-A[1,2] (vascular endothelial growth factor-A), Dll4[3] (Delta like ligand 4), and PDGF-B[4,5] (platelet derived growth factor-B). Therefore, pharmacological interference in the embryonic blood and lymphatic vasculature could complement genetic mouse models and could potentially be used to screen or investigate target substances for treatments.

Mouse embryos provide an advantageous system, as they present well-defined vascular systems, are inexpensive, and are more rapidly accessible than adult mice. In addition, pharmacological treatment of mouse embryos can be compared to genetic models, thus making them a good starting point for evaluating medicinal compounds or proteins. Here, we describe a method to investigate and manipulate *de novo* and sprouting blood and lymphatic vascular development in mouse embryos cultured *ex vivo* in whole embryo culture (WEC). This method was used to investigate and manipulate mouse blood and lymphatic vascular development and has led to new models and paradigms in vessel formation[6-13]. The protocol described here is suitable for E8.0, E8.75, E11.5, and E15.5 mouse embryos, thus covering different modes of blood and lymphatic vascular development, i.e. vasculogenesis[6,14,15], sprouting angiogenesis[16], *de novo* lymphatic vessel formation[13,17-19], and lymphatic sprouting angiogenesis[20-22].

Applications of the protocol

When cultured for 12 and 6 h (hours), respectively, E8.0 mouse embryos at the 1-2 somite stage (1-2 S) develop two dorsal aortae via vasculogenesis, which undergo lumenization between the 2 and 6 S stage, and E8.75 mouse embryos at the 12-13 S stage develop several intersomitic vessels (ISVs). Moreover, E11.5 embryos develop jugular lymph sacs (JLS) *de novo* when cultured for ~5 h, and E15.5 mouse embryos display lymphatic vessel sprouting in the dermis, which can be altered by experimental manipulation during a 0.5 h incubation.

Using a microinjector, pharmacological agents, including small molecules, antibodies, or Fc fusion proteins, can be injected into the embryos at each of these stages to modify both *de novo* formation and the sprouting of blood as well as lymphatic vessels[23]. Apart from the given examples, our protocol could also be applied to other aspects of vessel formation, such as the investigation of blood vessel maturation, which involves recruitment of vascular

smooth muscle cells and pericytes to developing blood vessels from E9.5 onwards[5,24], some aspects of lymphatic vessel maturation[21,25,26], or the generation of hematopoietic stem cells from vascular endothelium[27]. The protocol described here can also be adapted to manipulate and investigate developmental processes in other organs for which WEC has been previously used, e.g. heart[28,29], pancreas[30], liver[30 31], ear[32], or the central nervous system[33-35].

Comparison with previous protocols

The protocol described here uses gas compositions for WEC that were previously described for the culture of different embryonic stages[36]. In the past, WEC protocols primarily used rat serum for the cultivation of mouse embryos[6,7,9-13,27-32,36-39]. Consequently, the cultured embryos were soaked with rat antigens, and the rat anti-PECAM-1 (Platelet endothelial cell adhesion molecule-1, CD31) antibody (clone M13.3), the most frequently used antibody for blood vessel staining[3,6-9,11,13,14,17,18,25-27,40-44], could not be used successfully. In particular, the strong background staining rendered specific staining of endothelial cells virtually impossible (see for example Fig. 5 in [6]). The protocol described here circumvents this issue by using two different culture media: M16, a defined, serum-free medium based on a modified Krebs-Ringer solution, for the culture of E8.0 and E8.75 embryos (previously unpublished), and DMEM/FBS (80/20, Dulbecco's modified eagle medium/fetal bovine serum) for culture of E11.5 and E15.5 mouse embryos[13]. The use of M16 and DMEM/FBS as culture media allows PECAM-1 staining of sections and embryos following WEC, facilitating immunohistochemical analyses of vascular development if reporter lines are not available. In addition, the media used here reduce costs by as much as 90% compared to commercial rat serum, which is expensive or tedious to produce[45].The viability of embryos cultured in these media is sufficient for studying various aspects of blood and lymphatic vascular development (**Table 1**)**.** However, viability declines during long-term WEC (**Supplementary Table 1**), and therefore, rat serum might be necessary to culture embryos for longer than 24 h.

Advantages and limitations of this protocol

The development of blood and lymphatic vessels in mice is similar to the situation in humans (in particular the stages analyzed in this protocol). For example, humans and mice initially form two lateral dorsal aortae, which are connected to a 4-chambered heart[42], and the lymphatic vasculature develops from jugular lymph sacs, which derive mainly from the anterior cardinal veins[46]. Moreover, as mouse embryos deficient for drug targets such as VEGF-A[1,2] or Dll4[3] are available, the effects of pharmacological inhibition of these or other

targets in WEC can be compared to the effects of gene ablation to evaluate the specificity and selectivity of the pharmacological agents.

It is noteworthy that not all mechanisms of vascular development observed in mouse embryos apply to vascular development in adult mice and human pathologies (e.g.[47]). However, most vascular events are similar or even identical, as indicated by SU 5416 and VEGFR3-Fc that inhibit vascular development in mouse embryos as well as in tumors and developing metastases[48-50]

In contrast to mouse embryos, zebrafish embryos can be used in high-throughput screens, as embryos are available at a lower price and in higher quantity. However, several differences exist in blood and lymphatic vascular development between zebrafish and mice/humans. For example, in contrast to mice and humans, the zebrafish only contains a two- rather than four-chambered heart[42,51], a single aorta over most of the anterior-posterior axis, rather than two dorsal aortae[52,53], and hematopoiesis in zebrafish takes place in the kidney rather than in liver and bone marrow[54]. Therefore, mice are the model system of choice for preclinical studies, and pharmacologic manipulation of mouse embryos serves as a reasonable addition to high-throughput screens in zebrafish embryos.

In the current protocol, approximately 20 E8.0 mouse embryos and approximately 60 E11.5 mouse embryos can be manipulated by a single operator in one sitting. To facilitate the learning of embryo isolation and injection, four supplementary movies are provided (**Supplementary Videos 1-4**).

Finally, since the expenses for a micromanipulator, injector and WEC incubator do not exceed the costs for other common laboratory devices, such as a real-time PCR machine, this method can be set up in most laboratories.

Experimental design

WEC can be used on a variety of different mouse strains. Here, we use CD1 and C57BL/6J mice to show that different strains (out- and inbred) can be manipulated and cultured. CD1 mice are preferentially used because they give rise to 10-20 embryos per litter. In contrast, C57BL/6J mice give rise to fewer embryos, but can be better compared to gene-deficient C57BL/6J embryos. Finally, microinjection and WEC can also be performed on gene-deficient embryos, thus allowing the researcher to combine genetics with pharmacology[6,13]. For demonstration purposes, we use the VEGFR2 (VEGF receptor 2, also known as Flk1) receptor inhibitor SU 5416 as a small molecule that blocks both vasculogenesis[6] and angiogenesis[55], and VEGFR3-Fc as a protein agent that blocks lymphatic development[13,43,56]. We use different gas mixtures depending on the stage of the embryos to be cultured[36], and keep rotational speed continuously at 25 rpm for all stages. To illustrate the possibility to analyze different modes of blood and lymphatic vessel formation following manipulation of the embryos, we deliberately chose to immunostain sections of E8.0 and E11.5 embryos and whole-mount stain E8.75 embryos and E15.5 skin (for skin isolation, see **Supplementary Fig. S1**). However, all analyzed stages can be subjected to immunostaining of sections and whole-mount staining. Use of reporter lines, where available, can replace staining. For staining against PECAM-1, Lyve-1 (lymphatic vessel endothelial hyaluronan receptor-1), and the other markers utilized in this protocol, we fix embryos in 4% PFA (paraformaldehyde) after WEC; however, depending on the antibody that will be used for staining, alternative fixatives can be applied. An overview of the procedure for each of the four embryonic stages manipulated and analyzed is shown in **Fig. 1**.

Materials

Reagents

Mouse lines

- Pregnant CD1 mice (Janvier) at 8.0 or 8.75 days *post coitum* (E8.0 and E8.75)
- Pregnant C57BL/6J (Janvier) at 11.5 or 15.5 days *post coitum* (E11.5 and E15.5)

!CAUTION All animal experiments must be performed in accordance with the guidelines on the use of animals by the relevant authorities.

Embryo isolation

- Isoflurane (actavis), as inhalation anesthetics

!CAUTION harmful on inhalation! Use adequate ventilation (hood).

- PBS^{+} (PBS^{+} (Phosphate Buffered Saline with Mg^{2+} and Ca^{2+}), at 37°C

  We prepare PBS^{+} as described in reagent setup. All required chemicals are obtained from Carl Roth or Merck.

▲CRITICAL Embryos must be kept at 37°C during isolation, treatment and culture!

Treatment of mouse embryos

- Phenol Red powder (Sigma Aldrich, P3532)
- SU 5416 (Sigma Aldrich, S8442)
- DMSO (Dimethyl sulfoxide, Sigma Aldrich, D2650)
- VEGFR3-Fc (vascular endothelial growth factor receptor 3-Fc, Sigma Aldrich, V6633)
- Fast Green FCF C.I. 42053 (AppliChem, A1401)
- VEGF-C (vascular endothelial growth factor-C, R&D Systems, 2179-VC-025)
- Albumin Fraction V (bovine serum albumin, AppliChem, A1391)
- Ice, for storing injection reagents

Whole-embryo culture

For E8.0 and E8.75

- M16 medium (Sigma Aldrich, M7292), supplemented with HEPES
- HEPES buffer 1 M (mol/liter; GIBCO, Invitrogen, 15630)

  For use, dilute in M16 to 1% (v/v) final concentration.
- Gas mixture: 5% CO_2, 5% O_2, 90% N_2 (Air Liquide)

!CAUTION Gas mixture is stored in a pressurized container and must be kept in a safety cabinet.

For E11.5 and E15.5

- DMEM (Dulbecco's modified eagle medium, GIBCO, Invitrogen, 31885)
- FBS Mycoplex (fetal bovine serum, PAA, A15-105)
- Gas mixture: 5% CO_2, 95% O_2 (Air Liquide)

!CAUTION Gas mixture is stored in a pressurized container and must be kept in a safety cabinet.

Sectioning and Staining

- PFA (Paraformaldehyde, Sigma Aldrich, P6148), 4% in PBS
- Sucrose (Roth, 4661.1), 15% and 30% in H_2O
- Tissue-Tek O.C.T. Compound embedding medium (Sakura Finetek, #4583)
- Blocking solution (0.2% Triton X-100, 5% Normal Donkey Serum, 1% BSA (Bovine Serum Albumin) in PBS^+)
- Triton X-100, BioXtra (Sigma Aldrich, T9284), for blocking solution
- Normal donkey serum (Jackson Immuno Research, 017-000-001), for blocking solution
- Rat anti mouse PECAM-1 antibody (CD31, BD Bioscience, 550274), primary antibody to stain endothelial cells
- Goat anti mouse PODXL (Podocalyxin or gp135, R&D Systems, MAB1556), primary antibody to label apical cell surfaces of epithelial and endothelial cells (ECs)
- Goat anti Lyve-1 antibody (R&D Systems, AF2125), primary antibody to stain lymphatic endothelial cells (LECs)
- Rabbit anti mouse pH3 (phospho-Histone H3, Millipore, 06-570), primary antibody to stain proliferating cells
- Donkey anti rat IgG coupled to Alexa Fluor488 (Molecular Probes, Invitrogen, A-21208), secondary antibody
- Donkey anti goat IgG coupled to Cy3 (Jackson ImmunoResearch, 705-166-147), secondary antibody
- Donkey anti rabbit IgG coupled to Cy3 (Jackson ImmunoResearch, 705-166-152), secondary antibody
- DAPI (Sigma Aldrich, D9542)
- Mowiol 4-88 Reagent (Calbiochem, #475904)
- Nail polish

Imaging

- Agarose VII (Sigma Aldrich, A9414)

Equipment

Embryo isolation and skin isolation

- Water bath (at 37°C)
- Forceps, Dumont #55 (Fine Science Tools, 11255-20)
- Surgical scissors (Fine Science Tools, 14001-12)
- Vannas spring scissors (Fine Science Tools, 91500-09)
- Uncoated Petri dishes (e.g. VWR, 391-0880), 90 mm (milli-meter) diameter
- Stereomicroscope (e.g. Nikon SMZ1500)

Treatment of mouse embryos

- Reaction/ Microcentrifuge tubes (e.g. Brand or Eppendorf), 0.3 to 2 ml (milli-liter))
- Micropipettes (e.g. Gilson PipetMan or Eppendorf Reference)
- Ultrafine tips (e.g. Eppendorf, 5242 956.003)
- Borosilicate glass capillaries (GC100F-15, Harvard Apparatus, #30-0020) to pull needles

▲CRITICAL The capillaries should contain filaments. As the needles are backfilled with the injection solution, the filament aids the transport of the solution to the tip of the needle.

- Needle puller (e.g. Type PE-2, Narishige)
- Microinjector PV820 Pneumatic PicoPump (World Precision Instruments)
- Micromanipulator (World Precision Instruments, M3301R)

Whole embryo culture

- Plastic Pasteur pipettes (5 ml or more, e.g. VWR, 612-4494)
- Perforated Spoon (Fine Science Tools, #10370-18)
- Culture glass bottles for WEC (RKI Ikemoto)
- Rotatory WEC incubator (RKI Ikemoto scientific technology, Japan, No 10-0311)

Sectioning

- Embedding molds, Cryomold Intermediate (Sakura TissueTek, #4566), 10 x 10 x 5 mm
- Embedding molds, Peel-A-Way (T-12) truncated (Polyscience Inc., #18986), 22 mm square top tapered to 12 mm bottom
- Cryotome (e.g. Microm HM 560, Thermo Scientific)
- C35 carbon steel blades (Feather Safety Razor Co. LTD., e.g. pfm medical ag, #207500003), for E8.0 and E8.75 mouse embryos
- MX35 Premier, Microtome blade (Thermo Scientific, #3052835), for E11.5 and E15.5 mouse embryos
- Razor blades (e.g. Apollo)
- Superfrost® plus glass slides (Thermo Scientific, 4951PLUS)

Staining

- Washing box
- Staining box (humidified chamber)
- Covering foil (Parafilm M, Bemis)
- Fridge / cold room (4-8°C)
- Cover glass (Roth, H878), 24 x 60 mm, #1

Imaging

- Glass bottom culture dishes (MatTek, P35G-0-14-C), uncoated, 35 mm diameter, 14 mm microwell, No. 0 coverglass
- Confocal microscope, e.g LSM 710 (Zeiss) with image acquisition software, e.g. Zen (Zeiss)

Statistical Analysis

- Image processing software, e.g. Image J[57]
- Statistics software, e.g. Excel (Microsoft)

Reagent setup

PBS$^+$ preparation

To prepare 1 l of PBS with Mg^{2+} and Ca^{2+} (called PBS$^+$), add 0.2 g (gram) of KCl (5.4 mM), 0.2 g of KH_2PO_4 (3 mM), 1.15 g Na_2HPO_4 (1.3 mM), 8 g NaCl (0.27 M), 0.2 g $MgCl_2 \cdot 6\ H_2O$ (5 mM), and 0.264 g $CaCl_2 \cdot 2\ H_2O$ (9 mM) to 1 l of water. Stir well and autoclave. Can be stored at room temperature (16-26 degree Celsius) for several months.

SU 5416 solution

Dissolve SU 5416 in DMSO to 21 mM. Dilute in PBS$^+$ to 2.1 mM. Can be stored at -20°C for several months.

Phenol Red solution

Dissolve Phenol Red in PBS$^+$ (2% w/v). Can be stored at -20°C for years.

Fast Green solution

Dissolve Fast Green powder to 1% (w/v) in PBS$^+$. Can be stored at -20°C for years.

VEGFR3-Fc solution

Dilute VEGFR3-Fc to 100 µg/ml in PBS$^+$. Can be stored at -20°C for several months.

Control-Fc solution

Dilute Control-Fc to 100 µg/ml in PBS$^+$. Can be stored at -20°C for several months.

VEGF-C solution

Dissolve VEGF-C in PBS$^+$ with 0.1% BSA to 10 µg/ml. Can be stored at -20°C for several months. Dilute 1:10 in PBS$^+$ (to 1 µg/ml).

E8.0 and E8.75 injection solutions: VEGFR2-blocking solution

To prepare 5 µl injection solution, mix 0.6 µl SU 5416 solution (final conc. 250 µM) with 0.5 µl Phenol Red solution (final conc. 0.2% w/v) and fill to 5 µl with PBS$^+$. CRITICAL Must be prepared fresh.

E8.0 and E8.75 injection solutions: Ctrl solution

First dilute 0.5 µl of DMSO in 4.5 µl of PBS$^+$. To prepare 5 µl injection solution, add 0.5 µl Phenol Red solution (final conc. 0.2% w/v) to 0.5 µl of diluted DMSO and fill to 5 µl with PBS$^+$. CRITICAL Must be prepared fresh.

E11.5 injection solutions: VEGFR3-blocking solution

To prepare 10 µl injection solution, mix 1 µl Fast Green solution (final conc. 0.1%) with 1 µl VEGFR3-Fc solution (final conc. 10 µg/ml) and fill to 10 µl with PBS$^+$. CRITICAL Must be prepared fresh.

E11.5 injection solutions: Control-Fc solution

To prepare 10 µl injection solution, mix 1 µl Fast Green solution (final conc. 0.1%) with 1 µl Ctrl-Fc solution (final conc. 10 µg/ml) and fill to 10 µl with PBS^+. CRITICAL Must be prepared fresh.

E15.5 injection solutions: VEGFR3-blocking solution with VEGF-C

To prepare 10 µl injection solution, mix 1 µl Fast Green solution (final conc. 0.1%) with 1 µl VEGFR3-Fc solution (final conc. 10 µg/ml) and 1 µl VEGF-C solution (final conc. 100 ng/ml) and fill to 10 µl with PBS^+. CRITICAL Must be prepared fresh.

E15.5 injection solutions: Control-Fc solution with VEGF-C:

To prepare 10 µl injection solution, mix 1 µl Fast Green solution (final conc. 0.1%) with 1 µl VEGF-C solution (final conc. 100 ng/ml), 1 µl Ctrl-Fc solution (final conc. 10 µg/ml) and fill to 10 µl with PBS^+. CRITICAL Must be prepared fresh.

M16-based WEC medium (E8.0 and E8.75 embryos)

In a single WEC bottle, mix 2970 µl warm (37°C) M16 with 30 µl warm HEPES (final conc. 1% v/v) and equilibrate the bottle to 37°C and 5% CO_2 / 5% O_2 / 80% N_2 in the WEC incubator. CRITICAL Medium must be prepared fresh.

DMEM-based WEC medium (E11.5 and E15.5 embryos)

In a single WEC bottle, mix 1600 µl warm (37°C) DMEM with 400 µl warm FBS (final conc. 20% v/v), and equilibrate the bottle to 37°C and 5% CO_2 / 95% O_2 in the WEC incubator. CRITICAL Medium must be prepared fresh.

Blocking solution for whole embryo staining and staining of sections

The blocking solution is used for blocking and to dilute primary and secondary antibodies. 1 ml blocking solution is sufficient for 10-12 whole embryos or 3 slides. Make up 5 ml blocking solution by combining 0.05 g BSA, 250 µl NDS, 25 µl Triton X-100 and 4725 µl PBS^+. CRITICAL Blocking solution must be prepared fresh.

DAPI solution

Dissolve DAPI powder in H_2O to 1 mg/ml. Can be stored at -20°C for several months.

Primary antibody solution for staining of E8.0 sections for ECs (PECAM-1) and apical EC surfaces (PODXL)

Dilute 20 µl rat anti mouse PECAM-1 and 20 µl goat α mouse PODXL in 1 ml blocking solution (to 1:50, each). CRITICAL Prepare fresh.

Secondary antibody solution for staining of E8.0 sections for ECs (PECAM-1) and apical EC surfaces (PODXL)

Dilute 2 µl donkey anti rat IgG-Alexa Fluor 488, 2 µl donkey α goat IgG-Cy3, and 1 µl DAPI solution in 1 ml blocking solution. CRITICAL Prepare fresh.

Primary antibody solution for staining of E8.0 and E8.75 whole mounts for ECs (PECAM-1)

Add 20 µl rat anti mouse PECAM-1 antibody to 1 ml blocking solution (to 1:50). CRITICAL Prepare fresh.

Secondary antibody solution for staining of E8.0 and E8.75 whole mounts for ECs (PECAM-1)

Add 2 µl donkey anti rat IgG Alexa Fluor 488 to 1 ml blocking solution (1:500). CRITICAL Prepare fresh.

Primary antibody solution for staining of E11.5 sections for ECs (PECAM-1) and LECs (Lyve-1)

Dilute 10 µl goat anti mouse Lyve-1 and 20 µl rat α mouse PECAM-1 antibody in 1 ml blocking solution. CRITICAL Prepare fresh.

Secondary antibody solution for staining of E11.5 sections for ECs (PECAM-1) and LECs (Lyve-1)

Dilute 2 µl donkey anti rat IgG-Alexa Fluor 488, 2 µl donkey α goat IgG-Cy3, and 1 µl DAPI in 1 ml blocking solution. CRITICAL Prepare fresh.

Primary antibody solution for staining of E15.5 sections for LECs (Lyve-1) and proliferating cells (phospho-Histone H3)

Dilute 20 µl goat anti mouse Lyve-1 and 20 µl rabbit α mouse phospho-Histone H3 (pH3) in 1 ml blocking solution. CRITICAL Prepare fresh.

Secondary antibody solution for staining of E15.5 sections for LECs (Lyve-1) and proliferating cells (phospho-Histone H3)

Add 2 µl donkey anti goat IgG Alexa Fluor 488 and 2 µl donkey α rabbit IgG-Cy3 to 1 ml blocking solution. CRITICAL Prepare fresh.

Preparation and storage of agarose VII solution

To prepare 1% agarose solution for embedding of whole mount stained embryos, dissolve 10 mg agarose VII in 1 ml PBS^{+}. To dissolve, heat solution to 95°C. During use, keep at 37°C in water bath. Can be stored at 4°C in solid state for several weeks. 1 ml is sufficient for ~ 50 embryos.

Equipment setup

Glass capillaries

Prepare injection needles from glass capillaries with filaments. Insert capillaries in a vertical needle puller, type PE-2 (Narishige, Japan) and pull. Set heat to 7.5 and Magnet to 10. The shanks of the resulting needle (**Fig. 2 a**) should be thin and broaden only late (40 μm outside diameter after 5 mm, 95 μm outside diameter after 1 cm), so that one can break the tip of the needle several times and still be able to use it for injections. The total length of the needle should be 9.5 cm, sufficient to reach the specimen when injecting. Only one side of the capillary is used as an injection needle. Once pulled, the tip of the needle must be broken right before filling the needle under the microscope. To open and fill the needle, first, carefully break the tip. Avoid serration or disruption of the tip as this can damage embryonic tissues. After opening, the outside diameter should be ≤ 45 μm and the inside diameter ≤ 30 μm. The younger the embryo, the thinner the suggested tip. Transfer 3 μl injection solution into the backside of the needle using a micropipette with an ultrafine tip. Hold the needle upright and allow the solution to "sink" to the tip. Connect the needle to the microinjector.

Injection system / Injection apparatus

Connect the microinjector (PV820 Pneumatic PicoPump by World Precision Instruments to a pressurized air pipe (**Fig. 2, b, c**). Perform injection at a pressure of 8 psi.

WEC system

The WEC incubator (Ikemoto, contact: Mr. T. Sadatomi, TEL: 03-3811-4181, FAX: 03-3814-1360, email: ikemoto@ikemoto.co.jp, URL: http://www.ikemoto.co.jp, address: Ikemoto scientific technology co., LTD., 25-11, Hongo 3-chome, Bunkyo-ku, Tokyo 113-0033, Japan) is a roller culture system specifically designed for the cultivation of rodent embryos (**Fig. 2, d, e**). The incubator is 57x65x77 cm and is equipped with two airtight doors to maintain a constant temperature. Embryos are cultured in sterile, rotating glass bottles aerated with a CO_2 / O_2 mixture that is set according to the embryonic stage[36] and filtered through a gas-washing bottle with H_2O through a sterile rubber plug (see **Table 2**). Heat the incubator to 37°C and, when inserting bottles, open the incubator for a minimal amount of time to avoid temperature changes. Rotate the bottles at 25 rotations per minute (rpm). Temperature, rotation and aeration are supposed to mimic the conditions *in utero*.

Procedure

Preparation of WEC and injection ● TIMING 6 h (0.5 h effective working time)

1 Preheat incubator to 37°C at least 6 h before starting the experiment.

2 Prepare tools and equipment to avoid any delay after killing the mouse (forceps, scissors, microscope, microinjector, needles, Petri dishes, plastic Pasteur pipettes).

■**PAUSE POINT** Preparing equipment the day before and leaving them overnight is possible.

3 Warm up reagents to 37°C in a water bath. For steps 9-14, PBS^+ is always used at 37°C. For E8.0 and E8.75 embryos the required reagents are PBS^+, M16, and HEPES buffer (for E8). For E11.5 and E15.5 embryos the required reagents are PBS^+, DMEM and FBS.

4 Turn on the gas and set the flow of the incubator using the appropriate setting as detailed in **Table 2**. Start the motor (25 rpm). Prepare medium (see REAGENT SETUP) in a culture bottle. 3 ml M16/HEPES medium per bottle is sufficient for 5 E8.0 or E8.75 embryos. 2 ml DMEM/FBS medium per bottle is sufficient for 1-2 E11.5 or E15.5 embryos. Equilibrate the medium by incubating in the incubator for 30 min.

5 Prepare the injection solutions (see REAGENT SETUP) and place at 4°C or on ice. Prepare 5 µl solution for 10-20 injections.

6 Prepare a needle and backfill it with 3 µl injection solution, as described in EQUIPMENT SETUP. Fix needle to micromanipulator and injector and test ejection (in PBS^+).

Dissection of the uterus ● TIMING 10 min

7 Anesthetize the mouse. To do so, pipet 1 ml isoflurane on wadding in a small exsiccator. Anesthetize the mouse by incubation in the exsiccator for approx. one minute, until the mouse no longer shows a tail-pinch reflex. 1 ml of isoflurane is sufficient for anesthetizing at least 3 mice one after the other using the same exsiccator.

!CAUTION Isoflurane is harmful on inhalation! Use adequate ventilation (fume hood).

8 Sacrifice the mother mouse by cervical dislocation.

9 Dissect the uterus by cutting a V shape into the abdominal skin and membrane. Pull the uterus out of the body cavity with tweezers and cut off the birth canal, fatty tissue and both oviducts. Immediately transfer the uterus into warm PBS^+.

▲**CRITICAL STEP** Keep embryos at 37°C, until step 19.

Isolation of Embryos • **TIMING ~5 min/embryo, 1-2 h/per mouse, depending on strain**

10 Transfer the uterus into a Petri dish with PBS^+ and carefully cut the uterus into pieces containing single embryos (see **Supplementary video 1**).

11 Transfer a uterus segment containing one single embryo to another Petri dish with PBS^+ for isolation. If desired, the remaining uterus segments of E8.0 and E8.75 embryos or whole uteri (if more than one mouse is dissected) can be stored in warm PBS^+ (in a Petri dish or falcon tube in a water bath) for a maximum of 3 h. If desired the remaining uterus segments of E11.5 and E15.5 embryos can be stored for a maximum of 20 min.

12 Isolate the embryo under a stereomicroscope. Follow option A for E8.0 and E8.75 embryos and option B for E11.5 and E15.5 embryos. CRITICAL Perform this and steps 13-14 with the embryos submerged in PBS^+ to prevent the surface tension from rupturing the embryo or entire yolk sac.

▲**CRITICAL STEP** This step must be carried out as quickly as possible to avoid embryonic hypothermia.

(A) E8.0 and E8.75 embryos.

(i) Carefully remove the surrounding uterus.

(ii) Use forceps to peel away the uterus layers. This can be done by grabbing at the opening created by the incision in step 10.

(iii) Carefully remove the decidua with forceps by a horizontal cut at the top.

(iv) Separate the embryo and the ectoplacental cone from the decidua. Carefully remove the sticky Reichert's membrane (see **Supplementary videos 1 and 2**, respectively) with forceps and avoid damage to the embryo.

▲**CRITICAL STEP** For E8.0 embryos, do not cut off the ectoplacental cone.

▲**CRITICAL STEP** Avoid ruptures and large holes in the yolk sac.

(v) Stage the embryo by counting its somites.

?TROUBLESHOOTING

(B) E11.5 and E15.5 embryos

(i) Carefully remove the surrounding uterus.

(ii) Isolate the embryo, but leave the yolk sac, decidua and placenta connected. Remove the amnion. See **Supplementary videos 3** and **4** for further guidance.

Microinjection ● TIMING 5 min/embryo

13 Orient and fix the embryo for injection (see **Supplementary videos 1-4**). For E8.0 embryos, use the ectoplacental cone to grab the embryo with forceps. Orient the embryo with head up and the tail down (frontal view) with the upper surface parallel to the dish surface. For E8.75 embryos, use the yolk sac to grab the embryo close to the injection site. Place the embryo in side view (**Fig. 2 g**). Place E11.5 or E15.5 embryos in a single, separate drop of PBS^{+} to prevent the embryo from floating away during injection. Place the embryo in side view (**Fig. 2 h, i**).

14 Inject embryos with Ctrl solution or blocking solution using option A for E8.0, option B for E8.75, option C for E11.5 and option D for E15.5 embryos (also see **Supplementary videos 1-4**)

(A) E8.0 embryos

(i) Insert the needle into the mesenchyme to the left or right of the dorsal midline, below the cardiogenic plate. Minimal insertion is sufficient.

(ii) Inject 1.5 to 5 nl of control solution or VEGFR2-blocking solution.

CRITICAL STEP Injection is successful if the red color does not immediately disappear.

(i) Repeat steps i and ii on the other side of the embryo.

?TROUBLESHOOTING

(B) E8.75 embryos.

(i) Insert the needle (through the yolk sac, if necessary) into the 9^{th} or 10^{th} somite.

(ii) Inject 3 to 8 nl of control solution or VEGFR2-blocking solution. **▲CRITICAL STEP** Do not pierce through the embryo into the embryonic cavity, but inject into the mesenchyme. Avoid large holes in the embryo. Do not inject more substance than denoted. Avoid major damage to the yolk sac or embryo from improperly opened needles with broken or jagged edges. Small holes in the yolk sac (see **Supplementary video 2**), however, are generally tolerated.

(iii) Turn the embryo around if necessary and repeat steps i and ii on the other side.

(C) E11.5 embryos.

(i) Insert the needle into the jugular region (neck region) of E11.5 embryos.

(ii) Inject 4-8 nl of Control-Fc solution or VEGFR3-blocking solution).

(D) E15.5 embryos

(i) Insert the needle through the skin into the dorso-lateral region right below the dermis of E15.5 embryos.

(ii) Inject 4-10 nl Control-Fc solution with VEGF-C or VEGFR3-blocking solution with VEGF-C.

?TROUBLESHOOTING

Whole Embryo Culture • TIMING 1 – 13 h (depending on stage / time of cultivation. 1 h effective working time)

15 Transfer the injected embryo into a labeled flask in the incubator using a plastic Pasteur pipette prefilled with PBS^+ for E8.0 and E8.75 embryos or a perforated spoon for E11.5 and E15.5 embryos. Incubate the embryos at 25 rpm, 37°C using the appropriate flow rates and gas mixture as specified in **Table 2**. Note the time. CRITICAL STEP Transfer as little PBS^+ as possible.

?TROUBLESHOOTING

▲CRITICAL STEP Gas flow and mixture is dependent on the starting and end stage of the mouse embryos.

16 Repeat steps 12-15 with remaining embryos.

17 **I**ncubate E8.0 embryos with 1-2 S for approximately 12 h to study aortic lumen formation[6]. Incubate E8.75 embryos with 12-13 S for approximately 8 h to study formation of the posterior ISVs[58]. Incubate E11.5 embryos for 5 h to study jugular lymph sac expansion[13]. Incubate E15.5 embryos for 0.5 h to visualize changes in the proliferation rate of LECs in sprouting dermal lymphatic vessels. Changes in mitosis can be observed in LECs of E15.5 embryos within 0.5 h[13].

?TROUBLESHOOTING

18 After the appropriate incubation time, transfer single embryos to a Petri dish under the stereomicroscope. Check for viability by observing heart beat (in embryos with > 6 somites, see **Supplementary video 5** for an example of what should be seen), important developmental steps and morphological features (turning, limbs, etc.), color

(transparency; milky embryos are usually dead), hemorrhages/edema. Check for the development of additional somites in E8.0 and E8.75 embryos.

▲**CRITICAL STEP** A round and filled yolk sac already indicates healthy E8.0 and E8.75 embryos.

?TROUBLESHOOTING

Analysis of embryos and skin • TIMING 20-25 h for sections, 18-20 h for whole mounts

19 Sort the embryos according to their stage (number of somites) or phenotype and transfer them to 4% PFA at 4°C to fix them overnight.

■**PAUSE POINT** Fixed embryos can be transferred to PBS^{+} and then stored at 4°C for at least 4 weeks.

20 Prepare samples for immunostaining. If you are immunostaining sections, proceed with option A to prepare the samples and sections. If you are going to immunostain whole embryos (as an example here, E8.75 embryos), proceed with option B. If you are going to perform whole-mount staining of skin (as an example here, E15.5 embryos), prepare skin as described in option C.

(A) Sections

(i) Equilibrate the embryos with sucrose solution at 4°C. Use 30% sucrose for E8.0 embryos and 15% sucrose followed by 30% sucrose for E11.5 embryos. Equilibrate in each sucrose solution until the embryos sink to the ground.

■**PAUSE POINT** Incubation overnight in 15% sucrose at 4°C is possible. Embryos can be stored in 30% sucrose at 4°C for at least a week.

▲**CRITICAL STEP** Equilibration helps to avoid rupture during embedding and cutting.

?TROUBLESHOOTING

(ii) Embed embryos in transversal direction (head up, anterior aorta straight down) into a cryomold with O.C.T. embedding compound and freeze them on a flat surface of dry ice or the quick freezing block in the microtome. Use a 10x10x5 mm cryomold for E8.0 embryos and a Peel-A-Way cryomold for E11.5 embryos. Store embedded embryos at -80°C until sectioning.

!CAUTION Do not touch dry ice with bare hands.

▲**CRITICAL STEP** Upright embedding is crucial for comparable sections. Freeze embryos immediately after embedding to prevent the embryo from tilting.

(iii) Properly insert the block with the embedded embryo into the microtome. Cool the knife. Use a C35 blade cooled to -19°C and the object cooled to -17°C for E8.0 embryos. Use a MX35 blade cooled to -23°C and the object cooled to -21°C for E11.5 embryos.

(iv) Cut 12 μm thick sections and transfer them onto glass slides. Store the slides at -20°C until staining.

▲**CRITICAL STEP** The aortae can collapse or rupture during sectioning. Be very careful when sectioning E8.0 embryos.

■**PAUSE POINT** Frozen slides with sections can be stored at -20°C for months.

(B) Sample Preparation for whole mount staining

Isolate embryos by carefully removing the yolk sac with forceps under a stereomicroscope. Continue with step 21 B.

(C) Isolation of the back skin of the embryos.

(i) Remove the limbs and tail, then make a single cut at the abdomen and peel away the skin around the embryo with scissors (see **Supplementary Fig. S 1**).

▲**CRITICAL STEP** Carefully remove all thin subcutaneous skin layers, as they will interfere with the imaging.

(ii) Place the skin in 4% PFA. Appropriately discard the embryo. Continue with step 21 C.

■**PAUSE POINT** The fixed skin can be stored in 4% PFA for a week.

21 Prepare antibody solutions used for staining. Here, as an example, we stain sections of E8.0 embryos for endothelial cells and apical cell surfaces and sections of E11.5 embryos for lymphatic endothelial cells and endothelial cells (option A). Additionally, we stain for endothelial cells in E8.75 whole mount embryos (option B), and for lymphatic endothelial cells and proliferating cells in the skins of E15.5 embryos (option C). However, the desired markers and antibodies can be chosen by the researcher, depending on his/her interest.

(A) Sections (Here: E8.0 and E11.5 embryo sections)

(i) Prepare at least 3 ml blocking solution per 9 slides (see REAGENT SETUP).

(ii) Prepare antibody solutions. For 9 slides, prepare 1 ml of primary and 1 ml of secondary antibody solution (see REAGENT SETUP).

(B) Whole-mount staining (Here: E8.75 embryos)

(i) Prepare 500 μl blocking solution for 5 embryos (in a reaction tube).

(ii) Prepare antibody solutions. For 5-6 embryos, prepare 150 µl primary and 250 µl secondary antibody solution (see REAGENT SETUP).

(C) Whole mount skin staining (Here: E15.5 skin)

(i) Prepare 500 µl blocking solution for 5 skins (in a reaction tube).

(ii) Prepare antibody solutions. For 1-2 skins, prepare 150 µl primary and 250 µl secondary antibody solution (see REAGENT SETUP).

22 Stain sections (A), whole embryos (B) or embryonic skin (C) with fluorescent markers to analyze relevant molecules and processes as follows:

(A) Sections (Here: E8.0 and E11.5 embryo sections)

Wash slides in PBS^+ in a washing box on a rocking platform for 5 min. Wash again for 5 min with PBS^+ with 0.2% Triton X-100. Place slides (horizontally) in a humid staining chamber. Add 100 µl blocking solution to each slide and cover the slides with parafilm. Incubate in closed chamber for 1 h at RT.

Remove parafilm and solution from slides (by vertically pressing the side of the slides on a tissue paper). Add 100 µl of primary antibody solution per slide and cover with parafilm. Incubate in closed chamber for 1 h at RT or overnight at 4°C.

■**PAUSE POINT** Incubation overnight can last for up to 20 h.

Remove parafilm and transfer slides into washing box. Wash slides three times in PBS^+ on a rocking platform for 20 min. Wash again in PBS^+ with 0.2% Triton X-100. Place slides in humid staining chamber. Add 100 µl secondary antibody solution to each slide and cover the slides with parafilm. Incubate in closed, dark chamber for 50 min at RT. Remove parafilm and transfer slides into washing box. Wash slides four times in PBS^+ on a rocking platform for 20 min. Remove solution from slides (by vertically pressing the side of the slides on a tissue paper). Add 100 µl Mowiol and mount a coverslip on top. Let Mowiol dry for 15 min in the dark. Surround cover slip with nail polish to preserve. Store slides at 4°C in the dark.

■**PAUSE POINT** Mowiol can dry overnight, if necessary. Slides can be stored at 4°C in the dark for weeks.

(B) Whole mount staining (here: E8.75 embryos)

(i) Wash the embryos once in PBS^+ to rinse off the PFA. Carefully aspirate the PBS^+ and add 200 µl blocking solution. Incubate for 3 h at RT and 300 rpm on a thermomixer.

▲**CRITICAL STEP** Be careful when transferring embryos or skins or aspirating the solutions, to avoid damage or losing the objects.

(ii) Aspirate the blocking solution. Add 150 μl primary antibody solution. Incubate for 2 h at 33°C and 400 rpm on a thermomixer. Remove primary antibody solution and wash the embryos by adding 500 μl PBS^+ per tube. Incubate for 20 min at RT with 400 rpm. Repeat this step three times. Remove PBS^+ and add 150 μl secondary antibody to each tube. Incubate for 1 h at 33°C and 400 rpm on the thermomixer. Wash again three times with PBS^+ for 20 min at RT and 400 rpm on the thermomixer.

■**PAUSE POINT** Embryos can be stored at 4°C in the dark overnight.

(iii) Embed whole-mount stained embryos in agarose gel for optical sagittal sections. Prepare agarose VII solution and store it at 37°C. Place the embryos into a glass bottom culture dish. Carefully remove PBS^+ with a pipette. Cover embryo with 10-20 μl of agarose VII. Orient embryo sagittally (sagittal plane parallel to the dish bottom). Push embryo to the bottom of the dish with forceps until the agarose hardens. For long-term storage, cover the agarose drop with 50-100 μl Mowiol. Covering with Mowiol is also possible after step 23.

■**PAUSE POINT** Covered in Mowiol, embryos can be stored for several weeks.

(C) Whole mount skin staining (here: E15.5 skin)

Stain skins as described for embryos in (B). Afterwards, place the skin flat onto a slide with the inner side towards the coverslip. To avoid or remove wrinkles, use forceps to straighten and flatten the skin. Add 100 μl of Mowiol and mount a coverslip. Store slides at 4°C in the dark.

■**PAUSE POINT** Covered in Mowiol, skins can be stored for several weeks.

23 Analyze the slides (A), whole mounts of embryos (B) or whole mounts of skin (C) by confocal microscopy as indicated below. To visualize Alexa Fluor 488-stained antibody complexes, use an argon multiline laser to excite at 495 nm. Investigate emission at 519 nm. To visualize Cy3-stained antibody complexes, use a 543 nm Helium/Neon laser to excite at 550 nm. Investigate emission at 570 nm. To visualize DAPI staining, use a 405 nm laser diode. Investigate emission at 461 nm. Image and recolor the staining as required.

(A) Take single confocal images of sections (here: E8.0 or E11.5 embryos) with 40x magnification.

(B) Perform z-stacks of whole mounts (here: in the region of the ISVs in E8.75 embryos) with 10x magnification to get a 3D overview of this region.

(C) Prepare z-stacks with 63x magnification of whole mount skin staining to obtain 3D images (here: skin of E15.5 embryos to track individual lymphatic sprouts).

?TROUBLESHOOTING

Statistical analyses

24 Analyze images using an image processing software of choice (e.g. Image J). Perform adequate statistical analyses using a statistical software of choice (e.g. Excel). Here, perform a two-tailed Student's t-test after checking data for normal distribution to compare treatment and control condition. For all analyses, $p < 0.05$ is considered significant. Perform analyses of E8.0 dorsal aortae (A), E8.75 intersomitic vessels (E8.75) (B), E11.5 jugular lymph sacs (C), and E15.5 embryonic skin (D) as follows:

(A) In E8.0 embryos, measure the diameter of the aortic lumen to determine the percentage of lumenized aortae. A diameter ≥ 5 μm is considered lumenized.

(B) In E8.75 embryos, determine the last somite after which ISVs have formed in each embryo.

(C) In E11.5 embryos, count the number of endothelial cells in the JLS.

(D) In E15.5 embryos, count the number of proliferating LECs and all LECs in the lymphatic sprout.

Troubleshooting

See **Table 3** for troubleshooting guidance.

Timing

Steps 1-6, Preparation: 6 h (0.5 h effective working time)

Steps 7-9, Dissection of the uterus: 10 min

Steps 10-12, Isolation of embryos: 5 min/embryo or 1-2 h/mouse

Steps 13-14, Microinjection: 5 min/embryo

Steps 15-18, Whole embryo culture: 1 – 13 h (depending on stage. 1 h effective working time)

Steps 19-24, Analyses of embryos and skins: 20-25 h for sections, 18-20 h for whole mount stainings

Anticipated Results

We find that injection of small molecules or proteins followed by WEC for the times required for observing vascular changes allows survival of 83-94% of E8.0 - E8.75 embryos and 66-84% of E11.5 – E15.5 mouse embryos (**Table 1** and **supplementary video 5** show typical survival rates and typical rates of heartbeat seen in an E8.0 embryo after 12h of WEC, respectively). We have found that the heart rates after WEC of E8.0, E8.75 and E15.5 mouse embryos were similar to the heart rates of mouse embryos from *in utero* (see **Supplementary Table ST 2**).

Endothelial cell cords typically develop into lumenized blood vessels[6] in WEC of E8.0 mouse embryos (97% of analyzed aortae, see **Fig. 3 a, b**), and the formation of patent blood vessels is inhibited by around 75% upon injection of SU 5416 compared to control (**Fig. 3 b, c**). Due to the local injection, the effects should remain locally restricted, meaning that the dorsal aortae develop normally at a posterior position in the embryo (**Supplementary Fig. S 2**).

During WEC of E8.75 mouse embryos, approximately 5.4 additional posterior ISVs typically develop via sprouting angiogenesis from the dorsal aortae[58] (**Fig. 3 d, e**). These sprouting events are inhibited by injection of SU 5416 compared to control, meaning that only 3.5 sprouting ISVs will usually develop (**Fig. 3 e, f**).

In our setup, lymphatic endothelial cells (LECs) migrate from the cardinal vein (CV) to form and expand a jugular lymph sac (JLS) *in vivo* and *ex vivo* at E11.5[13] (**Fig. 3 g, h**), and the total number of LECs in the JLS can be significantly reduced by around 25% when VEGFR3-Fc is injected (**Fig. 3 h, i**).

VEGF-C dependent lymphatic vessel sprouting[44] can be observed in the dermis of E15.5 mouse embryos cultured in WEC (**Fig. 3 j**), and the number of proliferating LECs in these lymphatic vessel sprouts is typically reduced by 50% following injection of VEGFR3-Fc compared to Ctrl-Fc injection in the presence of VEGF-C (**Fig. 3 k, l**).

In conclusion, this method allows researchers to investigate the effects of pharmacological agents on many important steps in blood and lymphatic vascular development and likely other developmental and biological processes. Microinjection in combination with WEC can probably be set up in most laboratories and can be used with great success after a short learning phase, and it is easily applicable to multiple research areas at the intersection of basic science and medical applications.

References

1. Ferrara, N., *et al.* Heterozygous embryonic lethality induced by targeted inactivation of the VEGF gene. *Nature* **380**, 439-442 (1996).
2. Carmeliet, P., *et al.* Abnormal blood vessel development and lethality in embryos lacking a single VEGF allele. *Nature* **380**, 435-439 (1996).
3. Duarte, A., *et al.* Dosage-sensitive requirement for mouse Dll4 in artery development. *Genes Dev* **18**, 2474-2478 (2004).
4. Leveen, P., *et al.* Mice deficient for PDGF B show renal, cardiovascular, and hematological abnormalities. *Genes Dev* **8**, 1875-1887 (1994).
5. Lindahl, P., Johansson, B.R., Leveen, P. & Betsholtz, C. Pericyte loss and microaneurysm formation in PDGF-B-deficient mice. *Science* **277**, 242-245 (1997).
6. Strilic, B., *et al.* The molecular basis of vascular lumen formation in the developing mouse aorta. *Dev Cell* **17**, 505-515 (2009).
7. Strilic, B., *et al.* Electrostatic cell-surface repulsion initiates lumen formation in developing blood vessels. *Curr Biol* **20**, 2003-2009 (2010).
8. Randhawa, P.K., *et al.* The Ras activator RasGRP3 mediates diabetes-induced embryonic defects and affects endothelial cell migration. *Circ Res* **108**, 1199-1208 (2011).
9. Nagase, M., Nagase, T., Koshima, I. & Fujita, T. Critical time window of hedgehog-dependent angiogenesis in murine yolk sac. *Microvasc Res* **71**, 85-90 (2006).
10. Downs, K.M., Hellman, E.R., McHugh, J., Barrickman, K. & Inman, K.E. Investigation into a role for the primitive streak in development of the murine allantois. *Development* **131**, 37-55 (2004).
11. Kawasaki, K., *et al.* Ras signaling directs endothelial specification of VEGFR2+ vascular progenitor cells. *J Cell Biol* **181**, 131-141 (2008).
12. Bohnsack, B.L., Lai, L., Dolle, P. & Hirschi, K.K. Signaling hierarchy downstream of retinoic acid that independently regulates vascular remodeling and endothelial cell proliferation. *Genes Dev* **18**, 1345-1358 (2004).
13. Planas-Paz, L., *et al.* Mechanoinduction of lymph vessel expansion. *EMBO J* **31**, 788-804 (2011).
14. Xu, K., *et al.* Blood vessel tubulogenesis requires Rasip1 regulation of GTPase signaling. *Dev Cell* **20**, 526-539 (2011).
15. Parker, L.H., *et al.* The endothelial-cell-derived secreted factor Egfl7 regulates vascular tube formation. *Nature* **428**, 754-758 (2004).
16. Gerhardt, H., *et al.* VEGF guides angiogenic sprouting utilizing endothelial tip cell filopodia. *J Cell Biol* **161**, 1163-1177 (2003).
17. Wigle, J.T. & Oliver, G. Prox1 function is required for the development of the murine lymphatic system. *Cell* **98**, 769-778 (1999).
18. Karkkainen, M.J., *et al.* Vascular endothelial growth factor C is required for sprouting of the first lymphatic vessels from embryonic veins. *Nat Immunol* **5**, 74-80 (2004).
19. Kiefer, F. & Adams, R.H. Lymphatic endothelial differentiation: start out with Sox--carry on with Prox. *Genome Biol* **9**, 243 (2008).
20. Makinen, T., Norrmen, C. & Petrova, T.V. Molecular mechanisms of lymphatic vascular development. *Cell Mol Life Sci* **64**, 1915-1929 (2007).
21. Böhmer, R., *et al.* Regulation of developmental lymphangiogenesis by Syk(+) leukocytes. *Dev Cell* **18**, 437-449 (2010).
22. Tammela, T. & Alitalo, K. Lymphangiogenesis: Molecular mechanisms and future promise. *Cell* **140**, 460-476 (2010).
23. Kälin, R.E., Banziger-Tobler, N.E., Detmar, M. & Brändli, A.W. An in vivo chemical library screen in Xenopus tadpoles reveals novel pathways involved in angiogenesis and lymphangiogenesis. *Blood* **114**, 1110-1122 (2009).

24. Hellstrom, M., Kalen, M., Lindahl, P., Abramsson, A. & Betsholtz, C. Role of PDGF-B and PDGFR-beta in recruitment of vascular smooth muscle cells and pericytes during embryonic blood vessel formation in the mouse. *Development* **126**, 3047-3055 (1999).
25. Norrmen, C.*, et al.* FOXC2 controls formation and maturation of lymphatic collecting vessels through cooperation with NFATc1. *J Cell Biol* **185**, 439-457 (2009).
26. Sabine, A.*, et al.* Mechanotransduction, PROX1, and FOXC2 cooperate to control connexin37 and calcineurin during lymphatic-valve formation. *Dev Cell* **22**, 430-445 (2012).
27. Sasaki, T.*, et al.* Regulation of hematopoietic cell clusters in the placental niche through SCF/Kit signaling in embryonic mouse. *Development* **137**, 3941-3952 (2010).
28. Hang, C.T.*, et al.* Chromatin regulation by Brg1 underlies heart muscle development and disease. *Nature* **466**, 62-67 (2010).
29. Chang, C.P.*, et al.* A field of myocardial-endocardial NFAT signaling underlies heart valve morphogenesis. *Cell* **118**, 649-663 (2004).
30. Miki, R.*, et al.* Fate maps of ventral and dorsal pancreatic progenitor cells in early somite stage mouse embryos. *Mech Dev* **128**, 597-609 (2012).
31. Tremblay, K.D. & Zaret, K.S. Distinct populations of endoderm cells converge to generate the embryonic liver bud and ventral foregut tissues. *Dev Biol* **280**, 87-99 (2005).
32. Noda, T.*, et al.* Restriction of Wnt signaling in the dorsal otocyst determines semicircular canal formation in the mouse embryo. *Dev Biol* **362**, 83-93 (2012).
33. Calegari, F. & Huttner, W.B. An inhibition of cyclin-dependent kinases that lengthens, but does not arrest, neuroepithelial cell cycle induces premature neurogenesis. *J Cell Sci* **116**, 4947-4955 (2003).
34. Inoue, T. & Krumlauf, R. An impulse to the brain--using in vivo electroporation. *Nat Neurosci* **4 Suppl**, 1156-1158 (2001).
35. Gray, J. & Ross, M.E. Neural tube closure in mouse whole embryo culture. *J Vis Exp* doi: 10.3791/3132 (2011).
36. Takahashi, M., Nomura, T. & Osumi, N. Transferring genes into cultured mammalian embryos by electroporation. *Dev Growth Differ* **50**, 485-497 (2008).
37. Winn, L.M. & Tung, E.W. Assessment of embryotoxicity using mouse embryo culture. *Methods Mol Biol* **550**, 241-249 (2009).
38. Jones, E.A.*, et al.* Dynamic in vivo imaging of postimplantation mammalian embryos using whole embryo culture. *Genesis* **34**, 228-235 (2002).
39. Kwon, G.S.*, et al.* Tg(Afp-GFP) expression marks primitive and definitive endoderm lineages during mouse development. *Dev Dyn* **235**, 2549-2558 (2006).
40. Schmidt, M.*, et al.* EGFL7 regulates the collective migration of endothelial cells by restricting their spatial distribution. *Development* **134**, 2913-2923 (2007).
41. Boisset, J.C., Andrieu-Soler, C., van Cappellen, W.A., Clapes, T. & Robin, C. Ex vivo time-lapse confocal imaging of the mouse embryo aorta. *Nat Protoc* **6**, 1792-1805 (2011).
42. Drake, C.J. & Fleming, P.A. Vasculogenesis in the day 6.5 to 9.5 mouse embryo. *Blood* **95**, 1671-1679 (2000).
43. Veikkola, T.*, et al.* Signalling via vascular endothelial growth factor receptor-3 is sufficient for lymphangiogenesis in transgenic mice. *EMBO J* **20**, 1223-1231 (2001).
44. Skobe, M.*, et al.* Induction of tumor lymphangiogenesis by VEGF-C promotes breast cancer metastasis. *Nat Med* **7**, 192-198 (2001).
45. Garcia, M.D., Udan, R.S., Hadjantonakis, A.K. & Dickinson, M.E. Preparation of rat serum for culturing mouse embryos. *Cold Spring Harb Protoc* **2011**, pdb prot5593 (2011).
46. Schulte-Merker, S., Sabine, A. & Petrova, T.V. Lymphatic vascular morphogenesis in development, physiology, and disease. *J Cell Biol* **193**, 607-618 (2011).

47. Carmeliet, P.*, et al.* Synergism between vascular endothelial growth factor and placental growth factor contributes to angiogenesis and plasma extravasation in pathological conditions. *Nat Med* **7**, 575-583 (2001).
48. Akerman, S.*, et al.* Microflow of fluorescently labelled red blood cells in tumours expressing single isoforms of VEGF and their response to vascular targeting agents. *Med Eng Phys* **33**, 805-809 (2011).
49. Fong, T.A.*, et al.* SU5416 is a potent and selective inhibitor of the vascular endothelial growth factor receptor (Flk-1/KDR) that inhibits tyrosine kinase catalysis, tumor vascularization, and growth of multiple tumor types. *Cancer Res* **59**, 99-106 (1999).
50. Karpanen, T.*, et al.* Vascular endothelial growth factor C promotes tumor lymphangiogenesis and intralymphatic tumor growth. *Cancer Res* **61**, 1786-1790 (2001).
51. Bakkers, J. Zebrafish as a model to study cardiac development and human cardiac disease. *Cardiovasc Res* **91**, 279-288 (2011).
52. Jin, S.W., Beis, D., Mitchell, T., Chen, J.N. & Stainier, D.Y. Cellular and molecular analyses of vascular tube and lumen formation in zebrafish. *Development* **132**, 5199-5209 (2005).
53. Patan, S. Vasculogenesis and angiogenesis as mechanisms of vascular network formation, growth and remodeling. *J Neurooncol* **50**, 1-15 (2000).
54. Thisse, C. & Zon, L.I. Organogenesis--heart and blood formation from the zebrafish point of view. *Science* **295**, 457-462 (2002).
55. Mendel, D.B.*, et al.* The angiogenesis inhibitor SU5416 has long-lasting effects on vascular endothelial growth factor receptor phosphorylation and function. *Clin Cancer Res* **6**, 4848-4858 (2000).
56. Finnerty, H.*, et al.* Molecular cloning of murine FLT and FLT4. *Oncogene* **8**, 2293-2298 (1993).
57. Abramoff, M.D., Magalhaes, P.J. & Ram, S.J. Image Processing with ImageJ. *Biophotonics International* **11**, 36-42 (2004).
58. Walls, J.R., Coultas, L., Rossant, J. & Henkelman, R.M. Three-dimensional analysis of vascular development in the mouse embryo. *PLoS One* **3**, e2853 (2008).

Author contributions

M.Z., J.A. and E.L. wrote the text. M.Z. and J.A. prepared the figures. M.Z., J.A., B.S. and T.H. performed the blood vessel experiments. L.P.P. and J.A. performed the lymphatic vessel experiments.

Acknowledgements

The authors are grateful to Mary Gearing for proofreading the manuscript and to the other members of the Lammert lab for valuable discussions. The work was funded by the Deutsche Forschungsgemeinschaft DFG LA 1216/4-1 and 5-1, and by the CRC 974.

Conflict of interest

The authors declare that they have no conflict of interests.

Figure legends

Figure 1. Flowchart of *ex vivo* manipulation and cultivation of mouse embryos. Workflow to analyze *de novo* and sprouting blood and lymphatic vascular development, i.e. vasculogenesis (aorta formation in E8.0 mouse embryos), sprouting angiogenesis (intersomitic vessel (ISV) formation at E8.75), *de novo* lymphatic development (generation of the jugular lymph sac (JLS) at E11.5), and lymphatic vessel sprouting (at E15.5). Necessary steps for the successful analysis or culture of the given stage are shown in black. Variable steps, specifically selected for the analysis of blood and lymphatic vessels, are marked with grey letters and asterisks (*). α = anti.

Figure 2. Equipment setup and injection sites in mice at different embryonic stages. **(a-c)** Photographs of the isolation and injection equipment. **(a and a')** Image of the injection needle. **(a')** Magnification of the boxed region in a. **(b)** The image shows (left to right) a gooseneck lamp, microinjector, steromicroscope (with camera), and micromanipulator. **(c)** Close-up image of the equipment showing forceps, Petri dish with PBS^{+}, and micromanipulator. **(d, e)** Photographs of the WEC incubator. **(d)** The WEC incubator is shown with doors open and three incubation bottles connected to the rotator. At the top, temperature, rotational speed and gas flow-through can be regulated. **(e)** Close-up image of the interior showing WEC bottles connected to the rotator. **(f-i)** Side view photographs of embryos at the different stages after injection. Phenol red (**f,g**) and Fast Green (**h,i**) visualize the injection. **(f)** E8.0 embryo injected into the head region. **(g)** E8.75 embryo injected into the posterior somite region. For clarity, the needle was increased digitally. **(h)** E11.5 embryo injected into the jugular region. **(i)** E15.5 embryo injected into the dermis**.** The animal experiments were conducted and approved according to the German Animal Protection Laws.

Scale bars in c, 1 mm; c', 100 μm; **f, g**, 100 μm; **h, i**, 1 mm.

Figure 3. Typical confocal images of blood and lymphatic vascular development after microinjection in whole embryo culture (WEC). (a-c) Cross sections of E8.0 mouse embryos used to investigate vasculogenesis stained for PECAM-1 (red), PODXL (green) and nuclei (blue). (a) At the 1 S stage, the embryo shows non-lumenized endothelial cell cords. Schematic needle illustrates one of the two injections sites. (b) After control injection and 12 h WEC, embryos show lumenized aortae. *, aortic lumen (c) After SU 5416 injection and 12 h WEC, the vascular lumen is either absent (left) or reduced in size (right). Arrowheads point to the aortic regions. Mes, mesoderm; NE, neuroepithelium. Scale bars in a-c, 50 μm. (d-f) Maximum intensity projections of whole-mount PECAM-1 (red) stained E8.75 embryos in side view (head right, tail left) used to investigate intersomitic vessel (ISV) sprouting. (d) At the 12 S stage, the embryo shows ISVs up to the 9th somite (dashed line). Schematic needle illustrates one of the two injection sites. (e) After control injection and 8 h WEC, ISV formation proceeded up to the 14th somite (upper dashed line). The lower dashed line indicates the 9th somite. (f) After SU 5416 injection and 8 h WEC, ISV formation is impaired from the 9th somite onwards. Scale bars in d-f, 100 μm. (g-i) Cross sections of E11.5 embryos used to investigate *de novo* lymphatic development, i.e. formation of the jugular lymph sac (JLS) stained for Lyve-1 (green), PECAM-1 (red) and nuclei (blue). (g) At E11.5, a small JLS is present (arrowhead). (h) After control injection and 5 h WEC, the JLS is increased in size, shown by the increased cell number. (i) After VEGFR3-Fc injection and 5 h WEC, the JLS is reduced in size compared to control. JLS, jugular lymph sac, CV, cardinal vein, Ao, aorta. Scale bars in g-i, 50 μm. (j-l) Maximum intensity projections of whole mount stained dorsal skin of E15.5 embryos used to investigate cell proliferation in dermal lymphatic sprouts. Skins are stained for Lyve-1 (green), phospho-Histone H3 (red) and nuclei (blue). (j) A lymphatic sprout in the skin of an E15.5 embryo with proliferating lymphatic endothelial cells (proliferating LECs; arrowheads). (k) A lymphatic sprout after injection of VEGF-C + Control-Fc, and 30 min WEC. (l) A lymphatic sprout after injection of VEGF-C + VEGFR3-Fc and 30 min WEC. The animal experiments were conducted and approved according to the German Animal Protection Laws. Scale bars in j-l, 50 μm.

TABLE 1. Survival rates in relation to treatment and stage after WEC for the indicated times. 'Total' states the total number of embryos used in this study. Survival was assessed by a visible heartbeat.

Stage	Incubation time [h]	Treatment	Survived / Total	Survival rate [%]
E8.0	12	Control solution	15/17	88.2
		VEGFR2-blocking solution	5/6	83.3
E8.75	8	Control solution	32/34	94.1
		VEGFR2-blocking solution	20/23	87.0
E11.5	5	Control-Fc solution	14/17	82.4
		VEGFR3-blocking solution	6/9	66.7
E15.5	0.5	Control-Fc solution with VEGF-C	11/13	84.6
		VEGFR3-blocking solution with VEGF-C	5/7	71.4

TABLE 2. Gas flow, timing and flow rates of WEC.

Stage	Gas	Timing [h]	Flow [ml/min]
E8.0	5% CO_2, 5% O_2, 90% N_2	6 + 6	50 75
E8.75	5% CO_2, 5% O_2, 90% N_2	6 + 2	125 150
E11.5	5% CO_2, 95% O_2	5	50
E15.5	5% CO_2, 95% O_2	0.5	50

Table 3: Troubleshooting

Step	Problem	Reason	Solution
12	> Decidua floats to the surface during isolation. > Embryo „pops out“ while isolating	> Fat tissue not completely removed in step 10. > Decidua damaged in step 10 or too much pressure with forceps during isolation	> Remove fat tissue before embryo isolation. > Pull embryo packages apart, before separating (step 10). Use less force and intact forceps.
14 (A)	> Problems inserting the needle > Injection solution diffuses away	> Reichert’s membrane might still be in place > Needle is not inserted properly.	> Remove the delicate, thin and transparent Reichert’s membrane before injection > Insert needle only minimally. More acute angles of the needle usually facilitate entry
14	Problems injecting solution into the embryo	The tip of the needle might be clogged	Break the needle right behind the obstruction with forceps, avoid a jagged or broken tip, test ejection, and then continue
15	Problems transferring the embryo to the bottle	Embryo might be sticking to the inner wall of the pipette	Pick up embryo below surface of PBS^{+} used for injection
17	E8.75 embryos do not survive cultivation or do not develop as expected	E8.75 embryos less turned than 50% can have problems with turning	Use embryos turned more than 50%, (tail has moved ≥ 90° from its starting point in top view relative to the head; tail is lateral to the head)
18	Embryos die during cultivation	• Long storage before embryo isolation • Hypothermia • Perforation during injection • Incorrect gas flow rate	Work quickly, yet carefully; keep embryos warm; handle fewer embryos, e.g. open one uterus after another. (See ▲**CRITICAL STEP**s and **Tables 1** and **ST 1** for survival rates.)
20 (A)	Mold in sucrose solution	Sucrose solutions are good media for microorganisms	Only use fresh solutions
23	Bad staining / high background	• Wrong fixation • Blocking too short • Slides dried out	• Use TCA, methanol or different fixative • Block and wash longer • Keep slides moist

Supplementary information

Contents:

Supplementary Figure 1. Images to illustrate important steps of skin isolation as described in step 22B. (**a**) E15.5 mouse embryo after WEC. (**b-d**) Isolation of the torso. (**b**) Embryo after removal of yolk sac and placenta. (**c**) Removal of front limbs. (**d**) Embryo with removed limbs and tail. (**e, f**) Opening the abdominal skin. (**e**) Opening of the abdominal skin using forceps (or scissors). (**f**) Peeling of the skin, as far as possible without rupturing it. (**g, h**) Separation from the skin in the head region. (**g**) Opening of the skin at the ear using forceps or scissors. This step must be repeated on the other side. (**h**) Peeling of the skin without rupturing it on both sides of the embryo. Please note that the head skin is not removed. (**i-k**) Further skin separation from embryo. (**i**) Peeling of the skin using forceps along the whole back on both sides of the embryo. (**j**) Use scissors to remove the skin from the underlying tissue. (**k**) Complete final removal of skin from the embryo. (**l**) Straightening and flattening of the isolated skin using forceps. Scale bar for **a-l** in **l**, 1 mm.

Supplementary Figure 2. Transversal sections through mouse embryos after microinjection and whole embryo culture (WEC) illustrating the local effects of injected substances. (**a, b**) Complete transversal sections of E8.0 mouse embryos stained for PECAM-1 (red). (**a**) After control injection into the anterior region and 12 h WEC, embryos show lumenized aortae in the anterior head region as well as in the posterior tail region. (**b**) After SU 5416 injection into the anterior region and 12 h WEC, a vascular lumen is absent in the anterior head region, but present in the posterior tail region. Arrowheads point to non-lumenized endothelial cells in the aortic regions; *, aortic lumen; Mes, mesoderm; NE, neuroepithelium. Scale bars in a and b, 100 μm.

Supplementary TABLE 1. Survival rates of long-term WEC in M16. The total number of surviving embryos as indicated by heartbeat is given after the indicated time points. * = viability was assessed morphologically, as there is no beating heart at E8.0.

E8.0	**before WEC**	**WEC for 12 h**	**WEC for 24 h**			
n (alive embryos)	10*	9	5			
E8.75	**before WEC**	**WEC for 8 h**	**WEC for 16 h**	**WEC for 20 h**		
n (alive embryos)	11	11	11	9		
E9.0	**before WEC**	**WEC for 8 h**	**WEC for 12 h**	**WEC for 16 h**	**WEC for 18 h**	**WEC for 22 h**
n (alive embryos)	8	8	8	8	8	2
E9.5	**before WEC**	**WEC for 7 h**	**WEC for 8 h**	**WEC for 14 h**		
n (alive embryos) open yolk sac	10	8	7	3		
n (alive embryos) intact yolk sac	10	4	4	0		

Supplementary TABLE 2. Range of heart rates after WEC. The highest and lowest heart rates as well as the mean heart rate for each of the four stages (E8.0, E8.75, E11.5 and E15.5) are given. *In utero* refers to embryos grown *in utero,* but prepared according to the protocol used for embryo isolation for WEC. P values are determined by a student's t-test.

		Heartbeat			
	n	**[beats/min]**			
	(embryos)	**lowest**	**highest**	**mean**	**p =**
E8.5 *in utero*	3	35	56	44	0.17
E8.0 + 12 h WEC	19	14	69	32	
E9.0 *in utero*	4	40	84	61	0.17
E8.75 + 8 h WEC	10	67	92	78	
E11.5 *in utero*	16	23	65	38	0.02
E11.5 + 5 h WEC	12	14	134	72	
E15.5 *in utero*	6	68	88	75	0.16
E15.5 + 5 h WEC	3	14	94	52	

Supplementary Video 1. Uterus separation, isolation and injection of E8.0 mouse embryos are shown together with common mistakes.

Supplementary Video 2. Uterus separation, isolation and injection of E8.75 mouse embryos are shown together with common mistakes.

Supplementary Video 3. Uterus separation, isolation and injection of E11.5 mouse embryos are shown together with common mistakes.

Supplementary Video 4. Uterus separation, isolation and injection of E15.5 mouse embryos are shown together with common mistakes.

Supplementary Video 5. Heartbeat movie of an E8.0 mouse embryo after 12 h of WEC.

Zeeb et al., Fig. 1

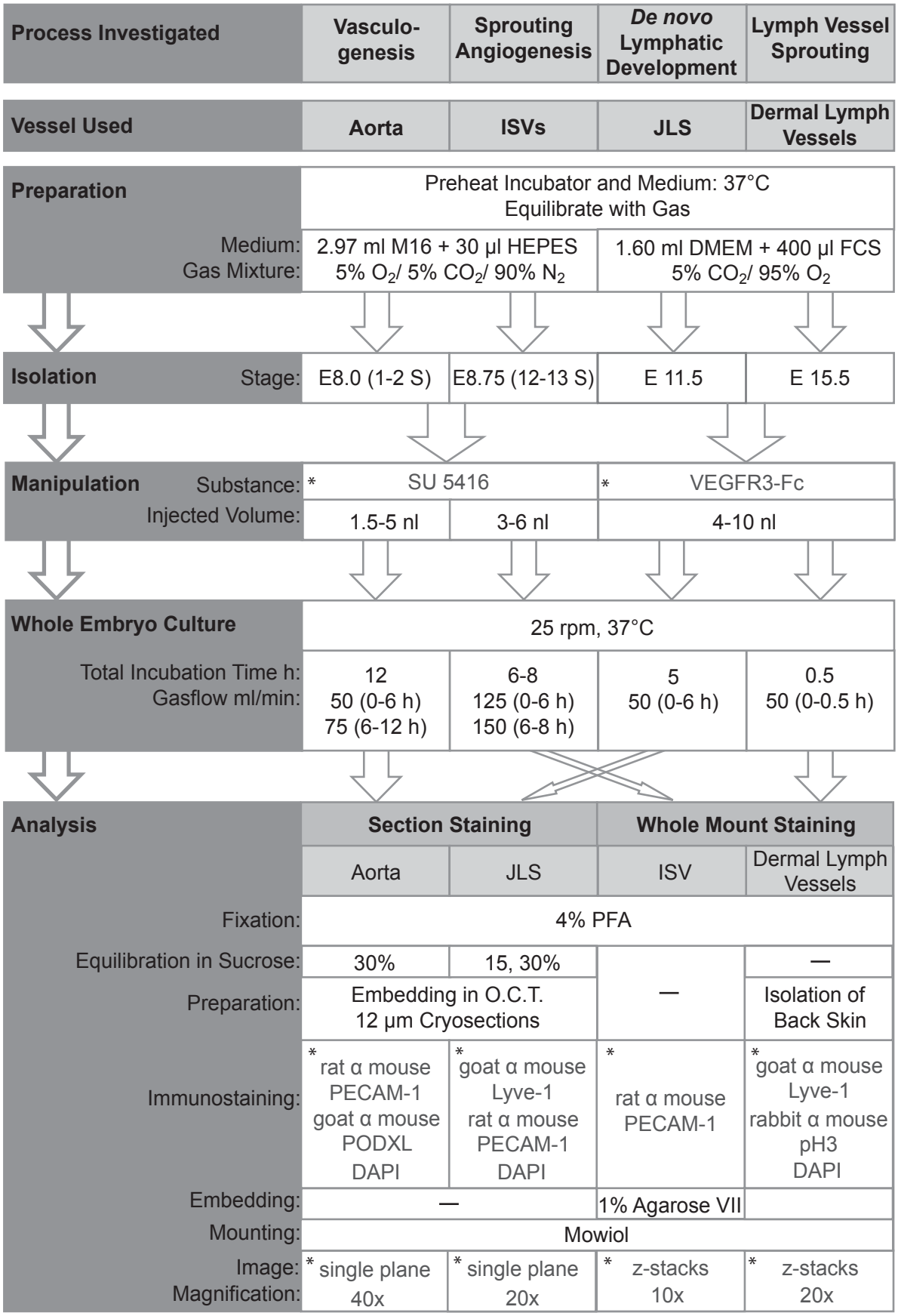

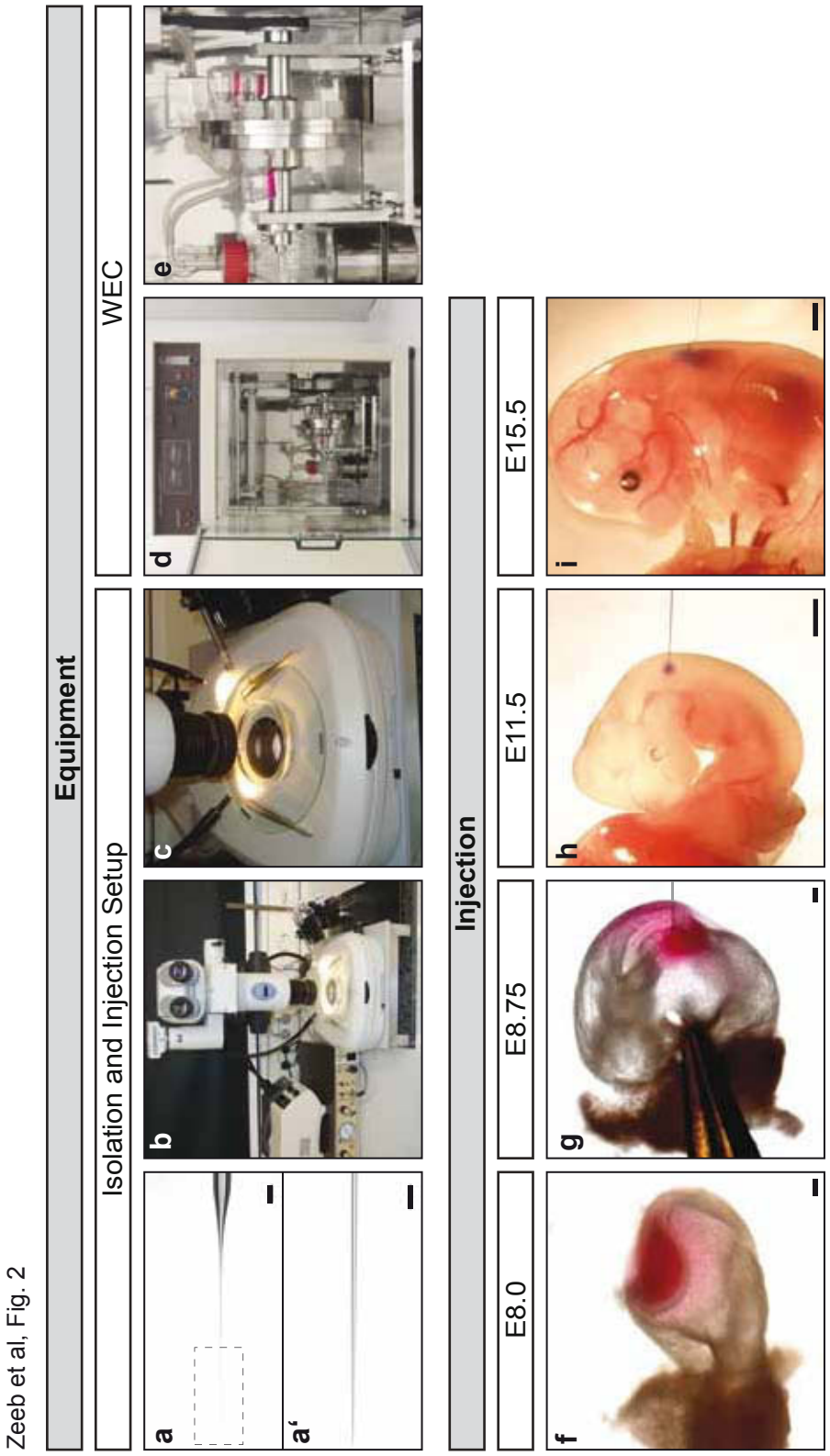
Zeeb et al, Fig. 2
Equipment
Isolation and Injection Setup
WEC
Injection
E8.0
E8.75
E11.5
E15.5
a
a'
b
c
d
e
f
g
h
i

Zeeb et al, Fig. 3

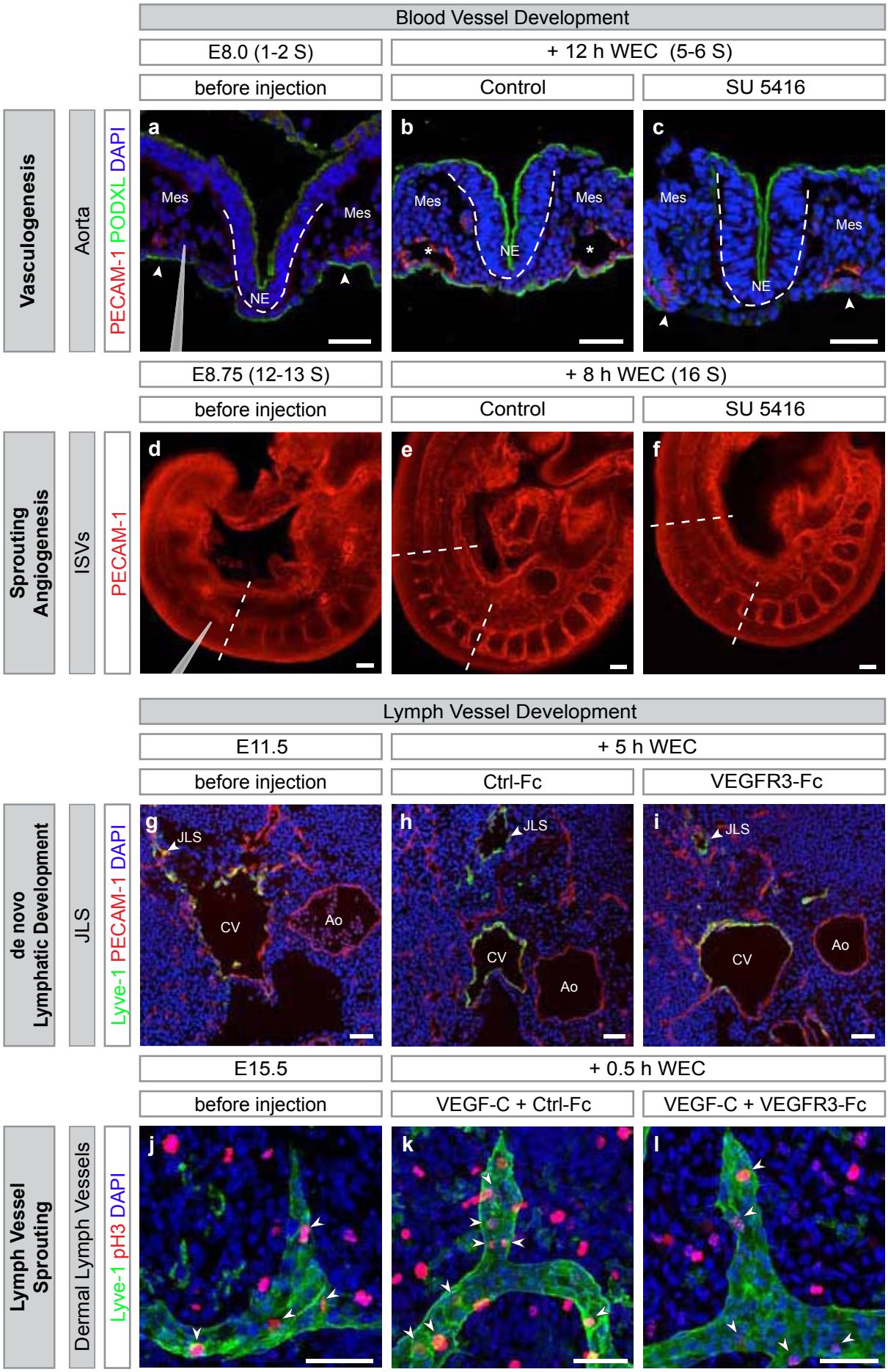

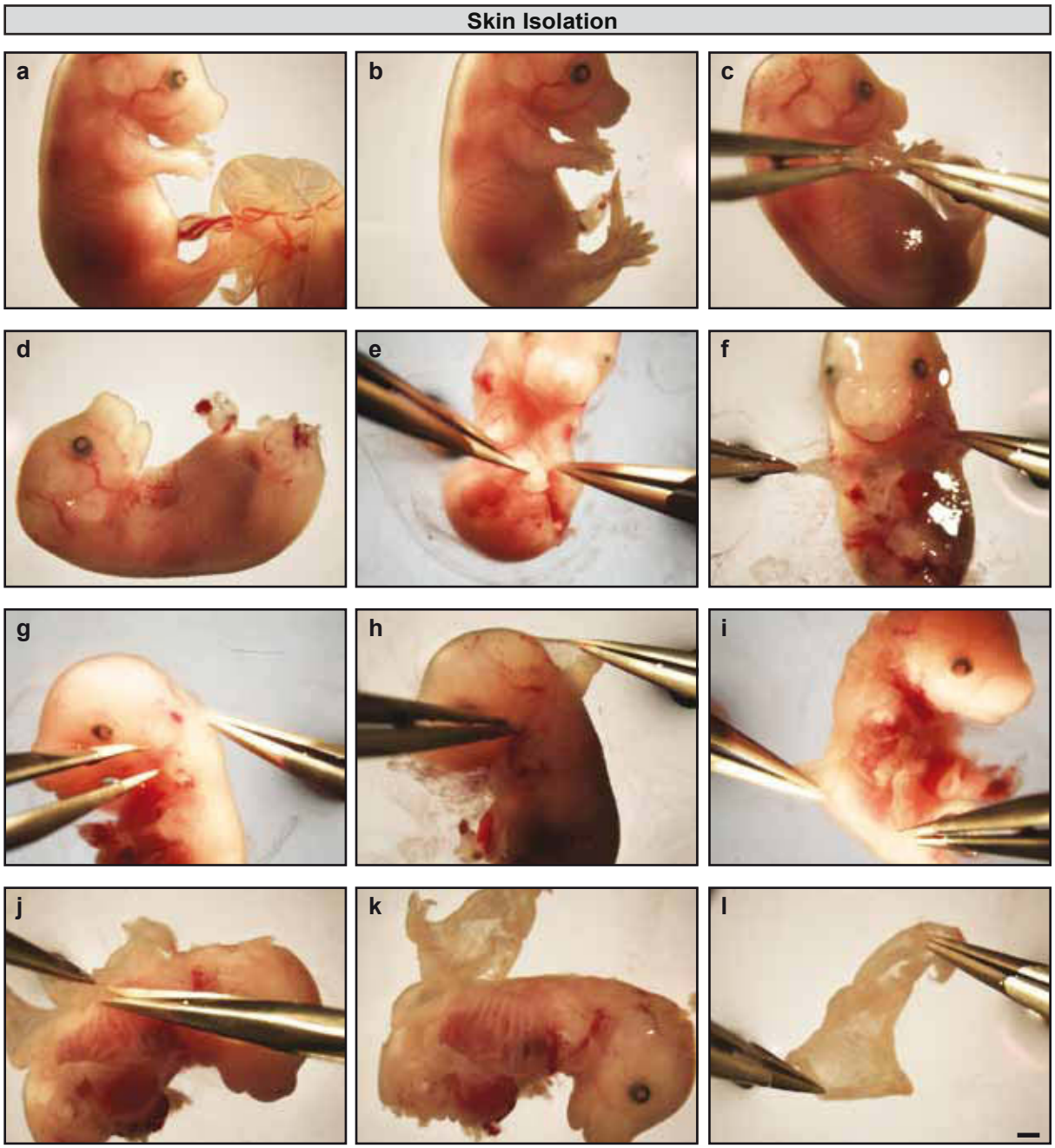
Skin Isolation
a
b
c
d
e
f
g
h
i
j
k
l

Zeeb et al., Fig. S 2
E8.0 (1-2 S) + 12 h WEC (5-6 S)
Control
SU 5416
Complete section
PECAM-1
Anterior
Posterior
a
b
NE
Mes
*

2.2.3 General information and personal contribution

Name of the journal	Nature Protocols
Impact Factor (2011)	9.924
Personal contribution	40 %
Author position	1st author, equal contribution
Tasks	Project planning, blood vessel experiments, manuscript writing and correction, figure preparation
Other	This work is also part of the master thesis of Jennifer Axnick and the bachelor thesis of Thorsten Hartmann, who were both supervised by Martin Zeeb. The protocol was unsolicitedly submitted.

Contribution in detail
This publication was initially planned and outlined by myself as a bachelor's thesis for Mr. Thorsten Hartmann. I took part in all cultivation experiments leading to the improved culture of mouse embryos. I performed the analysis of blood vessel development and subsequent refinements of the method together with Jennifer Axnick, as part of her Master's thesis. Writing the manuscript and preparation of the figures was performed in close collaboration with Jennifer Axnick. Correction of manuscript and figures was performed by myself, Jennifer Axnick and Prof. Eckhard Lammert.

2.3 Electrostatic cell-surface repulsion initiates lumen formation in developing blood vessels

2.3.1 Summary

Blood vessels function in the uptake, transport and delivery of gases and nutrients to and from tissues. A key question is how the central lumen of blood vessels develops within a cord of vascular endothelial cells. Here we demonstrate that sialic acids of apical glycoproteins localize to apposing endothelial cell surfaces and generate repelling electrostatic fields within an endothelial cell cord. Both in vitro and in vivo experiments show that sialic acids and their negative charge are required for the separation of endothelial cell surfaces and subsequent lumen formation. We also demonstrate that sulfate residues can substitute for sialic acids during lumen initiation. These results therefore reveal a key step in the creation of blood vessels, the most abundant conduits in the vertebrate body. Since negatively charged mucins and proteoglycans are often found on luminal cell surfaces, it is possible that electrostatic repulsion is a general principle also used to initiate lumen formation in other organs.

In this article we present for the first time a functional explanation for slit formation between apposing endothelial cells at the initiation of vascular lumen formation. The sialomucin PODXL was previously shown to localize to endothelial and epithelial apical cell surfaces, but its mechanistic role in lumen formation was unknown.
We identified the function of PODXL to separate apposing membranes by electrostatic repulsion, revealing a novel mechanism in shape generation of cells during tube formation.
Indeed, we could show that slit formation is critically dependent on the negative charges introduced by PODXL, as PODXL without negative charges did not promote vascular lumen formation, whereas artificial negative charges did.

In particular, using WEC, we showed that Neuraminidase (NA) treatment reduced the amount of sialic acids and vascular lumen formation in the dorsal aorta. Masking of negative charges by protamine sulfate (PS) showed similar results. To rescue this effect, artificial negative charges were introduced using dextrane sulfate (DS). DS restores negative charges and lumen formation in embryos treated with NA.
To confirm these findings, a novel assay was developed and established to assess EC-EC adhesion, termed bead-rolling assay (BRA). Therein, EC-covered microcarrier beads are placed on a tilted layer of ECs and the rolling distance of the beads is determined as an indicator of cell-cell adhesion. Both, NA and PS, result in shorter rolling-distances, indicating increased adhesion. Additionally, DS rescues NA treatment.
When measuring adhesion strength using single cell force spectroscopy (SCFS), PS and NA increased cell-cell adhesion and DS rescued NA treatment.
In a 3D in vitro sprouting assay, the effects of PS and NA treatment were similar, as both reduced lumen formation in the forming sprouts and DS partially restored NA's effect.

In total, we show that sialic acids and their negative cell-surface charges are required for de-adhesion of apposing endothelial cell surfaces during the initiation of lumen development in both angiogenesis and vasculogenesis.
Thus, this paper provides new insight into the mechanisms of initial lumen formation. We hypothesize that this mechanism could be applied in other systems as well, because PODXL or similar glycoproteins are expressed on the apical surface of many tubular organs.

2.3.2 Accepted publication

See pages 86 ff.

Electrostatic cell surface repulsion initiates lumen formation in developing blood vessels

Boris Strilić[1,2], Jan Eglinger[1], Michael Krieg[3], Martin Zeeb[1], Jennifer Axnick[1], Pavel Babál[4], Daniel J. Müller[3,5] and Eckhard Lammert[1,*]

[1]Institute of Metabolic Physiology, Heinrich-Heine-University of Düsseldorf, D-40225 Düsseldorf, Germany

[2]Department of Pharmacology, Max Planck Institute for Heart and Lung Research, W.G. Kerckhoff-Institute, D-61231 Bad Nauheim, Germany

[3]Biotechnology Center, University of Technology Dresden, D-01307 Dresden, Germany

[4]Department of Pathology, Comenius University, SK-81108 Bratislava, Slovakia

[5]Biosystems Science and Engineering, ETH Zürich, CH-4058 Basel, Switzerland

*To whom correspondence should be addressed. E-mail: lammert@uni-duesseldorf.de

Summary

Blood vessels function in the uptake, transport and delivery of gases and nutrients to and from tissues. A key question is how the central lumen of blood vessels develops within a cord of vascular endothelial cells. Here we demonstrate that sialic acids of apical glycoproteins localize to apposing endothelial cell surfaces and generate repelling electrostatic fields within an endothelial cell cord. Both *in vitro* and *in vivo* experiments show that sialic acids and their negative charge are required for the separation of endothelial cell surfaces and subsequent lumen formation. We also demonstrate that sulfate residues can substitute for sialic acids during lumen initiation. These results therefore reveal a key step in the creation of blood vessels, the most abundant conduits in the vertebrate body. Since negatively charged mucins and proteoglycans are often found on luminal cell surfaces, it is possible that electrostatic repulsion is a general principle also used to initiate lumen formation in other organs.

Highlights

- Sialic acids localize to the endothelial cell-cell contact at the onset of blood vessel lumen formation
- Sialic acids and their negative cell-surface charge are required for de-adhesion of apposing endothelial cell surfaces
- Sulfate residues can substitute for sialic acids during the initiation of lumen development
- It is concluded that electrostatic repulsion initiates blood vessel lumen formation

Results and Discussion

Mucins and proteoglycans are found on the luminal side of tubular organs in vertebrates, for example the gut, pancreas, salivary gland, lung, kidney and blood vessels [1-5]. In addition, these glycoproteins are found on the apical surfaces of invertebrate tubular organs, such as the retina, tracheae and wing imaginal discs of *Drosophila melanogaster*; the excretory cells of *Caenorhabditis elegans*; or the midgut of the *Anopheles* mosquito [6-10]. Interestingly, epithelial and endothelial cells express one such mucin, the CD34-sialomucin Podocalyxin/gp135 (PODXL), at the cell-cell contact (Fig. 1) [1, 11, 12]. As with many mucins, the CD34-sialomucin extracellular domain is decorated with oligosaccharides containing a large number of negatively charged sialic acids [13]. As the vascular lumen has been previously shown to develop through separation of adjacent endothelial cell (EC) surfaces during both vasculogenesis and angiogenesis [1, 14-16], we examined whether sialic acids of apical cell surface proteins contribute an electrostatic repulsion to initiate this process. We firstly analyzed the developing mouse aorta (Fig. 1), where a temporally and spatially defined transition from a non-lumenized EC cord to a lumenized tube takes place [1]. We find that sialic acids, detected using the *Tritrichomonas mobilensis* lectin [17], appear at the cell-cell contact (Fig. 1A, B) and co-localize with the apical marker PODXL at the cell-cell contact and luminal cell surfaces (data not shown). These data suggest that the sialic acids on apical cell surface proteins are positioned to separate apposing EC surfaces from each other to initiate blood vessel lumen formation in the developing mouse embryo.

It was previously shown that sialic acids can be removed from CD34-sialomucins by the enzymatic activity of neuraminidases, also known as sialidases [18]. To test whether sialic acids are required for vascular lumen formation *in vivo*, we injected

neuraminidase into the mesenchyme of mouse embryos at the onset of aortic lumen formation and allowed these embryos to develop in whole embryo culture (WEC) (Fig. 1) [1]. We found that the injection of neuraminidase significantly reduced the presence of sialic acids at the endothelial cell-cell contact (compare Fig. 1A and B with Fig. 1E and F). More importantly, these neuraminidase-treated embryos developed less lumenized aortae when compared with controls (compare Fig. 1C and D with Fig. 1G and H). The only lumenized dorsal aortae to develop were observed cranially and caudally, far away from the injection sites (data not shown).

Since sialic acids strongly contribute to the negative charge of apical cell surface proteins, we asked whether the negative charges of the apposing EC surfaces were required for vascular lumen formation. More precisely, we first asked whether re-introduction of negative charge to the neuraminidase-treated ECs could restore lumen formation (Suppl. Fig. S1). To this end, we injected dextran sulfate into mouse embryos, a negatively charged molecule that has been shown to bind to the apical cell surfaces of injured ECs *in vivo* [19, 20]. In our developing mouse aorta model we showed that dextran sulfate binds to the neuraminidase-treated apical cell surface of ECs (Suppl. Fig. S1I to K), and that it restores aortic lumen formation despite the absence of sialic acids (Suppl. Fig. S1I to M). In contrast, uncharged dextran does not rescue aortic lumen formation (Suppl. Fig. S1A to H). Importantly, neither treatment affected the EC viability or the expression of PODXL, moesin and F-actin at the apical cell surface (Fig. 1 and Suppl. Figure S1, and data not shown).

Secondly, we asked whether neutralization of the negative charge could inhibit lumen formation. We therefore injected into mouse embryos the cationic protamine sulfate, which was shown to neutralize the negative charge derived from sialic acids [21]. This injection significantly reduced the sialic acid staining, showing that

protamine sulfate effectively masked the sialic acids (compare Fig. 1A and B with Fig. 1I and J). More importantly, vascular lumen formation was reduced when compared with control (compare Fig. 1C and D with Fig. 1K and L). Taken together, these data strongly suggest that sialic acids and their negative charge are required on the apical EC surface for initiating a blood vessel lumen in the developing mouse embryo.

We next investigated whether sialic acids and their negative charge reduce adhesion of apposing EC surfaces (Fig. 2). To this end, we established a bead rolling assay (BRA) (Fig. 2A) in which human umbilical vein endothelial cells (HUVECs) expressing sialic acids at their apical EC surface were grown on collagen I-coated beads and cell culture dishes (Fig. 2A and B, and data not shown). The EC-covered beads were then transferred to the tilted EC monolayer to determine their rolling distance over time (Fig. 2A). This distance is an inverse measure for the adhesion of the apposing EC surfaces, since cell-cell adhesion is supposed to counteract gravity and thus inhibits the rolling of the beads. Indeed, the rolling distance of the beads increased with the steepness of the cell culture dish (Fig. 2J). Using the BRA, we found that neuraminidase-treated ECs had fewer sialic acids on their apical EC surface (compare Fig. 2A and B with Fig. 2D and E, and see Fig. 2K) and rolled over a significantly shorter distance compared with control (12% ±4%, $p < 0.01$) (compare Fig. 2C with 2F, and see Fig. 2L and Suppl. Movie M1). Moreover, addition of dextran sulfate, but not dextran, partially rescued the bead rolling, indicating that the negative charge is required for reducing cell-cell adhesion (Suppl. Fig. S2 and Suppl. Movie M2). Furthermore, treatment with protamine sulfate masked the sialic acids on apical EC surfaces (compare Fig. 2A and B with Fig. 2G and H, and see Fig. 2K), and the beads rolled over a shorter distance compared with the control (28% ±5%, *p*

< 0.001) (compare Fig. 2C with Fig. 2I, and see Fig. 2L and Suppl. Movie M1). Washing the HUVECs for 30 min and 24 hours reversed the effects of protamine sulfate and neuraminidase, respectively (Fig. 2L). These results demonstrate that sialic acids and their negative charge are required for reducing the adhesion between apposing EC surfaces.

Next, we quantified the adhesion strength between apposing ECs by using single-cell force spectroscopy (SCFS) (Fig. 3), which is based on atomic force microscopy (AFM) [22, 23]. Here the EC surfaces were brought into contact with each other and, after a dwell-time of 1, 10 or 20 seconds (s), we recorded the force needed to separate them (Fig. 3A to C). Neuraminidase treatment increased endothelial cell-cell adhesion after a contact time of 1 s (1.7x increase, $p < 0.001$ compared to control), 10 s (2.1x, $p < 0.001$ compared to control) and 20 s (2.9x, $p < 0.001$ compared to control) (compare Fig. 3A, D and G with Fig. 3B, E and H). Moreover, the low adhesion force between apposing ECs could be restored by adding dextran sulfate, but not by the addition of uncharged dextran (Suppl. Fig. S3). ECs treated with protamine sulfate also showed increasing cell-cell adhesion (1 s: 1.6x increase, 10 s: 2.1x, and 20 s: 2.3x, $p < 0.001$ compared to control) (compare Fig. 3A, D and G with Fig. 3C, F and I), but 30 min after washing, the low adhesion between ECs was restored at all contact times (data not shown). Thus, these force measurements directly confirm that ECs require sialic acids and their negative charge for lowering the cell-cell adhesion.

Lastly, we tested whether sialic acids and negative cell surface charge were also required for lumen formation during sprouting angiogenesis (Fig. 4), a process shown to be involved in blood vessel formation in the developing brain and retina as

well as in the growing tumor [24-27]. Here we employed an *in vitro* 3D sprouting angiogenesis assay [28], which reflects *in vivo* angiogenesis to a large extent [29-31]. We identified the vascular lumen in these sprouts based on brightfield and confocal light microscopic images. Using this assay, we found that sprouts harboring a small lumen developed into sprouts with virtually no vascular lumen upon neuraminidase treatment (compare Fig. 4A to C with Fig. 4D to F, and see Suppl. Movie M3). Importantly, lumen formation was partially restored by adding dextran sulfate, but not by the addition of uncharged dextran (Suppl. Fig. S4). In addition, sprouts treated with protamine sulfate also showed a reduction in vascular lumen development (compare Fig. 4A to C with Fig. 4G to I, and see Suppl. Movie M3). In both neuraminidase and protamine sulfate treatments, the apposing apical EC surfaces appear to adhere for longer times and thus have difficulties to separate in order to from a continuous and growing vascular lumen (Suppl. Movie M3). Therefore, sialic acids and negative cell surface charge are also required for lumen formation in angiogenic sprouts *in vitro*.

Taken together, our findings show that the blood vessel lumen develops from the electrostatic repulsion of apposing EC surfaces. Since negatively charged glycoproteins, such as mucins and proteoglycans, are found on most luminal cell surfaces, such as the ones of tracheae, gut tubes, kidney tubules, pancreatic ducts and the tubes of testis and mammary glands, it is possible that electrostatic repulsion is a general principle used to initiate lumen formation in many organs throughout the animal kingdom.

Experimental Procedures

Antibodies and reagents

Goat anti-PODXL (R&D Systems), rat anti-PECAM-1 (BD Bioscience), rabbit anti-moesin (abcam), Alexa Fluor 488 phalloidin (Invitrogen) and biotinylated *T. mobilensis* lectin [17] were used for immunostainings. DAPI (Sigma) was used to stain cell nuclei. Secondary antibodies were conjugated with AF488, AF633 (Molecular Probes), Cy3 or Cy5 (Jackson ImmunoResearch). Neuraminidase (0.5 U/ml, Sigma) or protamine sulfate (0.5 mg/ml, Sigma) were used for whole embryo culture (WEC), the bead rolling assay (BRA) and for single-cell force spectroscopy (SCFS) experiments. Low molecular weight dextran (Sigma) and dextran sulfate (Sigma) were used at 1 mg/ml for WEC and at 10 mg/ml for BRA and SCFS. FITC-conjugated dextran sulfate [32] was used at 1 mg/ml for labeling the neuraminidase treated apical cell surfaces of aortic ECs. For the 3D sprouting angiogenesis assay, fibrinogen (2.5 mg/ml, Sigma), aprotinin (0.15 U/ml, Sigma), thrombin (4 U/ml, Sigma), neuraminidase (0.06 U/ml), and protamine sulfate (0.5 mg/ml) were used. Poly-DL-alanine (0.5 mg/ml, Sigma) or PBS served as controls in each assay.

Mouse embryo isolation, embryonic injections and WEC

Isolated NMRI or CD1 mouse embryos (Janvier, France) were sorted by their numbers of somites. All embryos, after isolation or whole embryo culture (WEC), were fixed in 4% paraformaldehyde (PFA) in PBS and further processed for imaging. WEC was performed as previously described [1]. Briefly, all substances were injected into embryos at the 2S stage from the ventral side through the endoderm into the mesenchyme. After injection, embryos were roller-cultured for the indicated time periods and processed for immunostaining and imaging.

Immunostaining and imaging

Immunostaining and imaging was performed as previously described [1]. Images were acquired and analyzed by using a Zeiss Laser Scanning Microscope (LSM510 or LSM710) and ImageJ (NIH), respectively. For the identification of ECs, all sections were co-stained for PECAM-1.

Cell culture

Human umbilical vein endothelial cells (HUVEC, Lonza) of passages <P6 were used for all experiments. HUVECs and human skin fibroblast cells (HSF Detroit 551, Promochem) were grown in EGM-2 medium (Lonza) and MEM (supplemented with 10% FCS), respectively, and incubated at 37°C and 5% CO_2. The media were changed every other day.

Bead Rolling Assay (BRA)

HUVECs were seeded on collagen I-coated Cytodex-3 beads (GE Healthcare) and collagen I-coated wells of a 6-well plate. On the second day, ~100 HUVEC-coated beads were transferred to each well containing a confluent HUVEC monolayer, which was tilted by ~20 degrees. The rolling distance was subsequently recorded over 5 min (SMZ1500 and NIS-elements, Nikon) at 30 frames per minute. Neuraminidase or protamine sulfate were subsequently added for 30 min, and the measurements were repeated. In addition, the cells were subsequently washed with fresh medium and incubated for 30 min or 24 hours, and rolling distances were then determined using the BRA. Alternatively, dextran or dextran sulfate were added for 30 min to neuraminidase-treated cells, and measurements were repeated. Rolling distances of the respective treatments were normalized to the controls and analyzed using ImageJ (NIH).

Single-Cell Force Spectroscopy (SCFS)

SCFS experiments were conducted by using AFM as previously described [33]. In brief, HUVECs were cultured on a collagen I-coated coverslip. On the second day, the confluent coverslips were carefully rinsed with EGM-2 medium and built into a BioCell (JPK Instruments) for measurements at a physiological temperature (37°C), and JPK NanoWizard equipped with a CellHesion module (JPK Instruments) for long distance pulling. Next, 50 µl of a single cell suspension (~ 500 cells) was added into the BioCell, and a single cell was picked with a Concanavalin A-coated tipless AFM cantilever (NP-0, nominal spring constant 60 mN/m; Veeco Instruments) using a constant contact force of 1 nN. Adhesion measurements were carried out with an approach and retract velocity of 5 µm/s, a contact force of 1 nN and a contact time randomly changed between 1, 10 and 20 seconds at different spots of the underlying monolayer. Force-distance curves were analyzed using custom procedures in IgorPro (Wavemetrics, [23]). Before each experiment, spring constant measurements were performed on undecorated glass slides using the thermal noise method [34].

3D sprouting angiogenesis assay

The 3D sprouting angiogenesis assay was performed as previously described [28]. Briefly, collagen I-coated Cytodex-3 beads (GE Healthcare) were coated with HUVECs. On the next day, beads were resuspended in PBS containing fibrinogen and aprotinin and mixed with thrombin to yield a fibrin hydrogel. The solidified fibrin gel was subsequently overlaid with human skin fibroblasts (ATCC). PBS (control), neuraminidase or protamine sulfate were added when a vascular lumen started to develop, and sprouts were imaged on an inverted microscope (Zeiss Axio Observer Z1) every 20 min for 26 h. Per condition, six independent wells were imaged with five

fields of view per well. Sprouts of a minimal length of 50 µm were counted at the end of the treatment period, and classified as lumenized if more than 10% of the sprout length contained a visible lumen (measured from sprout stalk to sprout tip, starting at 20 µm distance from the bead). Sprout lumens were detected on the corresponding brightfield image as previously shown [31] and pseudo-colored in yellow.

Statistical Analysis

Data are presented as means ±SD or ±SEM (see Figure legends). Student's t-tests were used for statistical analyses. $p < 0.05$ was considered statistically significant.

Acknowledgements

We thank R. Yu, D. Lingwood and F. Oesterhelt, and all our friends and colleagues for helpful discussions. We are also grateful to R. Rieben and N. Bovin for their kind support and sharing the FITC-conjugated dextran sulfate. The German Research Foundation funded this project (DFG; LA1216/4-1).

References

1. Strilic, B., Kucera, T., Eglinger, J., Hughes, M.R., McNagny, K.M., Tsukita, S., Dejana, E., Ferrara, N., and Lammert, E. (2009). The molecular basis of vascular lumen formation in the developing mouse aorta. Dev Cell *17*, 505-515.

2. Tarbell, J.M., and Ebong, E.E. (2008). The endothelial glycocalyx: a mechano-sensor and -transducer. Sci Signal *1*, pt8.

3. Ng, A.N., de Jong-Curtain, T.A., Mawdsley, D.J., White, S.J., Shin, J., Appel, B., Dong, P.D., Stainier, D.Y., and Heath, J.K. (2005). Formation of the digestive system in zebrafish: III. Intestinal epithelium morphogenesis. Dev Biol *286*, 114-135.

4. Kesavan, G., Sand, F.W., Greiner, T.U., Johansson, J.K., Kobberup, S., Wu, X., Brakebusch, C., and Semb, H. (2009). Cdc42-mediated tubulogenesis controls cell specification. Cell *139*, 791-801.

5. Braga, V.M., Pemberton, L.F., Duhig, T., and Gendler, S.J. (1992). Spatial and temporal expression of an epithelial mucin, Muc-1, during mouse development. Development *115*, 427-437.

6. Jones, S.J., and Baillie, D.L. (1995). Characterization of the let-653 gene in Caenorhabditis elegans. Mol Gen Genet *248*, 719-726.

7. Dinglasan, R.R., Alaganan, A., Ghosh, A.K., Saito, A., van Kuppevelt, T.H., and Jacobs-Lorena, M. (2007). Plasmodium falciparum ookinetes require mosquito midgut chondroitin sulfate proteoglycans for cell invasion. Proc Natl Acad Sci U S A *104*, 15882-15887.

8. Ayers, K.L., Gallet, A., Staccini-Lavenant, L., and Therond, P.P. (2010). The long-range activity of Hedgehog is regulated in the apical extracellular space by the glypican Dally and the hydrolase Notum. Dev Cell *18*, 605-620.

9. Tian, E., and Ten Hagen, K.G. (2007). A UDP-GalNAc:polypeptide N-acetylgalactosaminyltransferase is required for epithelial tube formation. J Biol Chem *282*, 606-614.

10. Husain, N., Pellikka, M., Hong, H., Klimentova, T., Choe, K.M., Clandinin, T.R., and Tepass, U. (2006). The agrin/perlecan-related protein eyes shut is essential for epithelial lumen formation in the Drosophila retina. Dev Cell *11*, 483-493.

11. Meder, D., Shevchenko, A., Simons, K., and Fullekrug, J. (2005). Gp135/podocalyxin and NHERF-2 participate in the formation of a preapical domain during polarization of MDCK cells. J Cell Biol *168*, 303-313.

12. Martin-Belmonte, F., Gassama, A., Datta, A., Yu, W., Rescher, U., Gerke, V., and Mostov, K. (2007). PTEN-mediated apical segregation of phosphoinositides controls epithelial morphogenesis through Cdc42. Cell *128*, 383-397.

13. Nielsen, J.S., and McNagny, K.M. (2008). Novel functions of the CD34 family. J Cell Sci *121*, 3683-3692.

14. Parker, L.H., Schmidt, M., Jin, S.W., Gray, A.M., Beis, D., Pham, T., Frantz, G., Palmieri, S., Hillan, K., Stainier, D.Y., et al. (2004). The endothelial-cell-derived secreted factor Egfl7 regulates vascular tube formation. Nature *428*, 754-758.

15. Blum, Y., Belting, H.G., Ellertsdottir, E., Herwig, L., Luders, F., and Affolter, M. (2008). Complex cell rearrangements during intersegmental vessel sprouting and vessel fusion in the zebrafish embryo. Dev Biol *316*, 312-322.

16. Jin, S.W., Beis, D., Mitchell, T., Chen, J.N., and Stainier, D.Y. (2005). Cellular and molecular analyses of vascular tube and lumen formation in zebrafish. Development *132*, 5199-5209.

17. Babal, P., and Gardner, W.A., Jr. (1996). Histochemical localization of sialylated glycoconjugates with Tritrichomonas mobilensis lectin (TLM). Histol Histopathol *11*, 621-631.

18. Gelberg, H., Healy, L., Whiteley, H., Miller, L.A., and Vimr, E. (1996). In vivo enzymatic removal of alpha 2-->6-linked sialic acid from the glomerular filtration barrier results in podocyte charge alteration and glomerular injury. Lab Invest *74*, 907-920.

19. Eto, N., Kojima, I., Uesugi, N., Inagi, R., Miyata, T., Fujita, T., Johnson, R.J., Shankland, S.J., and Nangaku, M. (2005). Protection of endothelial cells by dextran sulfate in rats with thrombotic microangiopathy. J Am Soc Nephrol *16*, 2997-3005.

20. Laumonier, T., Mohacsi, P.J., Matozan, K.M., Banz, Y., Haeberli, A., Korchagina, E.Y., Bovin, N.V., Vanhove, B., and Rieben, R. (2004). Endothelial cell protection by dextran sulfate: a novel strategy to prevent acute vascular rejection in xenotransplantation. Am J Transplant *4*, 181-187.

21. Takeda, T., McQuistan, T., Orlando, R.A., and Farquhar, M.G. (2001). Loss of glomerular foot processes is associated with uncoupling of podocalyxin from the actin cytoskeleton. J Clin Invest *108*, 289-301.

22. Puech, P.H., Taubenberger, A., Ulrich, F., Krieg, M., Muller, D.J., and Heisenberg, C.P. (2005). Measuring cell adhesion forces of primary gastrulating cells from zebrafish using atomic force microscopy. J Cell Sci *118*, 4199-4206.

23. Krieg, M., Arboleda-Estudillo, Y., Puech, P.H., Kafer, J., Graner, F., Muller, D.J., and Heisenberg, C.P. (2008). Tensile forces govern germ-layer organization in zebrafish. Nat Cell Biol *10*, 429-436.

24. Tammela, T., Zarkada, G., Wallgard, E., Murtomaki, A., Suchting, S., Wirzenius, M., Waltari, M., Hellstrom, M., Schomber, T., Peltonen, R., et al. (2008). Blocking VEGFR-3 suppresses angiogenic sprouting and vascular network formation. Nature *454*, 656-660.

25. Gerhardt, H., Golding, M., Fruttiger, M., Ruhrberg, C., Lundkvist, A., Abramsson, A., Jeltsch, M., Mitchell, C., Alitalo, K., Shima, D., et al. (2003). VEGF guides angiogenic sprouting utilizing endothelial tip cell filopodia. J Cell Biol *161*, 1163-1177.

26. Hellstrom, M., Phng, L.K., Hofmann, J.J., Wallgard, E., Coultas, L., Lindblom, P., Alva, J., Nilsson, A.K., Karlsson, L., Gaiano, N., et al. (2007). Dll4 signalling through Notch1 regulates formation of tip cells during angiogenesis. Nature *445*, 776-780.

27. Stenman, J.M., Rajagopal, J., Carroll, T.J., Ishibashi, M., McMahon, J., and McMahon, A.P. (2008). Canonical Wnt signaling regulates organ-specific assembly and differentiation of CNS vasculature. Science *322*, 1247-1250.

28. Nakatsu, M.N., Sainson, R.C., Aoto, J.N., Taylor, K.L., Aitkenhead, M., Perez-del-Pulgar, S., Carpenter, P.M., and Hughes, C.C. (2003). Angiogenic sprouting and capillary lumen formation modeled by human umbilical vein endothelial cells (HUVEC) in fibrin gels: the role of fibroblasts and Angiopoietin-1. Microvasc Res *66*, 102-112.

29. Ridgway, J., Zhang, G., Wu, Y., Stawicki, S., Liang, W.C., Chanthery, Y., Kowalski, J., Watts, R.J., Callahan, C., Kasman, I., et al. (2006). Inhibition of Dll4 signalling inhibits tumour growth by deregulating angiogenesis. Nature *444*, 1083-1087.

30. Kleaveland, B., Zheng, X., Liu, J.J., Blum, Y., Tung, J.J., Zou, Z., Sweeney, S.M., Chen, M., Guo, L., Lu, M.M., et al. (2009). Regulation of cardiovascular development and integrity by the heart of glass-cerebral cavernous malformation protein pathway. Nat Med *15*, 169-176.

31. Nikolova, G., Strilic, B., and Lammert, E. (2007). The vascular niche and its basement membrane. Trends Cell Biol *17*, 19-25.

32. Laumonier, T., Walpen, A.J., Maurus, C.F., Mohacsi, P.J., Matozan, K.M., Korchagina, E.Y., Bovin, N.V., Vanhove, B., Seebach, J.D., and Rieben, R. (2003). Dextran sulfate acts as an endothelial cell protectant and inhibits human complement and natural killer cell-mediated cytotoxicity against porcine cells. Transplantation *76*, 838-843.

33. Puech, P.H., Poole, K., Knebel, D., and Muller, D.J. (2006). A new technical approach to quantify cell-cell adhesion forces by AFM. Ultramicroscopy *106*, 637-644.

34. Hutter, J.L., and Bechhoefer, J. (1993). Calibration of atomic force microscope tips. Rev Sci Instrum *64*, 1868-1873.

Figure Legends

Figure 1 Removal of sialic acids or neutralization of the negative charge inhibits blood vessel lumen formation

Confocal images of transverse sections through the developing mouse dorsal aortae and quantification of blood vessel lumen formation. (A to D) Effects of poly-DL-alanine (control), (E to H) neuraminidase and (I to L) protamine sulfate on the localization of sialic acids and podocalyxin (PODXL) at the endothelial cell-cell contact, and on aortic lumen formation (asterisks). (A, B, E, F, I, J) Confocal images showing (A, E, I) sialic acids or (B, F, J) PODXL on transverse sections through dorsal aortae after whole embryo culture (WEC) of mouse embryos from the 2S to 2-3S stage for 30 min. (C, G, K) Confocal images showing PECAM-1 endothelial staining on transverse sections through dorsal aortae after WEC from the 2S to 7S stage for 5-7 h after the treatment indicated on the left. Arrows point to the endothelial cell-cell contact. Arrowheads point to non-lumenized dorsal aortae, whereas asterisks mark the vascular lumen. EC, endothelial cell; En, endoderm; NE, neuroepithelium. Scale bars = 5 μm (A, B, E, F, I, J) and 20 μm (C, G, K).
(D, H, L) Quantification of EC cords (“No Lumen”, white bar) and vascular tubes (“Lumen”, black bar) after WEC from the 2S to 7S stage following the treatment indicated on the left. n ≥ 100 aortic sections of n ≥ 3 embryos per condition. All values are means ±SD.

Figure 2 Sialic acids and negative cell-surface charges are required for de-adhesion of apposing endothelial cell surfaces

(A, D, G) Schematic diagram of a bead rolling assay (BRA) experiment under (A) control conditions and after treatment with (D) neuraminidase or (G) protamine sulfate. The negative charges of sialic acids are shown in green (-) and the positive charges of protamine sulfate are shown in red (+). Black arrows indicate the rolling of the HUVEC-coated beads on the tilted HUVEC monolayer.

(B, E, H) Confocal images of transverse sections through endothelial cells (ECs) grown on collagen I-coated beads and stained for sialic acids after the treatment indicated on the left.

(C, F, I) Brightfield images of movies showing EC-coated beads rolling on a tilted EC monolayer. Time is indicated in min:sec. See also suppl. movie M1. Scale bars = 5 µm (B, E, H) and 100 µm (C, F, I).

(J) Quantification of the rolling distance in relation to the steepness of the monolayer. n ≥ 90 beads per angle (degree). All values are means ±SD.

(K) Quantification of the fluorescence intensity of sialic acid staining on the surface of ECs grown on collagen I-coated beads after the treatment indicated below. n ≥ 10 beads per treatment. *$p < 0.05$. All values are means ±SD.

(L) Quantification of the rolling distance of EC-coated beads on a tilted EC monolayer directly after treatment (black bars), 30 min after washing (grey bars) or 24h after washing (white bar). n ≥ 300 beads per treatment from n ≥ 3 independent experiments. *$p < 0.05$. All values are means ±SEM.

Figure 3 Quantification of adhesion forces between apposing endothelial cell surfaces after neuraminidase and protamine sulfate treatment by single-cell force spectroscopy (SCFS)

(A to C) Schematic diagram of an adhesion experiment under (A) control conditions and after treatment with (B) neuraminidase or (C) protamine sulfate. The negative charges of sialic acids are shown in green (-) and the positive charges of protamine sulfate are shown in red (+). An endothelial cell (EC) grown onto an atomic force microscopy (AFM) cantilever was brought into contact with the EC monolayer. Black dashed lines indicate the laser beam to measure the cantilever deflection. After a given contact time (1 s, 10 s, 20 s), the cantilever was withdrawn to separate the ECs and to measure their adhesive forces. Black arrows indicate the adhesive force between the single EC and the EC monolayer causing the cantilever to deflect downwards. The thickness of the arrow reflects the magnitude of the adhesive strength between the cells.

(D to F) Representative force-distance curves (20 s) after treatment indicated above. Approach curves of the cantilevers towards the EC monolayer are shown in grey. Withdrawal curves are shown in black and are used to estimate the maximum adhesion force (arrow).

(G to I) Quantification of the adhesion force between ECs and an EC monolayer after 1 s (black bar), 10 s (grey bar) and 20 s (white bar) contact times and treatment indicated above. $n \geq 12$ independent experiments with $n \geq 56$ measurements per condition and contact time. All values are means ±SEM. (H, I) Numbers on the bars indicate fold change compared to (G) control for the respective contact time.

Figure 4 Sialic acids and negative cell-surface charges are required for vascular lumen formation in angiogenic sprouts

(A, D, G) Schematic overviews on lumen formation in angiogenic sprouts under (A) control conditions and after treatment with (D) neuraminidase or (G) protamine sulfate. The negative charges of sialic acids are shown in green (-) and the positive charges of protamine sulfate are shown in red (+). The vascular lumen is indicated in yellow.

(B, E, H) Brightfield images of angiogenic sprouts 26h after the treatment indicated on the left. The vascular lumen is pseudocolored in yellow. See also suppl. movie M3. Scale bars = 20 μm.

(C, F, I) Quantification of lumen formation in sprouts 26h after the treatment indicated on the left. $n \geq 35$ sprouts from $n = 6$ experiments per treatment. All values are means ±SEM.

Inventory of Supplemental Items

Supplemental Figures S1 to S4 relate to Figures 1 to 4. They show that aortic lumen formation (Suppl. Fig. S1), bead rolling (Suppl. Fig. S2), cell-cell de-adhesion (Suppl. Fig. S3), and lumen formation in angiogenic sprouts (Suppl. Fig. S4) can be restored in de-sialylated endothelial cells by addition of negatively charged dextran sulfate, but not by the addition of non-charged dextran. Supplemental movies M1 to M3 show that (i) de-sialylation of endothelial cells or neutralization of their negative cell surface charges inhibits bead rolling (M1), (ii) de-sialylated endothelial cells start to de-adhere upon addition of negatively charged dextran sulfate but not upon addition of uncharged dextran (M2), and (iii) de-sialylation of endothelial cells or neutralization of their negative cell surface charges inhibits lumen formation in angiogenic sprouts (M3).

Suppl. Figure S1 Addition of negative charges restores vascular lumen formation in the developing mouse aorta after neuraminidase treatment

Confocal images of transverse sections through the developing mouse dorsal aortae and quantification of blood vessel lumen formation. Effect of (A to D) neuraminidase, (E to H) neuraminidase plus uncharged dextran (control), and effect of (I to M) neuraminidase plus negatively charged dextran sulfate on the presence of sialic acids and podocalyxin (PODXL) at the endothelial cell-cell contact and on aortic lumen formation. (A, B, E, F, I to K) Confocal images showing the location of (A, E, I) sialic acids, (B, F, J) PODXL and (K) FITC-labeled dextran sulfate on transverse sections through dorsal aortae after whole embryo culture (WEC) of mouse embryos from the 2S to the 2-3S stage for 30 min. Arrows point to the endothelial cell-cell contact. (C, G, L) Confocal images showing PECAM-1 endothelial cell staining on transverse sections through dorsal aortae after WEC from the 2S to 7S stage for 5-7 h after the treatment indicated on the left. Arrowheads point to non-lumenized dorsal aortae, whereas asterisks mark the vascular lumen. EC, endothelial cell; En, endoderm; NE, neuroepithelium. Scale bars = 5 μm (A, B, E, F, I to K) and 20 μm (C, G, L).

(D, H, M) Quantification of EC cords (“No Lumen”, white bars) and vascular tubes (“Lumen”, black bars) after WEC from the 2S to 7S stage following the treatment indicated on the left. n ≥ 90 aortic sections of n ≥ 3 embryos per condition. All values are means ±SD.

Suppl. Figure S2 Addition of negative charges restores de-adhesion of apposing endothelial cell surfaces after removal of sialic acids

(A, C, E, G) Schematic diagrams of a bead rolling assay (BRA) experiment under (A) control conditions (PBS) and after treatment with (C) neuraminidase, (E) neuraminidase plus dextran and (G) neuraminidase plus the negatively charged dextran sulfate. The negative charges of (A) sialic acids and (G) dextran sulfate are shown in green (-). Black arrows indicate the rolling of the HUVEC-coated beads on the tilted HUVEC monolayer.

(B, D, F, H) Brightfield images of movies showing EC-coated beads rolling on a tilted EC monolayer. Time is indicated in min:sec. See also suppl. movie M2. Scale bars = 100 µm (B, D, F, H).

(I) Quantification of the rolling distance of EC-coated beads on a tilted EC monolayer directly after the treatments indicated below. $n \geq 300$ beads analyzed per treatment in $n \geq 3$ independent experiments. $*p < 0.05$. All values are means ±SEM.

Suppl. Figure S3 SCFS-based quantification of adhesion forces between apposing endothelial cell surfaces after neuraminidase treatment and addition of dextran or dextran sulfate

(A to C) Schematic diagrams of an adhesion experiment after treatment with (A) neuraminidase, (B) neuraminidase plus dextran (control) and (C) neuraminidase plus the negatively charged dextran sulfate. The negative charges of dextran sulfate are shown in green (-). An endothelial cell (EC) grown onto an atomic force microscopy (AFM) cantilever was brought into contact with an EC monolayer. Black dashed lines indicate the laser beam to measure the cantilever deflection. After a given contact time (1 s, 10 s, 20 s), the cantilever was withdrawn to separate the ECs and to measure their adhesive forces. Black arrows indicate the adhesive force between the single EC and the EC monolayer causing the cantilever to deflect downwards. The thickness of the arrow reflects the magnitude of the adhesive strength between the cells.

(D to F) Representative force-distance curves (20 s) after the treatments indicated above. Approach curves of the cantilevers towards the EC monolayer are shown in grey. Withdrawal curves are shown in black and are used to estimate the maximum adhesion forces (arrow).

(G to I) Quantification of the adhesion force between ECs and an EC monolayer after 1 s (black bar), 10 s (grey bar) and 20 s (white bar) contact times and the treatments indicated above. $n \geq 7$ independent experiments with $n \geq 27$ measurements per condition and contact time. All values are means ±SEM. (H, I) Numbers on the bars indicate fold change compared to (G) for the respective contact time.

Suppl. Figure S4 Reduced vascular lumen formation in angiogenic sprouts after removal of sialic acids can be restored through addition of negative charge

(A, D, G) Schematic overviews on lumen formation in angiogenic sprouts after treatment with (A) neuraminidase, (D) neuraminidase plus dextran or (G) neuraminidase plus dextran sulfate. The negative charges of dextran sulfate are shown in green (-) and the vascular lumen is indicated in yellow.

(B, E, H) Brightfield images of angiogenic sprouts 48h after the treatment indicated on the left. The lumen is pseudocolored in yellow. Scale bars, 20 μm.

(C, F, I) Quantification of lumen formation in sprouts 48h after the treatment indicated on the left. n ≥ 50 sprouts from n = 6 experiments per treatment. All values are means ±SEM.

Supplemental movie M1

Bead rolling assay (BRA)

Representative time-lapse movies of HUVEC-coated beads on a tilted HUVEC monolayer, untreated (control) or after addition of neuraminidase or protamine sulfate (from left to right). Images were acquired every 2 seconds over a total time of 5 minutes.

Supplemental movie M2

Bead rolling assay (BRA)

Representative time-lapse movies of HUVEC-coated beads on a tilted HUVEC monolayer, untreated (control), after addition of neuraminidase, after addition of neuraminidase plus dextran, and after addition of neuraminidase plus negatively charged dextran sulfate (from left to right). Images were acquired every 2 seconds over a total time of 5 minutes.

Supplemental movie M3

3D sprouting angiogenesis

Representative time-lapse movies of angiogenic sprouts were started following no treatment (control) or treatment with neuraminidase or protamine sulfate (from top to bottom). Images were acquired every 20 minutes over a total time of 10 hours.

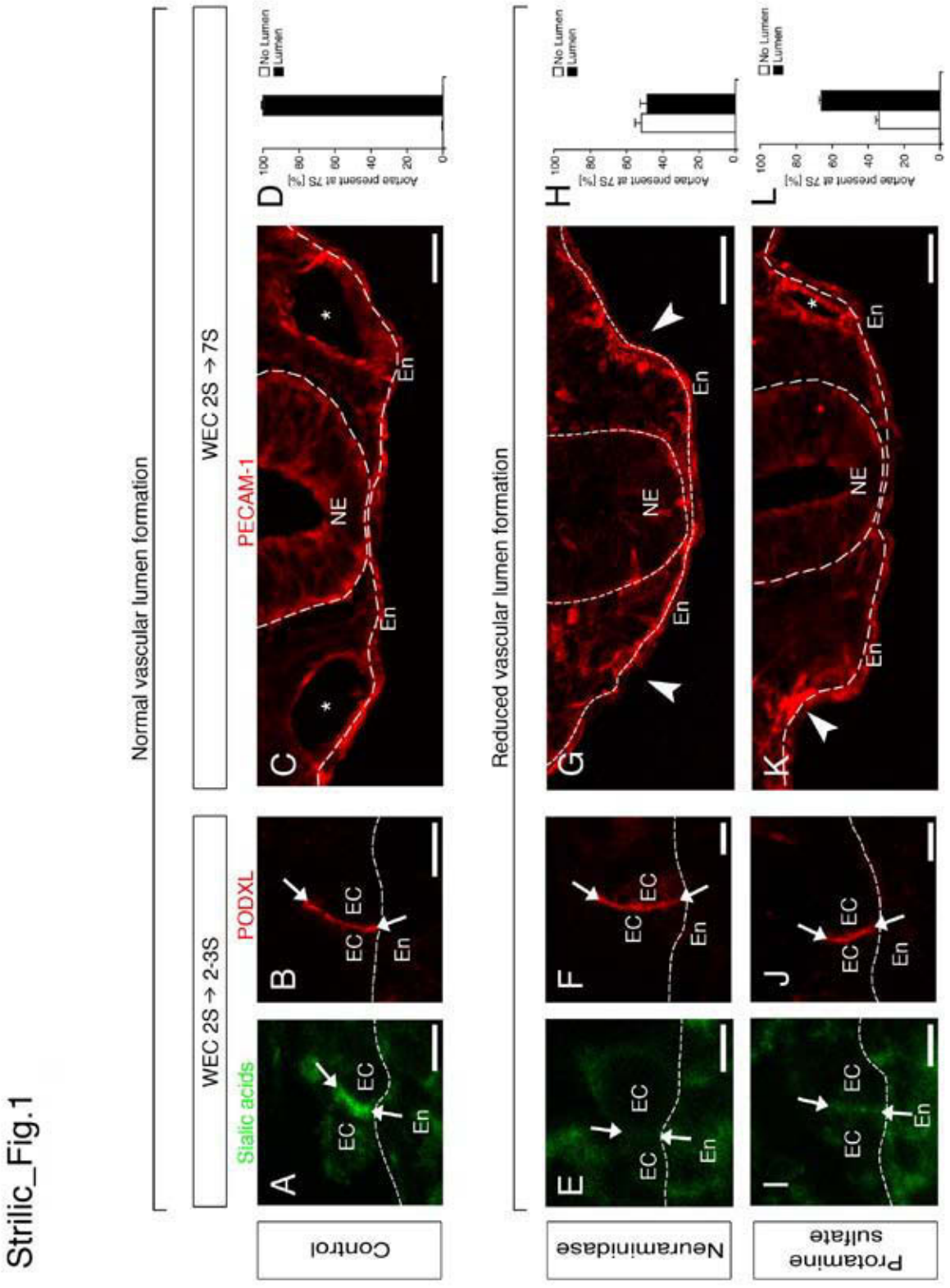
Strilic_Fig.1
Normal vascular lumen formation
Reduced vascular lumen formation
WEC 2S → 2-3S
WEC 2S → 7S
Control
Neuraminidase
Protamine sulfate
Sialic acids
PODXL
PECAM-1
No Lumen
Lumen
Aortae present at 7S [%]
EC
En
NE
A
B
C
D
E
F
G
H
I
J
K
L

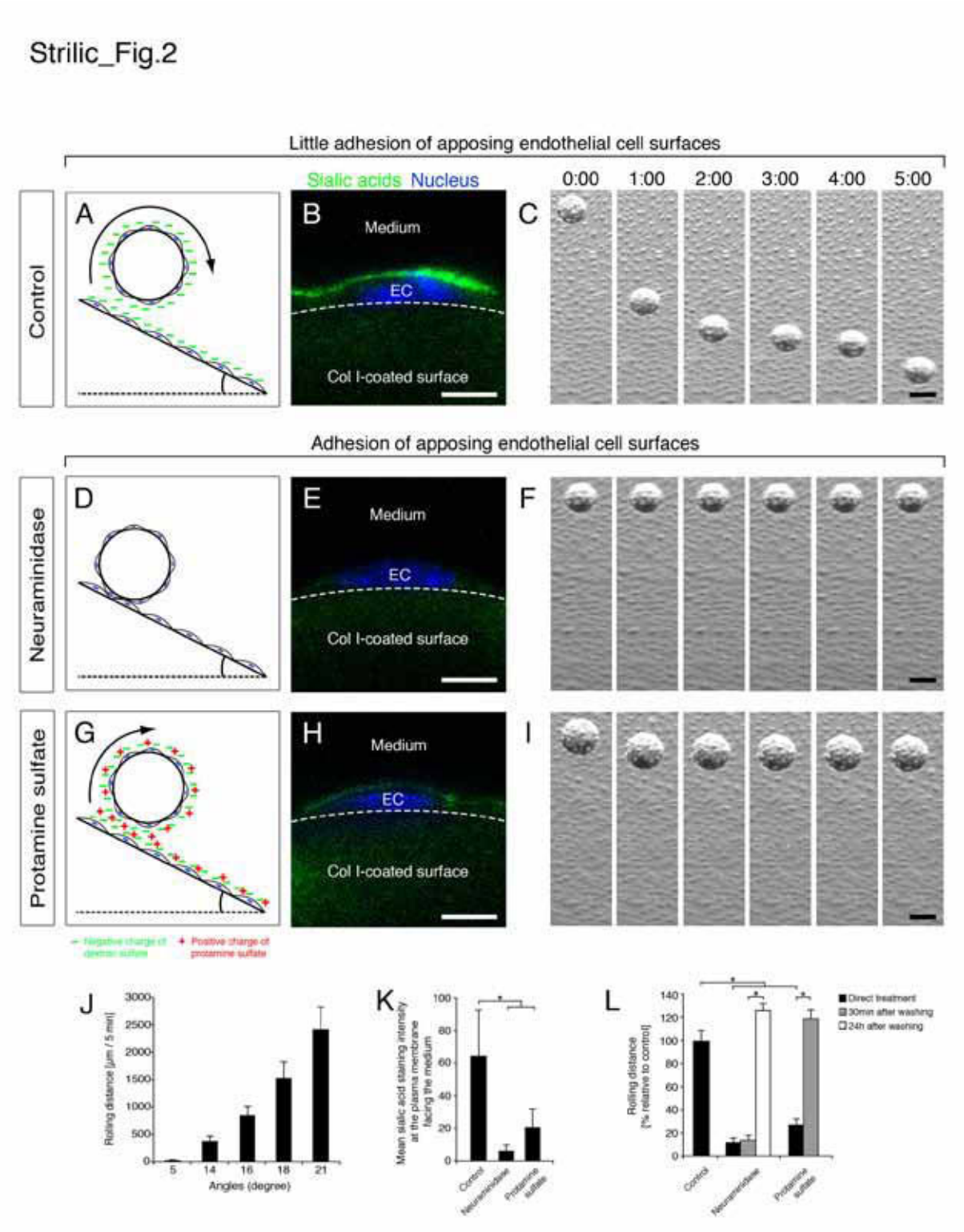
Strilic_Fig.2
Little adhesion of apposing endothelial cell surfaces
Sialic acids Nucleus
0:00
1:00
2:00
3:00
4:00
5:00
Control
A
B
Medium
EC
Col I-coated surface
C
Adhesion of apposing endothelial cell surfaces
Neuraminidase
D
E
Medium
EC
Col I-coated surface
F
Protamine sulfate
G
H
Medium
EC
Col I-coated surface
I
J
Rolling distance [µm / 5 min]
Angles (degree)
K
Mean sialic acid staining intensity at the plasma membrane facing the medium
Control
Neuraminidase
Protamine sulfate
L
Rolling distance [% relative to control]
Direct treatment
30min after washing
24h after washing
Control
Neuraminidase
Protamine sulfate

Strilic_Fig.3

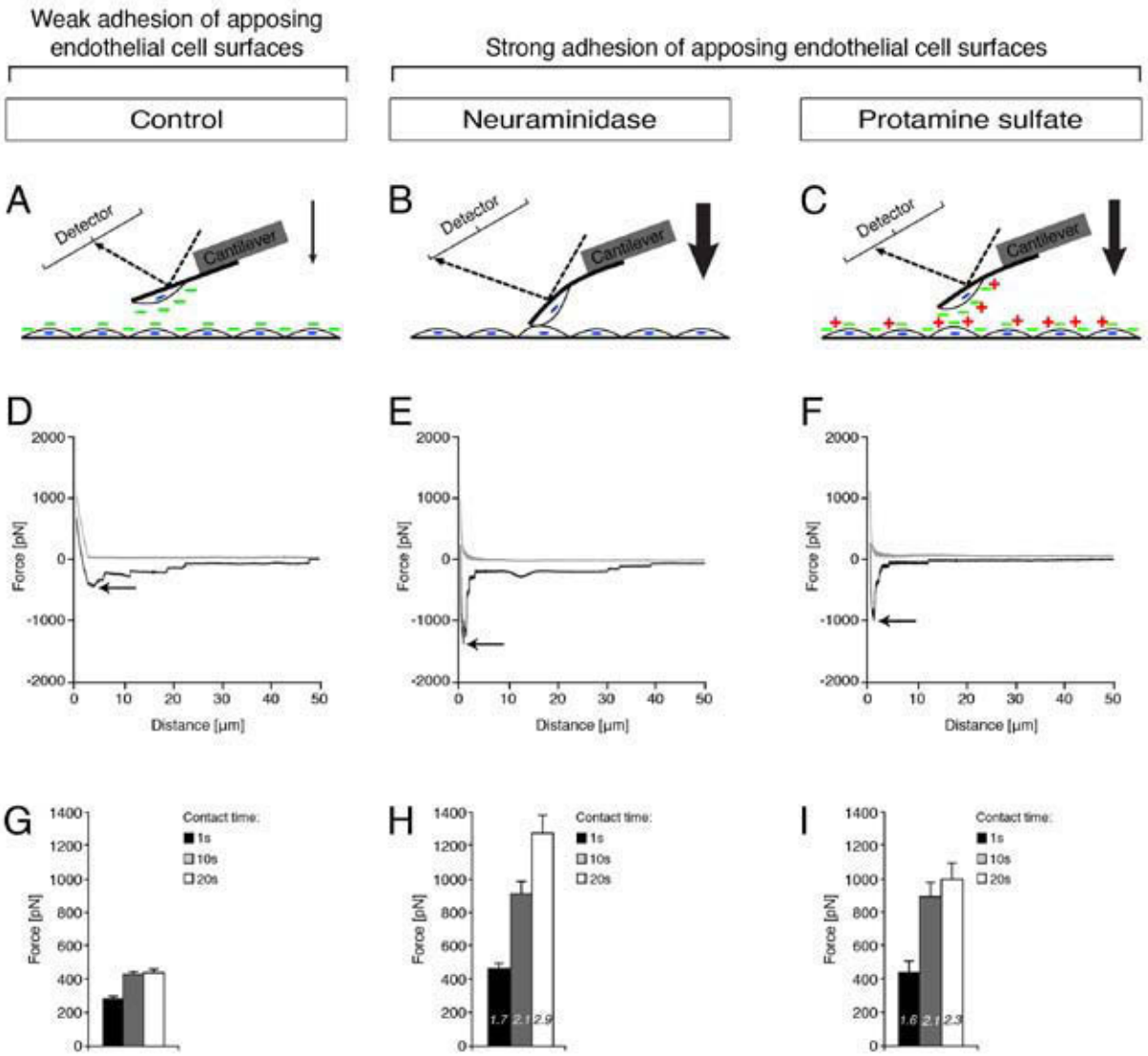

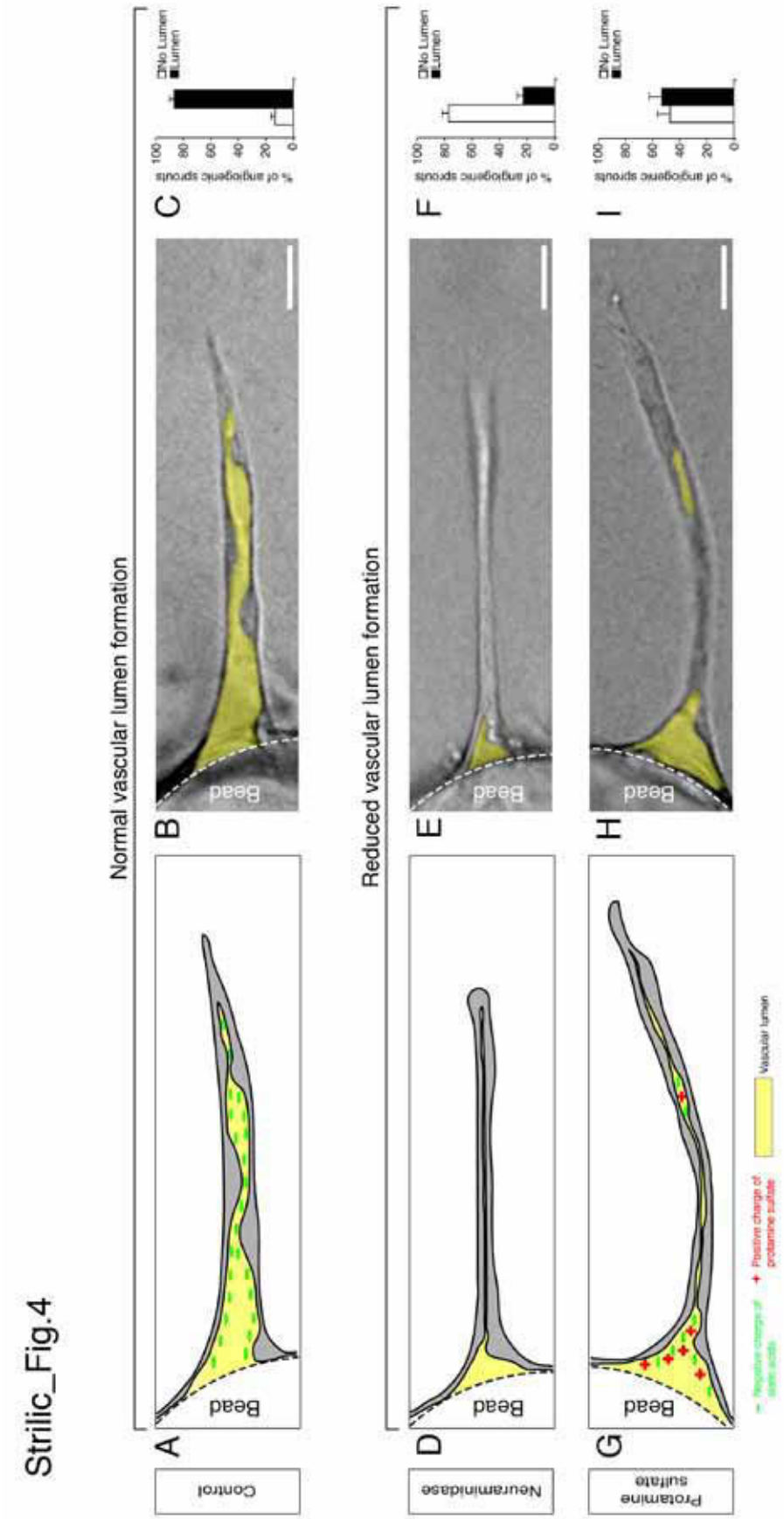
Strilic_Fig.4
Normal vascular lumen formation
Reduced vascular lumen formation
Control
Neuraminidase
Protamine sulfate
A
B
C
D
E
F
G
H
I
Bead
No Lumen
Lumen
% of angiogenic sprouts
Vascular lumen

Strilic_Suppl._Fig.S1

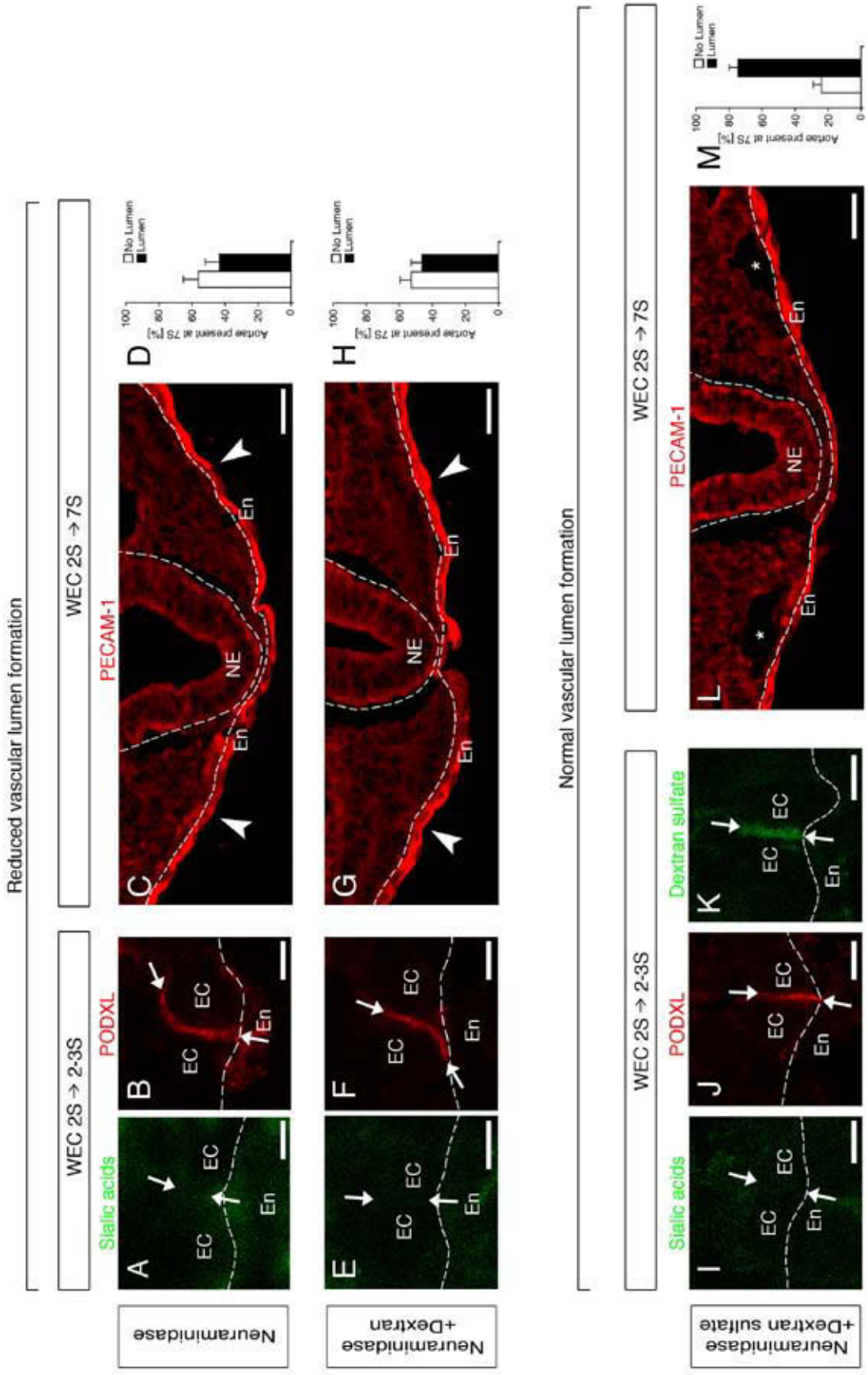

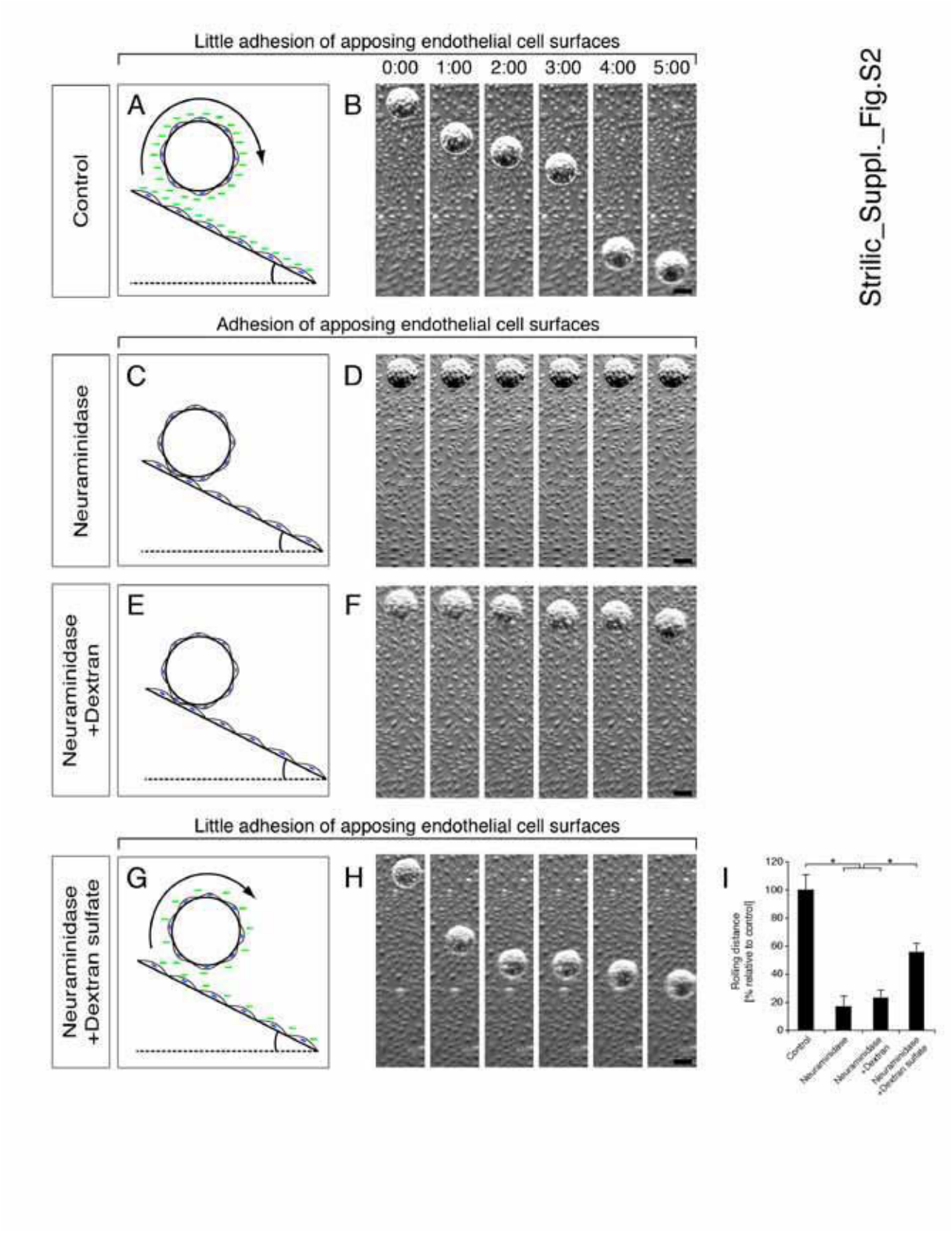
Little adhesion of apposing endothelial cell surfaces
0:00
1:00
2:00
3:00
4:00
5:00
Control
A
B
Adhesion of apposing endothelial cell surfaces
Neuraminidase
C
D
Neuraminidase +Dextran
E
F
Little adhesion of apposing endothelial cell surfaces
Neuraminidase +Dextran sulfate
G
H
I
Rolling distance [% relative to control]
120
100
80
60
40
20
0
Control
Neuraminidase
Neuraminidase +Dextran
Neuraminidase +Dextran sulfate
Strilic_Suppl._Fig.S2

Strilic_Suppl._Fig.S3

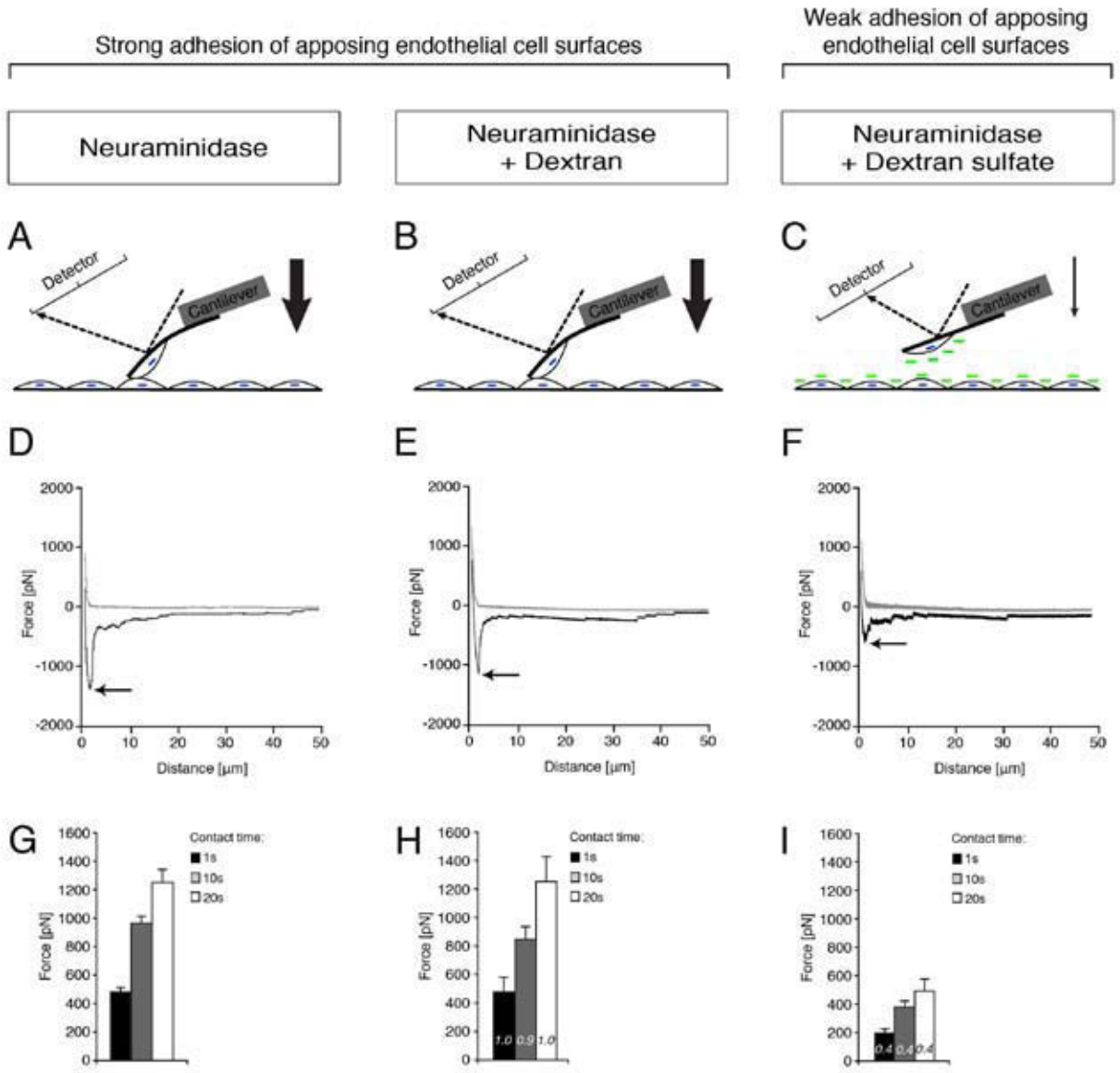

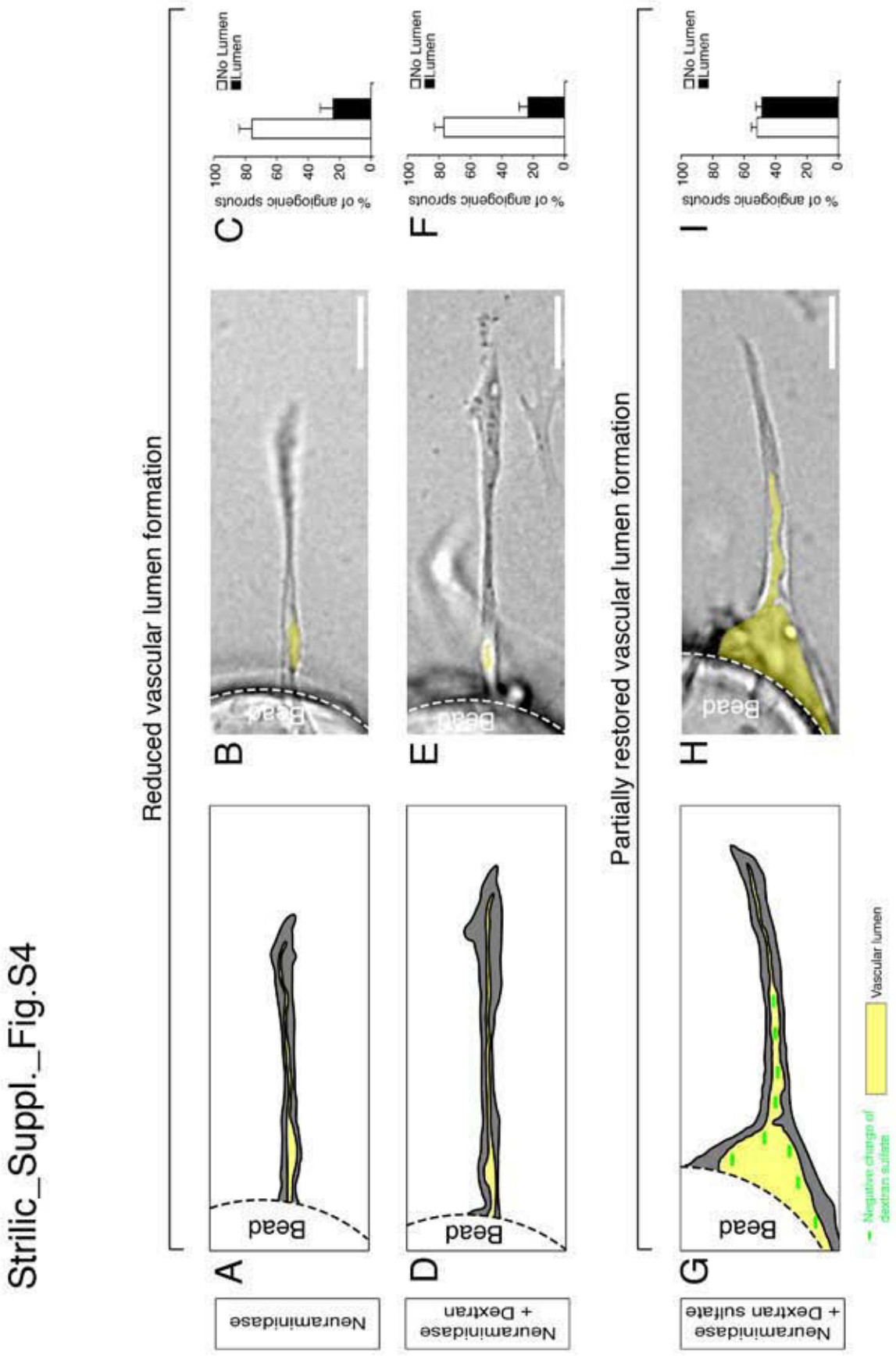
Strilic_Suppl._Fig.S4
Reduced vascular lumen formation
Partially restored vascular lumen formation
Neuraminidase
Neuraminidase + Dextran
Neuraminidase + Dextran sulfate
A
B
C
D
E
F
G
H
I
Bead
No Lumen
Lumen
% of angiogenic sprouts
Vascular lumen
Negative charge of dextran sulfate

2.3.3 General information and personal contribution

Name of the journal	Current Biology
Impact Factor (2011)	9.647
Personal contribution	5-10 %
Author position	4^{th} author
Tasks	Injection experiments and analysis
Other	-

Contribution in detail
My contribution to this work by Boris Strilic was the performance of injection experiments and the subsequent staining and analysis. This work was conducted together with Boris Strilic and Jennifer Axnick and resulted in figure 1 and supplementary figure 1.

3 Discussion and Outlook

3.1 Discussion

In the years during which this thesis was prepared, significant advance was made in the understanding of blood and lymphatic vessel formation.
Until 2008, lumen formation in blood vessels in general was thought to occur mainly intracellularly to form unicellular vessels that are later remodeled to the multicellular tubes that are observed in adulthood and later development (Kamei et al., 2006).
In recent years, this view diversified as reflected by our own findings (Strilic et al., 2009; Strilic et al., 2010a; Zeeb et al., 2010).
Today it is generally accepted and well established, that lumen formation can take place in different ways, dependent on the system and vessel that forms (Herbert et al., 2009; Axnick and Lammert, 2012). However lumen formation most commonly occurs extracellularly (Parker et al., 2004; Strilic et al., 2009; Herwig et al., 2011).

In zebrafish, intracellular lumen formation via vacuole coalescence was challenged and replaced as a model in the dorsal aorta (Parker et al., 2004; Jin et al., 2005), cardinal vein (Herbert et al., 2009), the DLAV (Herwig et al., 2011), and, in part, the ISVs (Blum et al., 2008; Ellertsdottir et al., 2010).
In particular, although lumen formation in the zebrafish DLAV was shown to frequently occur unicellularly, this type of lumen formation is extracellular via membrane invaginations and requires blood flow (Herwig et al., 2011).

In the mouse, the model was replaced by extracellular lumen formation between apposing endothelial cells (Strilic et al., 2009). Starting with the aforementioned study, many more molecular details were unraveled in the dorsal aorta or the arteries. Especially the molecular events regulating endothelial cell junctions (Kleaveland et al., 2009; Lampugnani et al., 2010) and the signaling mechanisms leading to polarization (Koh et al., 2008; Zovein et al., 2010; Xu et al., 2011) were elucidated. The molecules involved and studied can be grouped as cytoskeletal dynamics proteins, polarity regulators, and adhesion mediators (Iruela-Arispe, 2011).
Our study (Strilic et al., 2010a) advances our knowledge of lumen formation once polarity is established.
Although the glycocalyx was known to act as a repulsion zone for larger and small objects (Flessner, 2008), the active agent and molecular mechanism of this effect was unknown. PODXL is expressed on the apical surface of epithelial cells (Meder et al., 2005) and was used as a marker for the apical surface in endothelial cells (Strilic et al., 2009). As PODXL (gp135) is part of the CD34-sialomucin protein family, it is glycosylated and contains sialic acids resulting in a negative net charge (Nielsen and McNagny, 2008 J Cell Sci).
We could show that these negative charges are required for endothelial deadhesion and are the driving factor in mouse aortic lumen formation.
To date, no other mechanism has been proposed to explain the slit formation and initial separation of endothelial cells. Although targeted membrane and fluid delivery to the apical surface was suggested previously, both hypotheses were ruled out as no larger and not enough smaller vesicles were found in the EC cytoplasm. Additionally, the initial lumen was leaky, so fluid delivery would be futile (Strilic et al., 2009).

Interestingly, a PODXL homolog is localized on apical, luminal surfaces of zebrafish ISVs, as well (Herwig et al., 2011). Indeed, similar proteoglycans are expressed on many tubular organs such as kidney tubules and pancreatic ducts (Ng et al., 2005; Kesavan et al., 2009). Electrostatic repulsion could therefore constitute a potential general mechanism of lumen formation.

To summarize the emerging molecular details and align them with previous findings, we published the review article included in this thesis (Zeeb et al., 2010). The article cements and promotes extracellular and multicellular lumen formation and integrates the newest findings. However, many open questions remain, especially post polarization (Iruela-Arispe, 2011):
What drives endothelial cell shape changes during lumen formation? In the mouse aorta, formation of contractile fibres of actomyosin downstream of VEGFR-2 signaling was shown to be essential for lumen formation (Strilic et al., 2009). Yet, how these contractile fibers result in the dramatic cell shape changes is unknown.
How do endothelial junctions (VE-cadherin) relocate during endothelial cell polarization? The junctional molecules could be pushed to lateral positions by the same forces that generate the initial slit or could be endocytosed from the apical membrane. This step could turn out to be crucial, as proper formation of junctions is necessary for lumen formation as shown by the lethality of VE-cadherin null embryos and the CCM mutations (Carmeliet et al., 1999; Kleaveland et al., 2009; Strilic et al., 2009).
What is the exact role of the ECM in vasculogenesis and angiogenesis? β1-integrin was shown to influence EC polarization in arteries (Zovein et al., 2010), yet, a role for integrins in aorta formation is not known, probably due to the lack of basement membrane and surrounding pericytes.
Based on this last finding, further studies are also required to investigate the differences between lumen formation in the various systems, if any, especially regarding the known differences between the two most common model systems, zebrafish and mouse.

In order to promote the mouse as a model organism for vascular research and to allow researchers to study the mouse in molecular detail, we have improved the technique to culture mouse embryos *ex vivo* (Zeeb et al., 2012).
The mouse is advantageous as a model system, because it is a mammal that more closely resembles humans compared to zebrafish (Ellertsdottir et al., 2010). As there are many disease models for human diseases in *mus musculus*, many findings can directly be translated to the human patient and target substances can be tested for their efficacy.
It should be noted, that all pharmacological experiments *in vivo* contain a certain degree of uncertainty, due to side effects, cross-reactions, and redundancy.
However, because of the multitude of genetic models, pharmacological studies can easily be combined or compared with genetic approaches to increase their robustness.

The presented protocol offers optimal conditions for this kind of testing and work.
On the one hand, pharmacological substances can be tested and evaluated in a mammalian system *in vivo*. Testing benefits from the "simple" or rudimentary structures of the mouse embryo, such as the dorsal aorta prior to pericyte coverage. Additionally, the amount of substance required per embryo is low (few nanoliters) and survival rates are high ($\geq 80\,\%$), making the method robust and cheap.
On the other hand, the method allows for detailed analysis and manipulation of developmental processes from E8.0 to E10 or even to E15.5 if changes in development are detectable within shorter time. Any developmental process occurring within this timeframe can be analyzed, suitable analytical methods assumed, ranging from early development of the circulatory system, past the formation of liver or pancreas, to lymphatic vessel sprouting in the dermis. For example,

early attempts to image heart formation proved successful (data not shown).
If targeted injection is performed as described, internal controls can be used to study the effect of a substance in a single embryo, again resulting in a robust and cheap method.

The survival rates of the embryos after culture exceed 83 % in E8.0 embryos cultured for 12 hours and 87 % in E8.75 embryos cultured for 8 hours, irrespective of the treatment. In older embryos survival rates surpass 66 % and 71 %, in E11.5 embryos cultured for 5 hours and E15.5 embryos cultured for 0.5 hours, respectively. Viability of the embryos was assessed using the heartbeat of the embryos as an indicator.
In a long-term experiment, over half the embryos aged E9.0 and younger survived for 20 hours or more. After 18 hours however, survival dramatically declined (Zeeb et al., 2012). Survival rates dropped in an age-dependent manner. The older the embryos were at the beginning of cultivation, the shorter was the successful cultivation time. This might be due to two reasons. First, several different concentrations of O_2 in the gas mixture are required for the culture of mouse embryos (Takahashi et al., 2008). Unfortunately, we had to get by with 5 % and 20 % of oxygen in the mixture, at a time when 50 % are recommended (Takahashi et al., 2008). The O_2 concentration in the gas mixture has to increase to counteract the need for supply from the mother via the umbilical cord that is no longer present or functional, in the culture.
Second, older embryos probably require glucose and growth factors for survival and development, two traits that are not included in the culture medium.

Concerning the indicated price of the method, our improvement presents a dramatic reduction in running costs of up to 90 % compared to previous methods, while simultaneously increasing the staining quality. Previous WEC methods utilized rat serum as the culture medium of choice. Rat serum, while being effective, is expensive to buy or tedious to produce (Garcia et al., 2011). Additionally, rat serum prevents the use of rat antibodies, in particular the use of a well-established PECAM-1 antibody to detect endothelial cells, as the embryos are soaked with rat antigens. Our media avoid these disadvantages, as they contain no serum or calf serum, only. This allows staining the vasculature in whole embryos and imaging the results with a simple confocal microscope present in most labs. Thus, we circumvent the need for sophisticated staining techniques (Walls et al., 2008) and open up the method for a broad range of researchers and labs. Unfortunately, the initial investment for a WEC setup consisting of micromanipulator, injector and culture incubator amounts to 22,000 to 30,000 € limiting the broad applicability somewhat.

To test for healthy conditions in the culture, we compared cultivated embryos with embryos grown *in utero* at the corresponding stages. We could not detect notable morphological differences or differences in the somite number in these embryos. The heart rates of freshly isolated embryos and embryos in culture did not differ significantly, except for one condition, where the cultured embryos showed a slightly increased heart rate (Zeeb et al., 2012). However, we observed a rapid decline in the heart rate when embryos are not stored or cultured at 37 °C. Accelerated work or heating the workplace during isolation and injection is crucial for the proper development and survival of the embryos in our system.

On a time scale, our system allows to analyze the influence of two substances on vascular development with $n \geq 3$ embryos by a single researcher in one sitting, using a single CD1 mother mouse. When using multiple mice, a single researcher can perform a set of 30 to 40 injections in one sitting.

In total, the system provides vascular and developmental biologists with an affordable system

to analyze and manipulate the early development and to test biologically active compounds in a mammalian *in vivo* environment with high robustness. Vascular research will strongly benefit from the disease models and genetic applications of the mouse to complement the current zebrafish-based research.

3.2 Outlook

Although major "pieces of the puzzle" have been found and properly "placed" in context, many open questions still remain after these fruitful years in vascular research.
As mentioned earlier, several important pathways prior to and during lumen formation are unknown in any system. These include the role of the ECM and the signals leading to polarization, the mechanism of VE-cadherin translocation to lateral positions and the formation of stable junctions, the exact molecular mechanism of cell shape changes during lumen formation and the regulation of tube growth (Iruela-Arispe, 2011).
Currently, our lab focuses on cell shape changes during lumen formation and lumen expansion during mouse aorta vasculogenesis.
As we have shown previously that activation of RhoA and ROCK downstream of VEGF-A and VEGFR-2 are necessary for proper lumen formation (Strilic et al., 2009), we aim to elucidate the role of the contractile fibers and of actomyosin contractility formed by ROCK activation. Although in general, RhoA is known to increase actomyosin contractility, it is also reported to destabilize junctions, whereas Rac1 is reported to stabilize them (van Nieuw Amerongen and van Hinsbergh, 2001; Birukov, 2009). It is, however, quite likely that the activity is differentially regulated in different compartments of the endothelial cells, which could be achieved by the presence, tethering and activation of specific GEFs and GAPs (Lampugnani, 2010).
Additionally, we investigate the molecular mechanisms behind lumen enlargement and remodelling, focusing on the molecules influencing the actin cytoskeleton such as Rho and Src (Eliceiri et al., 2002; Im and Kazlauskas, 2007). Especially the Src family of kinases (SFKs) present a major candidate, as Src has been shown to regulate anisotropic growth of epithelial cells in the drosophila trachea (Nelson et al., 2012).

In order to support our molecular studies, we will continue to improve our method of investigation in our preferential model system, *mus musculus*.
First, we plan to reduce the stress of the embryos during isolation and injection to further increase viability and avoid potential side effects.
As we observed a dramatic decline in heart rate upon cooling of the embryos, heating the working surface during isolation should improve viability. Reducing the amount and pressure of injection is supposed to decrease damage and increase success of the injection process.
To increase usability and reputation of the mouse as a model system and to allow molecular studies of mouse ISVs, we test an improved method of whole-embryo imaging allowing for single-cell resolution and aiming at live-cell imaging as compared to the zebrafish. In that model system, live imaging in single-cell resolution is commonplace (Lawson and Weinstein, 2002; Blum et al., 2008), however, this was previously impossible in mouse. We plan to establish live imaging on a heated and gased microscope stage using GFP-reporter mice. As rotation is necessary for proper cultivation and survival of mouse embryos, live imaging will likely remain limited to a short period of time.
While improving the technique towards live-cell imaging, we will continue our research on the molecular details of mouse ISV formation with the method at hand. We plan to elucidate whether the mechanism of lumen formation is similar in mouse and zebrafish ISVs and whether

blood flow is required for these sprouting events.

We have previously tested injection of mouse-specific retroviruses in order to infect endothelial cells and to genetically alter their expression pattern. Although infection is in principle successful (data not shown), expression of encoded genes requires upwards of 20 hours. Although in principle, 20 hours of cultivation are possible (Zeeb et al., 2012), injection would have to take place 20 hours prior to the developmental process that is to be analyzed. To influence ISV sprouting or even aorta lumenization, injection would have to take place at E7.75 or E7.0, respectively. However, at this time, the embryo is still too small for targeted injection and too delicate, resulting in low viability.
Despite these limitations, injection with retroviruses to genetically manipulate developmental processes might provide a useful tool if longer cultivation or "faster" viruses become available.

Targeted injection can also be used for a different purpose that we are going to utilize in the study of inner organ formation. Injection of substances into the beating heart after the 6S stage will distribute the substance along the blood stream. This will prove especially useful to mark and target endothelial cells in the whole vasculature.

The planned refinements of WEC might prove useful to answer some of the open questions of vascular biology. In particular, our lab wants to focus on vascular lumen widening, cell-shape changes in aorta formation, the role of blood vessels in organ formation (Nikolova and Lammert, 2003), and the molecular events during lymphatic vessel formation.

With our work, we hope to contribute to a general understanding of blood and lymphatic vessel formation that is crucial for the development of new therapeutic targets for the multitude of diseases in which blood vessels are implicated. These diseases include varicose veins, arterial stenosis, atherosclerosis, and, most importantly, cancer. Especially against cancer, a general understanding of blood vessel formation is key, as many antiangiogenic treatments proved ineffective in certain types of cancer (Miles et al., 2010), probably because cancer "evades" general rules of vessel formation. Therefore, we aim to find necessities and underlying principles of lumen formation to provide novel targets for cancer treatment and to advance our knowledge of this crucial organ system.

4 References

Adams, R. H. and Alitalo, K. (2007) 'Molecular regulation of angiogenesis and lymphangiogenesis', Nat Rev Mol Cell Biol 8(6): 464-78.

Axnick, J. and Lammert, E. (2012) 'Vascular lumen formation', Curr Opin Hematol 19(3): 192-8.

Baum, O., Suter, F., Gerber, B., Tschanz, S. A., Buergy, R., Blank, F., Hlushchuk, R. and Djonov, V. (2010) 'VEGF-A promotes intussusceptive angiogenesis in the developing chicken chorioallantoic membrane', Microcirculation 17(6): 447-57.

Betsholtz, C., Lindblom, P. and Gerhardt, H. (2005) 'Role of pericytes in vascular morphogenesis', EXS(94): 115-25.

Billroth, T. (1856) Untersuchungen über die Entwicklung der Blutgefässe, nebst Beobachtungen aus der königlichen chirurgischen Universitäts-Klinik zu Berlin. Berlin: Georg Reimer.

Birukov, K. G. (2009) 'Small GTPases in mechanosensitive regulation of endothelial barrier', Microvasc Res 77(1): 46-52.

Blum, Y., Belting, H. G., Ellertsdottir, E., Herwig, L., Luders, F. and Affolter, M. (2008) 'Complex cell rearrangements during intersegmental vessel sprouting and vessel fusion in the zebrafish embryo', Dev Biol 316(2): 312-22.

Buschmann, T., Eglinger, J., Lammert, E. (2010) Angiogenesis and liver regeneration. in D. Häussinger (ed.) Liver regeneration. Berlin / Boston: De Gruyter.

Cai, W. and Schaper, W. (2008) 'Mechanisms of arteriogenesis', Acta Biochim Biophys Sin (Shanghai) 40(8): 681-92.

Carmeliet, P., Ferreira, V., Breier, G., Pollefeyt, S., Kieckens, L., Gertsenstein, M., Fahrig, M., Vandenhoeck, A., Harpal, K., Eberhardt, C. et al. (1996) 'Abnormal blood vessel development and lethality in embryos lacking a single VEGF allele', Nature 380(6573): 435-9.

Carmeliet, P., Lampugnani, M. G., Moons, L., Breviario, F., Compernolle, V., Bono, F., Balconi, G., Spagnuolo, R., Oosthuyse, B., Dewerchin, M. et al. (1999) 'Targeted deficiency or cytosolic truncation of the VE-cadherin gene in mice impairs VEGF-mediated endothelial survival and angiogenesis', Cell 98(2): 147-57.

Chung, A. S., Lee, J. and Ferrara, N. (2010) 'Targeting the tumour vasculature: insights from physiological angiogenesis', Nat Rev Cancer 10(7): 505-14.

Davis, G. E., Bayless, K. J. and Mavila, A. (2002) 'Molecular basis of endothelial cell morphogenesis in three-dimensional extracellular matrices', Anat Rec 268(3): 252-75.

Davis, G. E. and Camarillo, C. W. (1996) 'An alpha 2 beta 1 integrin-dependent pinocytic mechanism involving intracellular vacuole formation and coalescence regulates capillary

lumen and tube formation in three-dimensional collagen matrix', Exp Cell Res 224(1): 39-51.

Drake, C. J. and Fleming, P. A. (2000) 'Vasculogenesis in the day 6.5 to 9.5 mouse embryo', Blood 95(5): 1671-9.

Eichmann, A., Yuan, L., Moyon, D., Lenoble, F., Pardanaud, L. and Breant, C. (2005) 'Vascular development: from precursor cells to branched arterial and venous networks', Int J Dev Biol 49(2-3): 259-67.

Eliceiri, B. P., Puente, X. S., Hood, J. D., Stupack, D. G., Schlaepfer, D. D., Huang, X. Z., Sheppard, D. and Cheresh, D. A. (2002) 'Src-mediated coupling of focal adhesion kinase to integrin alpha(v)beta5 in vascular endothelial growth factor signaling', J Cell Biol 157(1): 149-60.

Ellertsdottir, E., Lenard, A., Blum, Y., Krudewig, A., Herwig, L., Affolter, M. and Belting, H. G. (2010) 'Vascular morphogenesis in the zebrafish embryo', Dev Biol 341(1): 56-65.

Ferrara, N., Carver-Moore, K., Chen, H., Dowd, M., Lu, L., O'Shea, K. S., Powell-Braxton, L., Hillan, K. J. and Moore, M. W. (1996) 'Heterozygous embryonic lethality induced by targeted inactivation of the VEGF gene', Nature 380(6573): 439-42.

Flessner, M. F. (2008) 'Endothelial glycocalyx and the peritoneal barrier', Perit Dial Int 28(1): 6-12.

Fong, T. A., Shawver, L. K., Sun, L., Tang, C., App, H., Powell, T. J., Kim, Y. H., Schreck, R., Wang, X., Risau, W. et al. (1999) 'SU5416 is a potent and selective inhibitor of the vascular endothelial growth factor receptor (Flk-1/KDR) that inhibits tyrosine kinase catalysis, tumor vascularization, and growth of multiple tumor types', Cancer Res 59(1): 99-106.

Garcia, M. D., Udan, R. S., Hadjantonakis, A. K. and Dickinson, M. E. (2011) 'Preparation of rat serum for culturing mouse embryos', Cold Spring Harb Protoc 2011(4): pdb prot5593, 391-393.

Gerhardt, H. and Betsholtz, C. (2003) 'Endothelial-pericyte interactions in angiogenesis', Cell Tissue Res 314(1): 15-23.

Graupera, M., Guillermet-Guibert, J., Foukas, L. C., Phng, L. K., Cain, R. J., Salpekar, A., Pearce, W., Meek, S., Millan, J., Cutillas, P. R. et al. (2008) 'Angiogenesis selectively requires the p110alpha isoform of PI3K to control endothelial cell migration', Nature 453(7195): 662-6.

Herbert, S. P., Huisken, J., Kim, T. N., Feldman, M. E., Houseman, B. T., Wang, R. A., Shokat, K. M. and Stainier, D. Y. (2009) 'Arterial-venous segregation by selective cell sprouting: an alternative mode of blood vessel formation', Science 326(5950): 294-8.

Herwig, L., Blum, Y., Krudewig, A., Ellertsdottir, E., Lenard, A., Belting, H. G. and Affolter, M. (2011) 'Distinct cellular mechanisms of blood vessel fusion in the zebrafish embryo', Curr Biol 21(22): 1942-8.

Im, E. and Kazlauskas, A. (2007) 'Src family kinases promote vessel stability by antagonizing the Rho/ROCK pathway', J Biol Chem 282(40): 29122-9.

Iruela-Arispe, M. L. and Davis, G. E. (2009) 'Cellular and molecular mechanisms of vascular lumen formation', Dev Cell 16(2): 222-31.

Iruela-Arispe, M. L. (2011) 'LUMENating blood vessels', Dev Cell 20(4): 412-4.

Jin, S. W., Beis, D., Mitchell, T., Chen, J. N. and Stainier, D. Y. (2005) 'Cellular and molecular analyses of vascular tube and lumen formation in zebrafish', Development 132(23): 5199-209.

Kamei, M., Saunders, W. B., Bayless, K. J., Dye, L., Davis, G. E. and Weinstein, B. M. (2006) 'Endothelial tubes assemble from intracellular vacuoles in vivo', Nature 442(7101): 453-6.

Kesavan, G., Sand, F. W., Greiner, T. U., Johansson, J. K., Kobberup, S., Wu, X., Brakebusch, C. and Semb, H. (2009) 'Cdc42-mediated tubulogenesis controls cell specification', Cell 139(4): 791-801.

Kleaveland, B., Zheng, X., Liu, J. J., Blum, Y., Tung, J. J., Zou, Z., Sweeney, S. M., Chen, M., Guo, L., Lu, M. M. et al. (2009) 'Regulation of cardiovascular development and integrity by the heart of glass-cerebral cavernous malformation protein pathway', Nat Med 15(2): 169-76.

Koh, W., Mahan, R. D. and Davis, G. E. (2008) 'Cdc42- and Rac1-mediated endothelial lumen formation requires Pak2, Pak4 and Par3, and PKC-dependent signaling', J Cell Sci 121(Pt 7): 989-1001.

Kucera, T., Strilic, B., Regener, K., Schubert, M., Laudet, V. and Lammert, E. (2009) 'Ancestral vascular lumen formation via basal cell surfaces', PLoS One 4(1): e4132.

Lammert, E. (2008) 'Developmental biology. Brain Wnts for blood vessels', Science 322(5905): 1195-6.

Lampugnani, M. G. (2010) 'Endothelial adherens junctions and the actin cytoskeleton: an 'infinity net'?', J Biol 9(3): 16.

Lampugnani, M. G., Orsenigo, F., Rudini, N., Maddaluno, L., Boulday, G., Chapon, F. and Dejana, E. (2010) 'CCM1 regulates vascular-lumen organization by inducing endothelial polarity', J Cell Sci 123(Pt 7): 1073-80.

Lawson, N. D. and Weinstein, B. M. (2002) 'In vivo imaging of embryonic vascular development using transgenic zebrafish', Dev Biol 248(2): 307-18.

Lubarsky, B. and Krasnow, M. A. (2003) 'Tube morphogenesis: making and shaping biological tubes', Cell 112(1): 19-28.

Meder, D., Shevchenko, A., Simons, K. and Fullekrug, J. (2005) 'Gp135/podocalyxin and NHERF-2 participate in the formation of a preapical domain during polarization of MDCK cells', J Cell Biol 168(2): 303-13.

Miles, D. W., Chan, A., Dirix, L. Y., Cortes, J., Pivot, X., Tomczak, P., Delozier, T., Sohn, J.

H., Provencher, L., Puglisi, F. et al. (2010) 'Phase III study of bevacizumab plus docetaxel compared with placebo plus docetaxel for the first-line treatment of human epidermal growth factor receptor 2-negative metastatic breast cancer', J Clin Oncol 28(20): 3239-47.

Nelson, K. S., Khan, Z., Molnar, I., Mihaly, J., Kaschube, M. and Beitel, G. J. (2012) 'Drosophila Src regulates anisotropic apical surface growth to control epithelial tube size', Nat Cell Biol 14(5): 518-25.

Ng, A. N., de Jong-Curtain, T. A., Mawdsley, D. J., White, S. J., Shin, J., Appel, B., Dong, P. D., Stainier, D. Y. and Heath, J. K. (2005) 'Formation of the digestive system in zebrafish: III. Intestinal epithelium morphogenesis', Dev Biol 286(1): 114-35.

Nielsen, J. S. and McNagny, K. M. (2008) 'Novel functions of the CD34 family', J Cell Sci 121(Pt 22): 3683-92.

Nikolova, G. and Lammert, E. (2003) 'Interdependent development of blood vessels and organs', Cell Tissue Res 314(1): 33-42.

Olsson, A. K., Dimberg, A., Kreuger, J. and Claesson-Welsh, L. (2006) 'VEGF receptor signalling - in control of vascular function', Nat Rev Mol Cell Biol 7(5): 359-71.

Parker, L. H., Schmidt, M., Jin, S. W., Gray, A. M., Beis, D., Pham, T., Frantz, G., Palmieri, S., Hillan, K., Stainier, D. Y. et al. (2004) 'The endothelial-cell-derived secreted factor Egfl7 regulates vascular tube formation', Nature 428(6984): 754-8.

Planas-Paz, L., Strilic, B., Goedecke, A., Breier, G., Fassler, R. and Lammert, E. (2012) 'Mechanoinduction of lymph vessel expansion', EMBO J 31(4): 788-804.

Risau, W. and Flamme, I. (1995) 'Vasculogenesis', Annu Rev Cell Dev Biol 11: 73-91.

Sabin, F. (1920) 'Studies on the origin of blood-vessels and of red-corpuscles as seen in the living blastoderm of chicks during the second day of incubation.', Contrib Embryol 9: 213-262.

Sato, Y., Watanabe, T., Saito, D., Takahashi, T., Yoshida, S., Kohyama, J., Ohata, E., Okano, H. and Takahashi, Y. (2008) 'Notch mediates the segmental specification of angioblasts in somites and their directed migration toward the dorsal aorta in avian embryos', Dev Cell 14(6): 890-901.

Shigei, T., Tsuru, H., Ishikawa, N. and Yoshioka, K. (2001) 'Absence of endothelium in invertebrate blood vessels: significance of endothelium and sympathetic nerve/medial smooth muscle in the vertebrate vascular system', Jpn J Pharmacol 87(4): 253-60.

Stratman, A. N., Schwindt, A. E., Malotte, K. M. and Davis, G. E. (2010) 'Endothelial-derived PDGF-BB and HB-EGF coordinately regulate pericyte recruitment during vasculogenic tube assembly and stabilization', Blood 116(22): 4720-30.

Strilic, B., Kucera, T., Eglinger, J., Hughes, M. R., McNagny, K. M., Tsukita, S., Dejana, E., Ferrara, N. and Lammert, E. (2009) 'The molecular basis of vascular lumen formation in the developing mouse aorta', Dev Cell 17(4): 505-15.

Strilic, B., Eglinger, J., Krieg, M., Zeeb, M., Axnick, J., Babal, P., Muller, D. J. and Lammert, E. (2010a) 'Electrostatic cell-surface repulsion initiates lumen formation in developing

blood vessels', Curr Biol 20(22): 2003-9.

Strilic, B., Kucera, T. and Lammert, E. (2010b) 'Formation of cardiovascular tubes in invertebrates and vertebrates', Cell Mol Life Sci 67(19): 3209-18.

Takahashi, M., Nomura, T. and Osumi, N. (2008) 'Transferring genes into cultured mammalian embryos by electroporation', Dev Growth Differ 50(6): 485-97.

Tortora, G. J., Derrickson, B.H. (2006) Anatomie und Physiologie: Wiley-VCH Verlag GmbH & Co. KGaA.

Tzima, E., Irani-Tehrani, M., Kiosses, W. B., Dejana, E., Schultz, D. A., Engelhardt, B., Cao, G., DeLisser, H. and Schwartz, M. A. (2005) 'A mechanosensory complex that mediates the endothelial cell response to fluid shear stress', Nature 437(7057): 426-31.

van Nieuw Amerongen, G. P. and van Hinsbergh, V. W. (2001) 'Cytoskeletal effects of rho-like small guanine nucleotide-binding proteins in the vascular system', Arterioscler Thromb Vasc Biol 21(3): 300-11.

Walls, J. R., Coultas, L., Rossant, J. and Henkelman, R. M. (2008) 'Three-dimensional analysis of vascular development in the mouse embryo', PLoS One 3(8): e2853.

Wigle, J. T. and Oliver, G. (1999) 'Prox1 function is required for the development of the murine lymphatic system', Cell 98(6): 769-78.

Woodfin, A., Voisin, M. B. and Nourshargh, S. (2007) 'PECAM-1: a multi-functional molecule in inflammation and vascular biology', Arterioscler Thromb Vasc Biol 27(12): 2514-23.

Xu, K., Sacharidou, A., Fu, S., Chong, D. C., Skaug, B., Chen, Z. J., Davis, G. E. and Cleaver, O. (2011) 'Blood vessel tubulogenesis requires Rasip1 regulation of GTPase signaling', Dev Cell 20(4): 526-39.

Yarnitzky, T. and Volk, T. (1995) 'Laminin is required for heart, somatic muscles, and gut development in the Drosophila embryo', Dev Biol 169(2): 609-18.

Zaret, K. S. and Grompe, M. (2008) 'Generation and regeneration of cells of the liver and pancreas', Science 322(5907): 1490-4.

Zeeb, M., Strilic, B. and Lammert, E. (2010) 'Resolving cell-cell junctions: lumen formation in blood vessels', Curr Opin Cell Biol 22(5): 626-32.

Zeeb, M., Axnick, J., Planas-Paz, L., Hartmann, T., Strilic, B. and Lammert, E. (2012) 'Pharmacological manipulation of blood and lymphatic vascularization in ex vivo-cultured mouse embryos', Nat Protoc 7(11): 1970-82.

Zovein, A. C., Luque, A., Turlo, K. A., Hofmann, J. J., Yee, K. M., Becker, M. S., Fassler, R., Mellman, I., Lane, T. F. and Iruela-Arispe, M. L. (2010) 'Beta1 integrin establishes endothelial cell polarity and arteriolar lumen formation via a Par3-dependent mechanism', Dev Cell 18(1): 39-51.

List of Abbreviations

SI units and their symbols were used throughout this thesis whereever possible.

PODXL	Podocalyxin
gp135	Glycoprotein 135
ECM	Extracellular matrix
EC	Endothelial cell
NMRI	Naval Medical Research Institute
E0.5	Embryonic day 0.5
ISV	Intersomitic vessels (in mouse)
	Intersegmental vessels (in zebrafish)
PECAM-1	Platelet endothelial cell adhesion molecule
CD31	Cluster of differentiation 31
VEGFR-2	Vascular endothelial growth factor receptor 2
KDR	Kinase insert domain receptor
Flk-1	Fetal Liver Kinase 1
VEGF-A	Vascular endothelial growth factor A
FGF	Fibroblast growth factor
Dll4	Delta-like ligand 4
9 S	9 somite stage
VE-cadherin	Vascular endothelial cadherin
ROCK	Rho-associated kinase
Par3	Partitioning defective 3
Cdc42	Cell division control protein 42
ccm	Cerebral cavernous malformation
DLAV	Dorso-lateral anastomotic vessel
Rasip1	Ras interacting protein 1
LEC	Lymphatic endothelial cell
JLS	Jugular lymph sack
VEGFR-3	Vascular endothelial growth factor receptor 3
Flt-4	Fms-related tyrosine kinase 4
Heg1	Heart of glass
PTEN	Phosphatase and Tensin homolog

ERM	Ezrin, Radixin, Moesin
WEC	Whole-embryo culture
NA	Neuraminidase
PS	Protamine sulfate
DS	Dextrane sulfate
BRA	Bead-rolling assay
SCFS	Single cell force spectroscopy
CD34	Cluster of differentiation 34
RhoA	Ras homolog gene family, member A
Rac1	Ras-related C3 botulinum toxin substrate 1
Src	from "Sarcoma"
SFK	Src-family of kinases
GFP	Green-fluorescent protein

Acknowledgements

I'd like to thank the Academy...
and...

... my boss and supervisor **Prof. Dr. Eckhard Lammert**
for the opportunity to do my thesis in his lab,
for good advice and supervision,
for freedom and guidance,
and for all the confidence he has shown me;

... my colleagues and former colleagues from the Lammert lab,
in particular **Dr. Jan Eglinger**
for all the help and support,
for all the HELP and SUPPORT, at any stage of this thesis,
for all his work he invests into the lab;

Dr. Boris Strilic
for handing the best project of all over to me,
for everything that you have taught me, in the lab and beyond,
for wonderful nightshifts;

and **Dr. Daniel Eberhard**
for an independent view,
for an open ear in all manners,
for a shared passion;

as well as, Jennifer Axnick, Astrid Wies, Dr. Lara Planas Paz, Dr. Ruchi Jain, Silke Jakob, Barbara Bartosinska, Dr. Deepak Jain, Tobias Buschmann, Dr. Jan Marquardt, Dr. Martin Kragl, Silke Otter, Dr. Alena Braun, Dimitrios Dimitroulis, Fatma Demir.

... my students **Jennifer Axnick** and **Thorsten Hartmann**
for teaching me as much as I taught them,
for all the excellent work you two have done,
for starting the best projects,
for all the load you have carried, Jenny;

... my second referee **Prof. Dr. Chris Bridges** and his lab.

... my collaborators and supporters,
Prof. Dr. Greg Beitel, Dr. Kevin Nelson (both Northwestern University, Chicago), Dr. Holm Zaehres (MPI Münster), Fabian Kuck, Dr. Roland Piekorz (HHU Düsseldorf), Matthias Pospiech (for the LaTeX templates)

... my family and my friends,
in particular **Carolin Knauber**
for your patience,
for still being with me,
for all the love you have given me;

and my parents **Marga** and **Artur Zeeb**
for always believing in me,
for supporting me throughout all situations in life;

as well as, Marcel Olkner, Rene und Kristin Reilard, Uwe Post, Marcus Malden, Christian Gienger, Merlind Pfeil, Regina Jäger, Claudia Fritschi, Michel Toppin, Thomas Pfau und Susa Merz.

. . . my bike shop owner **Robert Boehnke**
for mobility and good service.

..my favorite homepages and columnists LSV, Conley Woods, Simon Görtzen, HDStarcraft and Husky
for funny moments, and welcome distractions.

. . . my favorite bands and musicians Armin van Buuren, Wir sind Helden, Kettcar, Tomte, Coldplay, SEEED and ABBA
for the music.

Declarations

Erklärung

Hiermit erkläre ich, dass ich die vorliegende Dissertation eigenständig und ohne fremde und unerlaubte Hilfe angefertigt habe.
Ich habe keine anderen als die angegebenen Quellen und Hilfsmittel verwendet und habe alle Stellen in denen ich Bezug auf die Arbeit Anderer nehme als solche kenntlich gemacht.

Die vorliegende Arbeit wurde weder in dieser noch in ähnlicher Form bei einer anderen Institution eingereicht.

Vorherige, erfolgreiche oder erfolglose, Versuche zur Promotion wurden von mir nicht unternommen.

Gezeichnet

Martin Zeeb
Düsseldorf, den 21. November 2012

Declaration

I declare that I have written and prepared this thesis independently and without outside or forbidden help.
I did not use other sources, aids and appliances than those indicated and have marked all positions, where I have drawn from the work of others.

The work was not submitted to any other institution in this or any modified form.

I did not make any previous, successful or unsuccessful, attempts at any PhD thesis.

Signed

Martin Zeeb
Düsseldorf, 21st of November, 2012